W-AM-PM-Sy1 **INFERENCES ABOUT MOLECULAR MECHANISMS THROUGH FLUCTUATION ANALYSIS**
Charles F. Stevens, Department of Physiology, Yale University School of Medicine, New Haven, CT 06510.

The study of fluctuations has played an important role in the physical sciences and provided, at the turn of the century, crucial evidence for the reality of molecules. A chief significance of fluctuation analysis is that it permits inferences about the properties of individual molecules.

Fluctuation analysis works because the same physical properties of molecules that govern their average behavior--that usually observed in a laboratory--are also reflected in the inevitable randomness exhibited by such collections of molecules. This randomness is normally characterized by the spectrum of fluctuations around the mean value of some physical quantity: the spectrum represents the variance of the random process contributed by each of its frequency components. Spectra are usually calculated by the fast Fourier transform method, with careful attention being given to preparation of the data to eliminate artifacts known as aliasing and nonstationarity.

It is important to realize that spectra can only be interpreted in terms of molecular model. Probability theory provides straightforward recipes that permit us to start from a molecular mechanism for some process and predict the spectrum of fluctuations that the mechanism will produce. This approach permits us to check on the accuracy of a proposed mechanism and to derive properties of the molecules involved.

W-AM-PM-Sy2 SINGLE CHANNEL CURRENTS FROM EMBRYONIC HEART. Louis J. DeFelice and David E. Clapham, Department of Anatomy, Emory University, Atlanta, GA 30322.

Trypsin dissociated cells from embryonic chick heart were plated for several hours in a non-adhesive dish. During this period small clusters of cells form spontaneously. The cells were transferred to a Sylgard coated dish; individual cells, or clusters of about 12 cells, were selected under the microscope for approach with a patch electrode. Seals under suction were between 50 and 100 MΩ. Electrodes were filled with a balanced salt solution containing 1.3 mM K; tips were 1-3 μm in diameter. In spontaneously beating clusters of 7 day ventricle cells we observed action currents composed of a sharp inward phase followed by a slow, 200 msec duration, inward current, in turn followed by a noisy, outward current of approximately 10 pA amplitude that lasted between 200 and 400 msec but always ended abruptly. In TTX, the spontaneous beating stops and rectangular, outward, single channel currents are observed on a zero net current baseline. The single channel currents are 2 to 3 times larger than the peak-to-peak background noise bandlimited to 100Hz. Amplitudes range from 1 to 2 pA but in any one experiment are constant to within 15%. Average current duration is about 300 msec. In one experiment, the values were 280 msec ± 80 msec (n=20) at rest (approximately -60 mV) and at 32°C. At room temperature this time increases by a factor of about two. Occasionally, open times greater than one second were observed. The currents are absent in 4AP. Channel kinetics agree roughly with that expected from a noise analysis of K channels in the same preparation, but the single channel current is nearly 10 times too large. This may be due to an underestimate in K channel density in the noise calculations (less than one channel/μm^2). These single channel currents are tentatively identified as K channels. Compared to K channels in nerve, the channels we observe in heart have low density, long open times, and a larger single channel current near rest.

W-AM-PM-Sy3 NONSTATIONARY NOISE ANALYSIS OF MEMBRANE CURRENTS
F.J. Sigworth, Max-Planck-Institut für biophysikalische Chemie, D-3400 Göttingen, F.R.G.

Conventional stationary noise analysis of membrane currents requires that the ionic conductances be in a steady state. This condition is never rigorously met, and often is not even approximately fulfilled, for example because of inactivation or desensitization effects. I will discuss three approaches to the analysis of fluctuations in ionic currents that change with time.

(1) Compare the time-courses of mean and ensemble variance[1]. As in stationary noise analysis, the size of the fluctuations reflects the size and number of single-channel events. Changes in the mean and variance can sometimes be used to estimate the total number of channels as well.

(2) Compute the nonstationary covariance function. This is the analog of the usual power spectrum, and, for open-closed channels, reflects the open-time and other kinetic properties of the single channels. This function contains additional information that allows one to check for changes, in time, of the apparent channel lifetime. Such changes are in fact seen in Na^+ channels in nerve[2].

(3) Compute the power spectrum anyway. This is possible[3], and can give readily interpretable results. The limits of validity will be discussed, as will be the correction of raw spectra for nonstationary effects.

1. E.A. Schwartz, J. Physiol. 246: 617 (1975); F. Sigworth, J. Physiol. 307: 97 (1980)
2. F. Sigworth, Biophys. J. (in press; early 1981)
3. F. Conti et al., J. Physiol. (in press; 1980)

W-AM-PM-Sy4 ANALYSIS OF MEMBRANE PROPERTIES USING EXTRINSIC NOISE. R.T. Mathias, Department of Physiology, Rush University , Chicago, Illinois 60612.

The computation of power spectra or transfer functions describing single channels, patches of membranes or entire tissues is most accurately accomplished by frequency domain analysis. Recording potentials or currents from biological membranes requires specialized interface circuits, usually involving very high impedances. Because the impedances are so high, stray capacitances of a few picofarads will introduce relatively large shunt currents at frequencies of only a few kilohertz. We have developed several circuits which minimize the effects of stray capacitance and allow accurate microelectrode recording at frequencies up to 10 kHz. Once one has high fidelity analog records, these data must be digitized for subsequent analysis. When performing A/D conversions, one must always consider the bandwidth over which data is desired, the sample rate of the A/D's, and the errors due to aliasing; otherwise the fidelity of the analog data may be lost. The next stage of analysis is to digitally compute the power spectrum, or if extrinsic noise has been applied, the cross power spectrum and transfer function. At this stage it still is possible to lose the fidelity of the original recording, if the computations and signal averaging are not properly implemented. Once an accurate, low variance estimate of the spectra or transfer function is obtained, one must interpret these data in terms of the structure of the tissue being studied. This interpretation requires a theoretical model of the structure, whether the structure be a single channel or a syncytial tissue, and an explicit comparison of data with theoretical predictions. Measurement of the response to extrinsic noise allows computation of the phase function as well as power spectrum; thus, the comparison of data and theory can be made with more senstivity than with other techniques.

W-AM-PM-Sy5 FLUCTUATION STUDIES ON Na AND K CURRENTS OF MYELINATED AXONS. Wolfgang Nonner. Dept. of Physiology and Biophysics, Univ. of Miami, Miami FL 33136.

Noise analysis on biological membranes was pioneered by Verveen, and the first membrane studied was that of myelinated axons of frog. Their nodes of Ranvier provide natural small patches (ca. 50 μm^2) of exposed nerve membrane suitable for fluctuation measurements. Like in squid giant axons, the dominant ionic channels in this membrane are Na and K channels, the properties of which have been well studied under voltage clamp. Current noise is dramatically increased when such channels open upon a membrane depolarization. Fluctuation components attributable to current in either kind of channels have been separated by pharmacological block of Na or K current by Begenisich, Conti, Hille, Neumcke, Nonner, Sigworth, Stämpfli, Stevens, and Verveen's laboratory. Na current fluctuations have been analyzed by spectral analysis of stationary current and by variance analysis of transient current. The spectra are of the shape obtained by the superposition of several Lorentzian components with cutoff frequencies roughly reflecting the major kinetic events of Na channel gating, activation and inactivation. The nonstationary variance follows the time course of Na current as if it is due to random open-close transitions of Na channels. Single-channel conductances calculated on the assumption of a simple, open-close mechanism are in the range 5-8 pS and vary little with depolarization, which strongly modifies the distribution of channels among their kinetic states. Thus there is no sign that Na channels can have more than two levels of conductance. As a first attempt towards testing alternative kinetic models of gating by noise analysis, the possible coupling between activation and inactivation gating has been examined. Several models considered so far fail to predict the fluctuation properties. K current noise reveals spectra that are difficult to interpret in a mechanistic way. Estimates of K channel conductance range from 4 to 37 pS.

W-AM-PM-Sy6 SYNAPTIC NOISE. Vincent E. Dionne, Department of Medicine, University of California at San Diego, La Jolla, California 92093.

In cholinergic synapses the Acetylcholine Receptor mediates the transmission of electrical signals between cells with a coupled receptor-gating-channel mechanism. Acetylcholine and cholinomimetic compounds can reversibly bind at the receptor allowing the gating mechanism to open the channel for the transmembrane movement of small, dissolved cations; the channels spontaneously close after a few milliseconds. Noise analysis of ionic currents through the synaptic channels has been used to describe the kinetic relations between Receptor states and to estimate the average lifetime of states. Recent work has focussed on noise records exhibiting spectral densities composed of at least two Lorentzian components. Several fundamentally different mechanisms can produce such records. In order to select a correct class of mechanisms, supplemental experiments which make use of the Fluctuation-Dissipation relation must be employed. In these cases the characteristic noise frequencies cannot be identified with a single kinetic transition; rather, the characteristic frequencies are mixtures of several kinetic rates. Two different experimental examples will be presented to illustrated these points. In the slow muscle fibers of the garter snake the Acetylcholine Receptors produce complicated noise spectra because, after the receptor binds agonist, the channel can open several times before the agonist is released. In contrast, there are molecules with a local anesthetic-like property which block normal channels in their open configuration, and by this action produce multicomponent noise spectra.

This work was supported by USPHS grant NS 15344 from the NIH and contract N00014-79-C-079 from the Office of Naval Research.

W-AM-PM-Sy7 FLUCTUATION ANALYSIS OF EPITHELIAL ION TRANSPORT
B. Lindemann, 2nd Department of Physiology, 6650 Homburg/Saar, F.R.G.

Some of the ion-transporting channels in epithelial cell membranes show discontinuities of their translocation rate either spontaneously or after addition of reversibly acting blockers in suitable concentrations. Analysis of the noise signal recorded transepithelially from a large ensemble of such channels may require a one- or two-step correction for effects of series membranes and other ohmic or reactive elements contained in the preparation. The first correction deals with access impedance effects per se and merely requires the estimation of the transfer function from noise source to recording device. The second correction, for driving force effects, is more problematic but not required for many problems (Lindemann and DeFelice, 1981, in press). Subsequently, the computation of rate constants, single channel currents and area densities of channels proceeds in the usual way. Data will be presented which show that the estimation of channel area densities derived from ensemble shot-noise is of particular interest for the understanding of epithelial function: epithelia which face solutions of varying ionic composition on the luminal side are controlled by extracellular signals (e.g. hormones) and local (cell residing) permeability-changing mechanisms which vary predominantly the area densities (e.g. Li, Palmer, Edelman and Lindemann, Pflügers Arch. 382: R13, 1979).

W-AM-PM-Sy8 SINGLE CHANNEL RECORDING. Joseph B. Patlak, Department of Physiology and Biophysics, University of Vermont, Burlington, VT 05405.

One of the goals of electrophysiology is to determine the properties of the macromolecules which give rise to transmembrane currents. Because "whole-cell" recording techniques measure the signals from 10^3 to 10^6 simultaneously functioning channels, noise analysis must be used to calculate a single channel's conductance and kinetics. The currents through individual channels in a wide variety of preparations can now be recorded using the patch clamp method of Neher and Sakmann. The recording of single channel signals is a more direct and sensitive method of determining a channel's conductance and kinetics than noise analysis. In particular, measurement of the channel's conductance is not model dependent. Also, individual kinetic components can be better separated because noise analysis often measures only the sum of related parameters, and because slow kinetic components tend to swamp fast ones in noise signals since they carry more signal power per event. Recent developments of the patch recording technique have extended the range of channels for which single channel analysis is possible. These developments include a drastic improvement in resolution with the Gigohm-seal technique of Neher, and the ability to fully control transmembrane potential and internal bathing solution in excised membrane patches. Useful new insights of Na^+ and ACh-activated channel properties have been the result. The patch recording technique is applicable to many different preparations and channel types, with the primary constraint that the cell's membrane be "clean". Some channel currents are too small to be resolved as discrete events. Examples are Ca^{++} currents or currents near their reversal potentials. However, the patch clamp method is also well suited to standard noise analysis, thereby extending the usefulness of this technique.

W-AM-PM-Sy9 STRUCTURAL ANALYSIS OF ELECTRICAL PROPERTIES. R.S. Eisenberg, Dept. of Physiology, Rush University, Chicago, IL 60612.

The electrical properties of most cells and all syncytial tissues are the composite of the properties of different membranes and systems of small extracellular space. For example, the electrical properties of epithelia are determined by the distinct properties of the apical membrane, the basal membrane (which may, or may not, be distinct from the lateral membrane), and the lateral intercellular spaces. Similarly, the electrical properties of the lens, a highly specialized syncytial tissue derived from an epithelium, are determined by the properties of inner and outer membranes and by the properties of a narrow tortuous extracellular space within the tissue. And, most extensively studied of all, the electrical properties of skeletal muscle are determined by the surface membrane, the lumen of the t-system, the t-system membrane, with perhaps some contribution from current flow across a specialized junction into the sarcoplasmic reticulum.

The function of these tissues is mediated by the specialized properties of each membrane and system of extracellular space. Thus, physiological analysis must parse the composite electrical properties of the tissue into the properties of each component. Structural analysis requires morphological measurements, theory, and physiological experiments. The morphological measurements determine the topology and amount of structure. The theory predicts the expected properties of the structure and thereby allows analysis of physiological experiments. Physiological experiments, applying extrinsic noise to measure the impedance, determine the composite electrical properties of the heterogeneous tissue. Fitting of the structural theory to the measured impedance determines the properties of the individual components of the tissue.

W-AM-A1 PHOTOREACTIVATING ENZYME FROM E. COLI: SPECTROSCOPIC EVIDENCE FOR SECONDARY STRUCTURE IN THE RNA COFACTOR OF NATIVE HOLOENZYME. George D. Cimino* and John Clark Sutherland, Biology Dept., Brookhaven National Laboratory, Upton, NY 11973. *Graduate Student from the Dept. of Molecular Biology and Biochemistry, University of California, Irvine, CA 92664

Photoreactivating enzymes monomerize cyclobutane pyrimidine dimers in DNA in a light (300-450nm) requiring reaction. The enzyme from E. coli is a single polypeptide with a small RNA cofactor, the role of which is unknown. To investigate the conformation of the RNA within the enzyme, we have measured a thermal melting profile of the RNA by monitoring the absorption at 260nm and correcting for scattering changes as a function of temperature. Absorption melting transitions are observed at 14°C, 25°C and 40°C. We also measured the circular dichroism (CD) of the RNA at λ=270nm and λ=300nm as a function of increasing temperature (4°C to 70°C). The melting transition at 14°C is accompanied by a decrease in the amplitudes of both CD peaks at 270nm and 300nm. Melting transitions occuring at higher temperatures are seen only in the CD peak at 270nm. These data are consistent with a model of the E. coli photoreactivating enzyme in which the RNA cofactor is partially double stranded. The double stranded segment of the RNA melts at 14°C under our experimental conditions (0.01M ionic strength, pH=7.0). To estimate the fraction of double stranded RNA, we fit the absorption difference spectrum between denatured and native enzyme to a linear combination of basis spectra for the melting of A:U and G:C base pairs. This analysis yields two base pairs per enzyme molecule; a single A:U and a single G:C.

(Supported by Department of Energy and RCDA from the National Cancer Institute [CA00465] to JCS).

W-AM-A2 PYRIMIDINE DIMER RATIOS IN MAMMALIAN DNA AS A FUNCTION OF IRRADIATING WAVELENGTH. R. B. Setlow and Eleanor Grist. Brookhaven National Laboratory, Upton, NY 11973.

Important indications that DNA is the target for many of the deleterious effects of UV on mammalian cells are the similarities between the action spectra and the yield of pyrimidine dimers as a function of wavelength and that if cells contain photoreactivating enzyme, the deleterious effects are photoreversible--a process specific for pyrimidine dimers. However, the action spectra do not coincide with the absorption spectrum of DNA, but compared to 265nm are high at 280-297nm and low at 313nm (1,2). A possible explanation for the differences might be in changes in relative yields of C=T versus T=T. We irradiated dThd-labeled Chinese hamster DNA in vitro and in vivo with wavelengths 265, 280, 289, 297 and 313nm and measured chromatographically the radioactivity in C=T and T=T after acid hydrolysis. There were no significant differences between the ratios of DNA irradiated in vivo and in vitro. At low doses the ratios of T=T to C=T were 3.3-3.6 at 265 and 280nm; 2.9-3.0 at 289 and 297nm; and 3.0 at 313nm. Hence a large change in T=T/C=T is not the explanation for the differences between action and absorption spectra. (Research supported by the U.S. Department of Energy.)

1. G. J. Kantor, J. C. Sutherland, and R. B. Setlow, Photochem. Photobiol. 31, 459 (1980).
2. B. S. Rosenstein and R. B. Setlow, Photochem. Photobiol. 32, 361 (1980).

W-AM-A3 ULTRAVIOLET CROSS SECTIONS FOR PRE-MUTAGENIC AND ERROR-PRONE REPAIR INDUCTION IN E. COLI, AT FIVE WAVELENGTHS. D. J. Fluke, E. C. Pollard, and Deno Kazanis. Dept. of Zoology, Duke University, Durham, NC 27706.

Leucine revertant mutagenesis in E. coli WU3610.89, a uvr B/r strain, is known from other work to involve primarily a suppressor mutation and to exhibit three different modes of response by magnitude of exposure. The revertant per survivor ratio (R/S) shows two-photon response at low UV exposures, linear (or less) at higher exposures, and a higher order response at largest exposures. Our results at five UV wavelengths from 234.5 to 313 nm can be represented reasonably by the following relation:

$$R/S = k_1 D(1 - \exp(-k_2 D)) + (k_4 D)^n.$$

Cross sections k_1 and k_2, for pre-mutagenic damage and error-prone repair induction respectively, show wavelength dependence concordant with DNA absorption and differ in magnitude by about 300,000. Quantum efficiencies can be 10^{-4} for k_2 in relation to one E. coli genome and for k_1 in relation to 10 to 15 base pairs. It is suggested that the latter number relates to the specific sites for suppressor mutation, and that the whole genome may be the target for error-prone repair induction. The k_4 cross section is roughly DNA-indicative and similar to k_1 in magnitude. Its exponent, n, is closest to 4, averaging over the five wavelengths. It can also be remarked that a possible cross section for UV-induced decline of induced error-prone repair (k_3) is now indicated to be nil. (This work has been assisted by Mr. John K. Douglass, by Mr. Steven M. Nolte, and by D.O.E. Contract No. DE-AS05-76EV03631).

W-AM-A4 NEAR UV MUTATION OF TRANSFORMING DNA. E. Cabrera-Juarez and J. K. Setlow, Brookhaven National Laboratory, Upton, NY 11973.

We previously observed that near UV radiation is not a mutagen for Haemophilus influenzae cells in the presence or absence of oxygen, although we were able to mutagenize purified transforming DNA by such radiation. Three different hypotheses could account for these results: (1) premutational lesions induced by near UV in the DNA are repaired by the cells; (2) DNA inside the cells is protected against the formation of premutational lesions, and (3) lethal lesions are formed much more readily than premutational lesions, so that the mutagenized cells are nonviable. To test these hypotheses we irradiated streptomycin-resistant cells at 334 and 365 nm, and then lysed them and assayed the DNA for mutations and for the ability to transform sensitive cells to streptomycin resistance. Inactivation of transforming ability was similar to that observed in vitro with highly purified transforming DNA. The transforming DNA irradiated in vivo was mutated by radiation at both wavelengths, but not so efficiently as was purified transforming DNA. Neither incubation of the cells after irradiation and before lysis nor freezing and thawing the cells three times before irradiation significantly changed the amount of mutation. It is concluded that hypothesis (1) is not correct, since we find no evidence of repair of premutational lesions, and hypothesis (2) is not entirely correct, since the cellular milieu does not completely protect the DNA against mutation, whether the cells are initially viable or killed by freezing and thawing. Thus we favor the hypothesis that the lethal lesions for inactivation of cells are much more readily induced than the premutational lesions.

This research was carried out at the Brookhaven National Laboratory under the auspices of the U.S. Department of Energy, and partially supported by Project No. CBA-79 from the DIDET and a fellowship from the DEDICT-COFAA of the National Polytechnic Institute, Mexico.

W-AM-A5 INDUCED RADIORESISTANCE: RELATION TO INDUCED REPAIR. E.C.Pollard, D.J.Fluke and Deno Kazanis*,Zoology Department, Duke University, Durham, N.C. 27706.

Induced radioresistance (i.r.r.) in Escherichia coli is a phenomenon associated with induced (or S.O.S.)repair. It requires the recA and lexA genes to be functional. We suggest thati.r.r. is due to increased efficiency in the repair of damage requiring a second duplex to provide the information for repair. We term this "repair by molecular synapsis." By observing the separation between cells that divide normally after an inducing dose and those that divide less, we also separate sensitive and resistant cells. The fraction, f, of normally dividing and sensitive cells we take to be uninduced and, to a first approximation, 1-f to be induced. Comparing this last with the dose-yield curve for the recA gene product (p-recA) it can be seen that in the limit more p-recA is made than is needed for i.r.r. We further find that the diminution of f with dose is similar to the diminution of colony forming ability in $lexA^-$ cells. These are deficient in molecular synapsis repair. We suggest that both the killing of $lexA^-$ cells and the induction of wild type cells are due to an insult that requires molecular synapsis for repair.

Cells grown on lean medium can have only one genome per cell. Nevertheless, such cells show i.r.r. They also show septum inhibition, thus adding more genomes in the same envelope. This must also be a factor in i.r.r. We thus suggest that radiation damage to both strands of a duplex very close to one another causes activation of the recA gene product. This activated p-recA inactivates the lexA repressor and derepresses recA. The gene product of lexA causes septum inhibition; the gene product of recA facilitates molecular synapsis. Hence repair and resistance.

We acknowledge support from D.O.E. contract DE-AS05-76-EV03631.

W-AM-A6 DIRECT DETERMINATION OF INTACT DNA SURVIVAL CURVES BY VISCOELASTOMETRY. Christopher S. Lange, Dept. Rad. Oncology, SUNY Downstate Med. Ctr., Brooklyn, NY 11203.

The viscoelastic relaxation behavior of shear-stressed DNA in solution determines the size (from the terminal slope of the retardation curve) and the number concentration (from the intercept (Γ_{11}) of this slope with the time of ending the externally applied torque) of largest such molecules present. Thus, for an initially monodisperse, intact size, population of molecules (genomes), the change in Γ_{11} (corrected for shear-stress) with radiation dose yields a dose response curve for the survival of intact full-size molecules. Similarly, after post-irradiation incubation, an estimate of the completion rejoining rate can be obtained. Unlike the sucrose gradient method, where average breaks and rejoinings per molecule are seen, visco elastometry yields the rates of induction of the FIRST break/molecule and of restitution of INTACT molecules. These parameters are more likely to be of biological importance than the average breakage and rejoining rates. Using this method, the $_{DNA}D_{37}$ of intact T4c was found to be 474 ± 23 Gy while the $_{PFU}D_{37}$ was 410 ± 4.5 Gy. Thus for oxic irradiation, one double-strand break/genome yielded 86.5% of all lethal events, in agreement with Freifelder's (1965) sedimentation data. Based on these data, target theory predicts a $_{PFU}D_{37}$ of 1760 Gy for T7 which agrees well with Freifelder's 1750 Gy measured value. A test of the validity of the Kavenoff-Zimm L_1 equation will also be presented. This work was supported by DOE contracts # DE-AS02-76EV-03501 and DE-AC02-80EV-0503.

W-AM-A7 BINDING (DYNAMICS) OF ACRIDINE ORANGE AND PROFLAVINE TO DNA INVESTIGATED BY A NOVEL TRIPLET PROBE METHOD. N.E. Geacintov, T. Kolubaev, J. Waldmeyer and V. Kuzmin, Chemistry Department and Radiation and Solid State Lab., New York University, New York, N.Y. 10003.

Polynuclear aromatic dyes such as acridine orange (AO) and proflavine (PF), bind to DNA by a reversible, non-covalent mechanism. These dye-DNA complexes exhibit not only the usual prompt fluorescence (decay of excited singlet state S_1), but also delayed fluorescence which is due to thermal population of the S_1 state from the excited triplet state T_1 of the dye (1). The T_1 lifetime in de-oxygenated DNA solutions (pH 7, 25°C) increases strongly with increasing DNA concentration. The lifetime varies from τ_f=0.40 ms in the buffer solution without DNA, to a limiting value of $\tau_b \simeq 30$ ms for DNA concentrations exceeding 2×10^{-3}M (DNA phosphorous). Furthermore, regardless of the DNA concentration, the triplet decay profiles are strictly exponential indicating a rapid exchange of the dye between bound and unbound states. The observed lifetime τ varies with DNA concentration according to the expression

$$\tau = \frac{\tau_f + \tau_b\, K(DNA)}{1 + K(DNA)}$$

The binding constant is found to be $4000M^{-1}$ for AO and PF indicating that the delayed fluorescence originates from weakly bound sites, since the binding constants normally measured are larger than this value. The exchange rates between these weakly bound and unbound states is of the order of $10^4 s^{-1}$.

(1) T. Prusik and N.E. Geacintov, FEBS Lett. 71, 236 (1976).

W-AM-A8 SUPEROXIDE DISMUTASE (SOD) ACTIVITY IN SYRIAN HAMSTER EMBRYO (SHE) CELLS AND ITS ROLE IN OXYGEN TOXICITY. S. Lesko and S. Yang, Division of Biophysics, The Johns Hopkins University, Baltimore, Md. 21205.

Oxygen is universally toxic to living cells and only be developing special defense mechanisms can organisms survive the omnipresence of oxygen. There is evidence, mostly from studies with prokaryotes (I.Fridovich, Science 201, 873:1978), to indicate that superoxide (O_2^-) is an important agent in oxygen toxicity and that SOD provides an essential defense. In this investigation, SOD activity has been measured in two types of SHE fibroblasts, viz., BP6T, a tumorigenic line and SHE 21f Cl-2, a non-tumorigenic line. SOD was assayed spectrophotometrically be measuring its ability to inhibit O_2^--mediated autoxidation of pyrogallol at 420 nm. The 10,000 g sonicates of BP6T and SHE 21f Cl-2 cells contained 6.4 $\pm$ 0.6 and 3.6 $\pm$ 0.5 units of SOD activity per mg protein, respectively. The activity was inhibited 84% by 5mM KCN. Disc gel electrophoresis with 7.5% polyacrylamide revealed the presence of 3 bands of activity in the 10,000 g sonicates. Two very prominent faster moving bands migrated with the same mobility as pure bovine Cu-Zn SOD and did not appear when the gels were developed in the presence of 5nM KCN. A faint, slower moving band was not inhibited by KCN and is most likely Mn SOD. Treatment of BP6T cells with diethyldithiocarbamate (DDC), a copper chelator, for 1.5 hrs reduced the SOD activity to 1.3 $\pm$ 0.2 units per mg protein (80% inhibition). The activity gradually returned to normal after removal of the DDC and further growth in DDC-free medium (~22 hrs). BP6T cells treated with 3mM DDC are more sensitive to the cytotoxic action of oxygen. The surviving fraction was reduced to 37% by exposure of normal BP6T cells to 95% O_2 for 28 hrs or 70% O_2 for 35 hrs and DDC-treated cells to 95% O_2 for 10 hrs or 70% O_2 for 14 hrs. (Supported by NIH grant ES 01659 and DOE Contract DE-AC02-76-EVO-3280).

W-AM-A9 BROAD-BAND, TIME RESOLVED ATTEMPT TO MEASURE PHOTO-ASSISTED CHARGE TRANSFER Albert Chang and Robert Austin, Department of Physics, Princeton University

Theories of electron transfer in biological systems predict the presence of a charge transfer band whose extinction coefficient and wavelength absorption maximum contain valuable information about the physics of the charge transfer process. In a time-resolved Nd:YAG laser excitation experiment we were unable to verify the results of Potasek et al who claimed to observe a charge transfer band in the cytochrome c-iron hexacyanide system. The effort reported here utilizes a 1000 joule flash lamp in a highly efficient geometry in a broad band attempt to detect charge transfer bands. A discussion of the sensitivity of the apparatus and the relevance of our results to present theories of electron transfer will be made.

W-AM-A10 ENERGY TRANSFER IN SYSTEMS EXPOSED TO IONIZING RADIATION. E.S. Kempner, J.T. Harmon and C.J. Steer, NIAMDD, NIH, Bethesda, MD 20205.

Exposure of macromolecular systems to ionizing radiation results in deposition of massive amounts of energy. Each interaction involves the average transfer of 60 electron volts (~1500 kcal/mol) which must be rapidly dissipated. After irradiation of lyophilized or frozen samples of membranes or enzymes, the surviving biochemical activity was determined. Target analysis indicates that discrete transfers of large amounts of energy between polymer chains are rare. In order to destroy function (enzymatic activity, hormone binding, regulatory action) the initial ionization must occur within the same covalently-bound structure as that possessing the activity. Furthermore, the ionization can occur anywhere in that structure, implying significant energy transfer along the length of the polymer chain. Gel electrophoresis of irradiated proteins shows a progressive decrease in chain length with increasing radiation dose. These points will be illustrated by radiation inactivation studies of tryptophan synthetase, prothrombin and receptors for insulin, glucagon and asialoglycoproteins. Many examples of these phenomena are also observed in irradiated polyethylene, polystyrene and other plastic homopolymers and copolymers. Because of the large amount of energy involved, the dissipation will involve many different mechanisms. Extensive experimental evidence has already been provided for secondary electron emission, fluorescence, free radical formation, etc. In addition, the temperature dependence of radiation sensitivity has been found to be quantitatively similar in protein, DNA and plastics. This suggests that in the polymer backbone the relative motion of atoms affects the efficiency of this energy transfer.

W-AM-A11 **PICOSECOND PRIMARY PHOTOPROCESSES OF BILIRUBIN BOUND TO HUMAN SERUM ALBUMIN.** A. A. Lamola, B. I. Greene, and C. V. Shank, *Bell Laboratories, Murray Hill and Holmdel, New Jersey.*

The fluorescence quantum yield of bilirubin (BR) bound to its most affinitive site on human serum albumin (HSA) increases from values of the order of 0.001 near room temperature to about 0.5 at 77°K. The quantum yield for configurational ($Z \rightarrow E$) photoisomerization about the *meso* double bonds decreases from about 0.22 to less than 0.01 over the same temperature range in reciprocal relation to the fluorescence yield. The fluorescence lifetime of BR/HSA at 77°K, 2.7ns, indicated an excited state lifetime near room temperature of the order of 10ps. Absorption spectra recorded over the time range 2 to 100ps after excitation with a 0.4ps pulse of 307nm light revealed a transient with a lifetime of 19 ± 3ps at 22° and 35 ± 7ps at 2°C, which was assigned as the excited singlet state. No other transient was observed. BR undergoes the same photoisomerization reaction in chloroform solution. The excited state lifetime in chloroform, observed directly by picosecond spectroscopy, was 17 ± 7ps at 22°C.

From these and other data we conclude that configurational isomerization of BR is the predominant nonradiative pathway that competes with pigment fluorescence, that photoisomerization proceeds via a short-lived ($\ll$18ps) partially twisted excited singlet state intermediate, and that BR remains relatively unhindered with respect to photoisomerization when bound to HSA.

W-AM-A12 LIQUID XENON AS A SOLVENT FOR BIOLOGICAL MOLECULES. P. M. Rentzepis and D. C. Douglass. Bell Laboratories, Murray Hill, New Jersey 07974.

We show by means of infrared, UV and NMR spectroscopy that liquid xenon is a useful solvent for many chemical and biological molecules at modest pressures (58 atmos) near room temperature ($T < 16.6$°C) (critical point). The transparency of xenon from the vacuum UV through the infrared is a unique advantage compared to conventional solvents. Liquid xenon solutions may also be easily converted to a clear glass matrix below -118°C. The fluid solutions give promise as a medium for studies of biological and chemical structure and reaction while the low temperature glasses (i.e. 4 K) provide a means for studying spectra of biological or heat sensitive molecules that may not be vaporized for use in conventional matrix isolation techniques.

W-AM-B1 ELECTRON MICROSCOPY OF FIBRINOGEN AND OF THROMBIN-INDUCED FIBRIN OLIGOMERS. Robley C. Williams, Dept. of Molecular Biology, Univ. of Calif., Berkeley, CA 94720

Bovine fibrinogen (Miles) was examined after adsorption to carbon films, followed by rotary shadowing with tungsten or by negative staining with uranyl formate or acetate. Very lightly shadowed preparations showed the well-known features: an apparently symmetrical, elongated molecule with two terminal knobs and one at the center of symmetry. In addition, a rod-like structure connecting the knobs and about 4 nm across was distinctly evident. Molecules stained with either uranyl salt showed some heretofore unreported features: (a representational drawing of a well-preserved molecule in negative stain is shown below.) The main body appeared rod-like, about 4.0 nm across, and almost always moderately sigmoidal in shape. The handedness of this contour, as seen on the microscope viewing screen, was invariably that shown if the grid was positioned with its specimen side up. No mirror-images of the contour shown were ever seen. Some molecules showed a central "knot". The protuberances at the ends of the main body were oblong, 9.0 × 4.0 nm, when the fibrinogen was adsorbed to the specimen film while in ammonium formate solution (50 mM). But when 1-2 mM Ca^{2+} was added many cases were found in which each terminal protuberance was seen to consist of two spheres, about 3.5 nm across. The earliest observable events in thrombin-induced clot formation were studied. These showed end-to-end aggregations of fibrin monomers, most frequently combined with limited side-to-side binding to form short, bifilar arrays. Most notably, the side-to-side aggregation was always staggered, with the end protuberance of one molecule apparently bound to the central knot of its lateral neighbor. Supported by Research Grant PCM80-10650 from the National Science Foundation.

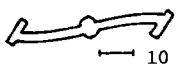

W-AM-B2 ELECTRON MICROSCOPY OF C1q FROM THE BULLFROG, RANA CATESBEIANA. H. S. Slayter, Sidney Farber Cancer Institute, Dept. of Physiology, Harvard Medical School, Boston, MA 02115; R. J. Alexander* and L. A. Steiner, Dept. of Biology, MIT, Cambridge, MA 02139.

The first component of complement, C1, is a calcium-dependent complex of 3 proteins. One of these, C1q, binds to antigen-antibody complexes and activates C1r, which in turn activates C1s, thereby triggering the classical complement cascade. Human C1q is a very unusual protein consisting of six triple-stranded subunits, each with a globular head that binds immunoglobulin and a collagen-like tail that binds C1r and C1s (Porter and Reid, Nature *275:* 699, 1978). When examined in the electron microscope, human C1q has a unique appearance with the six globular regions merging into extended strands that are collected into a central compact structure, the whole molecule having the appearance of a bunch of tulips. The strands and the central structure are composed of the collagen-like domains (Shelton *et al.*, Proc. Nat. Acad. Sci. U.S.A. *69:*65, 1972; Svehag *et al.*, Nature New Biol. *238:*117, 1972; Knobel *et al.*, Eur. J. Immunol. *5:*78, 1975; Brodsky-Doyle *et al.*, Biochem. J. *159:*279, 1976). We have recently obtained evidence that C1q from a lower vertebrate, the bullfrog *Rana catesbeiana*, resembles human C1q in function and in a number of structural features (Alexander and Steiner, J. Immunol. *124:*1418, 1980). We report here that the two proteins are also very similar when examined in the electron microscope. Like the human protein, bullfrog C1q appears to be composed of six peripheral globular regions connected by strands to a compact central structure that presumably consists of the terminal portions of the six strands. The dimensions of the human and bullfrog proteins are similar. Evidently, the major structural features of the C1q molecule have been preserved in evolution, at least since the appearance of the class Amphibia.

(Supported by NIH grants GM-14237, FR-05526, and AI-08054.)

W-AM-B3 ELECTRON MICROSCOPY OF CROSS-LINKED HUMAN COMPLEMENT COMPONENT C1. Candace J. Strang, Richard C. Siegel, Martin L. Phillips, Pak H. Poon and Verne Schumaker. Department of Chemistry and the Molecular Biology Institute, University of California, Los Angeles, 90024.

The C1 subcomponents were isolated by differential elution after serum C1 was bound to an IgG-Sepharose column. C1r and C1s were eluted from the column with EDTA in the presence of NPGB to prevent activation. Ca^{++} was added to reform the $C1r_2C1s_2$ tetramer, and it was further purified. Both the C1q and the $C1r_2C1s_2$ tetramer were shown to be pure by ultracentrifugation, SDS-PAGE, and electron microscopy. The $C1r_2C1s_2$ tetramer was less than 10% activated as shown by SDS-PAGE. C1q and $C1r_2C1s_2$ were reconstituted into C1 by mixing in the presence of Ca^{++} and at slight $C1r_2C1s_2$ molar excess. Cross-linking was performed at pH 6 using 0.1M 1-ethyl-3(3-dimethylaminopropyl) carbodiimide. After this treatment, the C1 remained associated as a 16s complex even in the presence of EDTA. Fields of C1 negatively stained with uranyl formate showed some easily discernible top and side views. The $C1r_2C1s_2$ tetramer appeared to be extensively folded among the six fibril arms of C1q. The C1q heads were visible and did not appear to be binding with the tetramer. The rod-like central portion of C1q was mostly visible as well. It was impossible to elucidate the $C1r_2C1s_2$ domain substructure which could easily be seen in electron micrographs of the elongated $C1r_2C1s_2$ tetramer alone, nor could it be determined whether the tetramer was positioned inside or outside the cage formed by the six C1q arms. We would like to thank the NSF for research grant PCM 77-17577.

W-AM-B4 BINDING OF PROTONS AND 2,3-DIPHOSPHOGLYCERATE TO OXY- AND DEOXY- HUMAN HEMOGLOBIN A_o. Mitchell K. Hobish and Dennis A. Powers (Intr. by Michael Beer). Mergenthaler Laboratory for Biology, The Johns Hopkins University, Baltimore, MD 21218.

The linkage relationships between the binding of protons, organic phosphate, and oxygen to hemoglobin are well-documented phenomena. The interactions provide a model for the investigation of linkage equilibria. The binding of 2,3-diphosphoglycerate (DPG) to oxy- and deoxy-hemoglobin as a function of pH was investigated using the rapid rate equilibrium dialysis technique of Colowick and Womack (1969) as modified by Greaney, Hobish, and Powers (1980). Contrary to reports by others, our results indicate that DPG binds to both oxy- and deoxy-hemoglobin. The apparent association constants are maximized at low pH values, indicating that DPG binding is facilitated by protons. The isotherm for binding to oxy- hemoglobin is shifted to lower pH values relative to deoxy-hemoglobin. Several thermodynamic schemes have been constructed. Computer simulations and data analysis have been used to test the relative fitness of these models. (Supported, in part, by NSF Grant DEB79-12216 and NIH Training Grant #HD00139).

W-AM-B5 ELECTROSTATIC INTERACTIONS IN BOVINE PANCREATIC TRYPSIN INHIBITOR. Keith L. March, Stephen H. Friend, David G. Maskalick and Frank R. N. Gurd, Department of Chemistry and Medical Science Program, Indiana University, Bloomington, IN 47405

The electrostatic interactions within bovine basic pancreatic trypsin inhibitor (BPTI) have been considered as a function of pH and ionic strength using the modified Tanford-Kirkwood theory. Such forces are dependent upon the geometry of the protein insofar as it determines not only separations between charge sites but also the degree of their burial within the low-dielectric medium of the protein. Alternative methods of inclusion of static burial parameters within the calculation have been evaluated. The possible implications of the delocalized nature of the charge systems of carboxylate and guanidinium moieties have been assessed, as have the consequences of varying certain of the intrinsic pK values invoked as model parameters. Experimental studies determining pK values for given ionizable groups largely via NMR titration analyses have been confirmed, and are well-predicted theoretically particularly with respect to the range of variation of values within each residue class. Electrostatic contributions to structural stability have been estimated. BPTI is shown to possess a spacial distribution of charged groups as well as solvent exposures which disfavors net destabilizations, reducing hindrance to the compact folding of such a highly-charged structure at physiological pH. Since a majority of the charged sites possess a comparatively great solvent exposure, a rather minor status is ascribed to most individual electrostatic interactions in this system, although a significant dipole is computed. The distribution of charges in BPTI points to their major role in maintaining solubility, or modulating interprotein interactions, rather than in serving specific stabilizing functions, as they also seem to in heme proteins thus far investigated. (Supported by PHS Grants HL-05556 and HL-14680 and by an Insurance Medical Research Fellowship to K.L.M.)

W-AM-B6 THE TRANSITION METAL BINDING SITE OF BLEOMYCIN. COBALT(III) BLEOMYCIN. M. Tsukayama, C. R. Randall, F. S. Santillo and J. C. Dabrowiak, Department of Chemistry, Syracuse University, Syracuse, New York 13210.

In an approach similar to that used to study the metal binding sites of certain metalloenzymes, we have used the labile and exchange inert cation pair, Co(II,III) to elucidate the structure of the metal binding site of bleomycin (BLM). Subjecting Co(III)BLM (produced by areobic oxidation of Co(II)BLM) to mild acid hydrolysis, followed by chromatography yielded a Co(III) complex containing a fragment of bleomycin. The fragment which was found to be missing the gulose, mannose and bithiazole moieties of the antibiotic was subsequently identified as pseudotetrapeptide-A of bleomycin. With the help of a variety of physical techniques, among them high resolution ^1H nmr (400 MHz), potentiometric titrations and conductance measurements, the structure of the Co(III) hydrolysis product was determined to be analogous to that of Cu(II) P-3A.[1] The structure of the binding site in light of the proposed metal mediated mechanism of action of bleomycin will also be discussed.

1. Y. Iitaka, H. Nakamura, T. Nakatani, Y. Muraoka, A. Fujii, T. Takita, and H. Umezawa, J. Antibiot., 31, 1070 (1978).

W-AM-B7 IN VITRO SUBSTITUTION OF INTRINSIC Zn WITH Co IN E. COLI RNA POLYMERASE. Dipankar Chatterji and Felicia Y.-H. Wu. State University of New York at Stony Brook, Stony Brook, New York 11794.

Earlier studies from our laboratory indicated that both holo($\alpha_2\beta\beta'\sigma$) and core($\alpha_2\beta\beta'$) RNA polymerases (RPases) contain 2 g-atoms of Zn per mol of enzyme. One Zn is located in the β' subunit while the other may be in the β subunit. In vivo substitution of Zn in holoenzyme with Co yielded the Co-Co RPase which is catalytically active but differs from the Zn-Zn RPase in promoter recognition and specific RNA chain initiation. To further elucidate the structural and functional role of the intrinsic Zn, we have performed in vitro substitution of Zn in core enzyme with Co by a sequential denaturation and reconstitution process in the presence of 10^{-5} M ^{57}Co. The substituted holoenzyme retaining 75% of the original enzyme activity has one Co and one Zn as proven by radioactivity determination and atomic absorption spectroscopy. The Co-Zn RPase was oxidized from Co(II) to Co(III) with H_2O_2 to freeze the Co in its perspective binding site and the enzyme subunits were separated by Affi-Gel Blue column chromatography in the presence of urea. SDS-gel electrophoretic analysis of the column fractions revealed that one Co is present in the β subunit. Comparison of the ^{1}H-NMR spectra of the substrate ATP in the absence and presence of Co-Zn RPase showed selective broadening of the H_8 peak and general broadening of the ribosyl protons by the enzyme-bound Co. The proton H_3' is more affected than proton H_2' favoring the proposed catalytic mechanism that the metal may coordinate with 3'-OH. Attempts to monitor the effect of enzyme-bound Co on the relaxation rates of water and substrate protons are in progress. The results will reveal the spatial relationship between the substrate and metal binding sites. (Supported in part by NIH Grant GM 28057).

W-AM-B8 THE EFFECT OF IONIC STRENGTH ON THE POLYMERIZATION OF TMV PROTEIN. Ragaa A. Shalaby and Max A. Lauffer, Biophysical Laboratory, Department of Biological Sciences, University of Pittsburgh, Pittsburgh, PA 15260.

An intermediate in the entropy-driven polymerization of TMV protein is the 20S component. The loading concentration, C, at which the first trace of 20S appears in the ultracentrifuge can be used to investigate the effect of temperature, pH and ionic strength, μ, on polymerization. When nonideality is related to salting-out and an electrical work term is added to the enthalpy, for a reaction in which n 4S particles combine with m H^+ ions to form 20S, $\log C = \text{constant} - \Delta S^*/(2.3R) + (\Delta H^* + \Delta We1^*)/(2.3\ RT) - K\acute{s}\ \mu + \zeta\ pH$. ΔS^*, ΔH^* and $\Delta We1^*$ are, respectively, the changes in entropy, enthalpy and electrical work per mole of 4S, $K\acute{s}$ is the salting-out constant and ζ is m/n. This equation has been derived for isodesmic polymerization, for an n-order process, and for a phase separation process, the only difference being in the anatomy of the constant. If $\Delta We1^*$ is $\phi q^2/\sqrt{\mu}$, where ϕ is a constant and q is the charge per monomer, at constant T and pH, $\log C = \text{constant} + (\phi q^2/RT)(1/\sqrt{\mu}) - K\acute{s}\ \mu$. Triplicate sedimentation experiments were carried out on three different TMV protein preparations at 15°C and pH 6.7 with values of μ between 0.03 and 0.15. Appearance of 20S was reversible. When $\log C$ was plotted against μ, the above equation could be fitted to the composite data. Values were found for $K\acute{s}$ and for $\phi q^2/2.3\ RT$ of the same order of magnitude as those obtained previously by a different method. The same method was used previously to investigate the effect of T at constant μ and pH. Previous data on the effect of pH at constant μ and T have been re-evaluated in terms of the above theory.

(Supported by NIH Grant GM 21619 and HRSF Grant W-1)

W-AM-B9 PROPERTIES OF VARIANT NITROGEN FIXING ENZYME FROM AZOTOBACTER VINELANDII MUTANT GROWN ON TUNGSTEN, G.D. Riddle, J.G. Simonson and H.D. Braymer, Department of Microbiology and B.J. Hales* Department of Chemistry, Louisiana State University, Baton Rouge, LA 70803

Experiments on a nitrogen fixing enzyme extracted from a mutant of *Azotobacter vinelandii* (ATCC 12837) grown on tungsten-containing medium show it to be different from the normal dinitrogenase enzyme complex found in wild-type strains grown on molybdenum. The difference, apparently, is in component 1 of this normal two component enzyme. For example, in the wild-type strain, component 1 is a molybdenum- and iron-containing protein possessing a unique esr spectrum with inflection points at g-factors of 4.3, 3.6 and 2.0. On the other hand, the new or altered component 1 extracted from the tungsten-grown mutant lacks the 3.6 inflection normally attributed to the molybdenum containing enzyme.

Preliminary results will be presented on acetylene reduction and dinitrogen fixation with this variant enzyme component along with esr, optical and CD spectra comparing it to the wild-type enzyme.

W-AM-B10 SEDIMENTATION EQUILIBRIUM AS A COLLIGATIVE PROPERTY OF MACROMOLECULAR SOLUTIONS. Charles L. Stevens. Dept. of Biological Sciences, Univ. of Pittsburgh, Pittsburgh, PA 15260.

Certain properties of solutions change in proportion to the concentration of solute. For osmotic pressure and light scattering of ideal solutions, the functions take the form below.

$$\pi/RT = (1/M)c \qquad \tau/H = Mc$$

Here, τ is turbidity, H is the light scattering factor, π is osmotic pressure and c is the weight concentration of solute. Molecular weight (M) and 1/M are the proportionality constants. For an ideal, two-component system in the ultracentrifuge, concentration at any position r is given in terms of that at some reference position r_o, as $c(r) = c(r_o) \exp [-M(1-\bar{v}\rho)\omega^2(r_o^2-r^2)/2RT]$. Define the exponential as X; subtracting both sides from $c(r_o)$ and rearranging, one gets $[c(r_o)-c(r)]/(1-X) = c(r_o)$. Thus, the left-hand side of this equation can be regarded as a colligative property with respect to sedimentation. We have called this function $\Xi(X)$. For ideal polymeric solutes, X is defined using the molecular weight of the monomer. It will be shown that, in the limit as $X \to 1$, the proportionality constant is the weight-average degree of polymerization, $\bar{N}_w$. Thus, the expression becomes

$$\Xi(1) = \bar{N}_w c(r_o)$$

For osmotic pressure and light scattering of ideal polymers, the analogous equations are

$$\pi/RT = (1/\bar{M}_n)c \qquad \tau/H = \bar{M}_w c$$

showing more clearly the similarities of the three equations and the fundamental character of the $\Xi(X)$ function. The explicit form of $\Xi(X)$ will be given for several systems and its evaluation will be discussed Supported by NIH Grant GM 22558.

W-AM-B11 IDENTIFICATION OF HISTOLOGICALLY-DETERMINATE CANCERS BY 2-DIMENSIONAL ELECTROPHORESIS K.M. Anderson, J. Baranowski, S.G. Economou,[1] Departments of Medicine, Biochemistry and Surgery,[1] Rush Medical College, Chicago, Ill. 60612.

In order eventually to use the pattern of tissue proteins determined by 2-dimensional electrophoresis as an aid in identifying histologically indeterminate cancers, representative distributions of proteins from several identified human cancers have been examined. Proteins extracted from identified cancers were separated according to their isoelectric points and molecular weights, stained with Coomassie blue dye and their distributions compared. Although many proteins appear to be represented in most samples, significant differences in the distribution of others are present. These "difference patterns" may characterize particular cancers. "Noise" due to red blood cells and plasma can be identified. Comparing the qualitative content of proteins in histologically identified cancers should provide a basis for determining the origin, based on the residual homologies with identified cancers arising from comparable tissue "stem" cells of histologically undifferentiated cancers for which no definitive pathological diagnosis presently can be made. In other words, the hypothesis being tested is that even in cancers, biochemical ontogeny will recapitulate phylogeny, albeit in a less organized manner. Use of 2-dimensional polyacrylamide gel electrophoresis to identify the origin of histologically indeterminate cancers will require the collection of a "catalogue" of representative protein profiles from histologically identified primary and metastatic cancer of diverse origin, and eventually, analysis by photoelectrical scanning and digital analysis of their similarities and differences. (Supported by NCI CA-22246).

W-AM-C1 REGULATION OF ACTIN-ACTIVATED ATPASE ACTIVITY OF ARTERIAL MYOSIN. Samuel Chacko and Arline Rosenfeld. Department of Pathobiology, University of Pennsylvania, School of Veterinary Medicine, Philadelphia, PA 19104 (Introduced by Joel Rosenbloom)

Actomyosin isolated from swine arterial muscle contains the endogenous light chain kinase and phosphatase. Myosin is separated from other proteins by gel filtration on Sepharose 4B agarose column. The amount of phosphate covalently bound to the 20,000 dalton light chains of purified myosin is controlled by phosphorylation or dephosphorylation using the endogenous enzymes prior to column purification. The purified myosin serves as substrates for exogenously added light chain kinase and phosphatase but the myosin itself is free of the activities for both enzymes. The ATPase activity of myosin is activated by actin only when the 20,000 dalton light chain is phosphorylated. The level of activation correlates with the amount of phosphate bound to the light chain. The maximum activation by pure actin is observed when the molar ratio of myosin to actin is 1:20. The activation is dependent on the amount of phosphate bound to the myosin light chain at all levels of actin concentrations. The actin-activated ATPase activity of arterial myosin is not dependent on Ca^{2+} concentration once the myosin is phosphorylated, and is free of kinase and phosphatase activity. The highest level of activation is observed when the myosin is fully phosphorylated and the actin is complexed with tropomyosin at a molar ratio of 1:6 (Tm:A). The potentiation of actin-activated ATP hydrolysis by tropomyosin is not dependent on Ca^{2+}. These data indicate that the tropomyosin plays a major role in the actin-activated ATP hydrolysis by arterial smooth muscle myosin in the absence of other regulatory proteins. Supported by HL 22264 and HL 23779.

W-AM-C2 ISOLATION AND ENZYMATIC PROPERTIES OF MYOSIN LIGHT CHAIN KINASE FROM VASCULAR SMOOTH MUSCLE. J. DiSalvo, J. Miller, D. Blumenthal, & J.T. Stull (Intr. by M. Behbehani). Dept. Physiol. Univ. Cinn., Ohio & Dept. Pharmacol., Univ. Texas, HSCD.

Modulation of contractile activity in vascular smooth muscle (VSM) involves Ca^{++} dependent phosphorylation of the phosphorylatable myosin light chains (PLC). Since myosin light chain kinase (MLCK) from VSM has not been characterized we isolated the enzyme from bovine aortic muscularis (BAM) and determined some of its kinetic properties. More than 90% of extractable MLCK in skeletal muscle was solubilized after a single homogenization. In contrast, only 40% of extractable MLCK was solubilized after a single homogenization of BAM. Three additional consecutive homogenizations released respectively 30, 20, and 10% of the extractable activity. Parallel purification of MLCK from the first (H_1) and fourth (H_4) homogenization by ion exchange on DEAE-cellulose, $(NH_4)_2SO_4$ fractionation and affinity chromatography on calmodulin-sepharose and Affi-gel blue yielded a single protein of 120,000 daltons on SDS electrophoresis. MLCK from either H_1 or H_2 required Ca^{++} and calmodulin for activity and had similar pH-optima, Kms for ATP(100μM), Kms (118-129μM) and V_{max}s (27-30μmol ^{32}P/min/mg) for cardiac PLC suggesting that the same enzyme was isolated from H_1 and H_2. Further studies showed that the Km for skeletal muscle PLC was 88μM but V_{max} was only 0.6μmol ^{32}P/min/mg, whereas the Km for aortic PLC was markedly lower (10μM) and V_{max} was markedly greater (40μmol ^{32}P/min/mg). Results obtained with graded concentrations of Ca^{++} (2-100μM) and calmodulin (1-330nM) showed that $K_{Ca^{++}}$ (12μM) and K_{CM} (0.6nM) were similar to corresponding values obtained with skeletal muscle MLCK and that the activating moiety was Ca_4^{++}·calmodulin. These observations suggest that different MLCK isozymes exist in different types of muscle but that the mechanism of MLCK activation by Ca^{++} and calmodulin is similar.

W-AM-C3 PROTEIN PHOSPHORYLATION IN BARNACLE MUSCLE FIBERS. M. Bárány, S.R. Hager, E.E. Bittar and J. Nwoga*, Dept. Biochem., Univ. Il. Med. Ctr., Chicago, 60612 and Dept. Physiol., Univ. Wi., Madison, 53706

Single fibers dissected from barnacles (Balanus nubilus) were injected with carrier-free ^{32}P-orthophosphate. After 40 minutes the fibers were frozen and ^{32}P incorporation determined. The major phosphorylated protein migrated as a doublet (with molecular weights of 26,000 and 28,000) on SDS-urea gels. Two-dimensional gel electrophoresis also indicated that the major ^{32}P-incorporation takes place into two similar proteins. On the basis of analogy with experiments carried out in our laboratory, these two proteins probably are inhibitors of phosphoprotein phosphatase. Fractionation of ^{32}P-labeled barnacle muscle showed that the 26,000- and 28,000-dalton proteins are localized in the 251,800 x g supernatant fraction. Several other proteins were also found to be phosphorylated in ^{32}P-injected fibers; 40,000-, 50,000-, 100,000-, 120,000- and 150,000-160,000-daltons. If the barnacles were injected with aldosterone prior to injection of the ^{32}P into the muscle fibers, an overall increase in protein phosphorylation was found which ranged from 1.5 to 2-fold as compared to aldosterone-untreated barnacles. Injection of cAMP, cGMP, or GTP into the muscle fiber along with the ^{32}P, or depolarization with KCl did not reproduce the aldosterone effect. Virtually no ^{32}P-labeling of the phospholipids was found under the above conditions. However, if barnacle fibers were incubated with ^{32}P, instead of being injected, the phospholipids became labeled and the pattern of protein phosphorylation also differed from that of the injected fibers. (Supported by NS-12172 from NIH and MDA).

W-AM-C4 RABBIT MYOSIN LIGHT CHAINS: ISOELECTRIC FORMS: S. P. Scordilis and C. W. Mahoney, Dept. of Biological Sciences, Smith College, Northampton, Mass 01063.

Structural and functional studies have been carried out on myosin light chains from rabbit fast skeletal muscle (FSM), cardiac muscle (CM), and uterine muscle (UM). Two dimensional gel electrophoresis was carried out on the isolated light chains. The subscripts following the designation LC (light chains) are the apparent molecular weights (M_r) on the second SDS dimension of the gels. NP, P and pI stand for non-phosphorylated, phosphorylated, and isoelectric point respectively. These studies yielded the following data: FSM, LC_{25}pI 5.22 and 5.16, $LC_{18.5}$NP pI 4.91, P pI 4.84, LC_{16} pI 4.72; CM, LC_{27} pI 5.36 and 5.31, LC_{20}NP pI 5.09, P pI 5.04; UM, LC_{20}NP 5.14, P pI 5.09, LC_{15}pI 4.75.

It is apparent from these data that phosphorylation of the P-light chains of these myosins changes the isoelectric points of these proteins by about 0.05 pH units. Furthermore, it was unexpectedly found that the FSM-LC_{25} and CM-LC_{20} consist of two populations of light chains.

(Supported in part by Grants from the Muscular Dystrophy Association of America, Inc. and the Blakeslee Fund for Genetics Research to Smith College).

W-AM-C5 THE ROLE OF LIGHT CHAINS IN THE ATPASE ACTIVITY OF MYOSIN SUBFRAGMENT-1 ISOENZYMES. K. George and P. Dreizen. Biophysics Program and Department of Medicine, State University of New York Downstate Medical Center, Brooklyn, New York 11203.

The subfragment-1 isoenzymes, S-1 (LC1) and S-1 (LC3), which are produced by chymotryptic digestion of rabbit fast-twitch muscle myosin, have been reported by Weeds and associates (1975, 1977, 1979) to show significant differences between Vmax and Km for actin-activated ATPase, whereas myosin ATPase is the same for the two isoenzymes. The differences in actin-activated ATPase occur at KCl concentrations approaching zero; however, myosin ATPase has been measured only at higher KCl concentrations. We here report a systematic study of myosin ATPase of the two isoenzymes. Pure S-1 isoenzymes were obtained by a modification of the conventional chromatographic procedure, involving the use of KCl gradient. The two isoenzymes exhibit equivalent Ca-ATPase activity in both 0.5 M KCl and 30 mM KCl, at 25°C, pH 8.0, as previously reported. However, K/EDTA-ATPase is approximately 10% higher for S-1 (LC3) than S-1 (LC1) in 0.5 M KCl, and Ca-ATPase is approximately 35% greater for S-1 (LC3) than S-1 (LC1) in 5 mM KCl. These differences are not due to selective denaturation of either isoenzyme. Concomitant studies of actin-activated ATPase in 5 mM KCl indicate values of Vmax approximately 50% greater for S-1 (LC3) than S-1 (LC1), and values of Km approximately two-fold greater for S-1 (LC3) than S-1 (LC1). The differences in actin-activated ATPase of the two isoenzymes are greatly diminished at higher KCl concentrations, although prolonged storage may result in selective denaturation with apparent differences between the isoenzymes even at higher KCl concentrations. These results indicate that the two isoenzymes differ with respect to myosin ATPase as well as actin-activated ATPase at low KCl concentration, and imply that the essential light chains (LC1 and LC3) have a role in ATP catalysis, as well as in the interaction of myosin with actin.

W-AM-C6 PROTEIN PHOSPHORYLATION IN SLOW AND FAST CHICKEN MUSCLE. F.L. Homa*, M. Bárány and S.R. Hager, Dept. Biochem. Univ. IL. Med. Ctr., Chicago, 60612. (Intr. by Akira Ōmachi).

Comparative protein phosphorylation abilities of chicken latissimus dorsi muscles, slow anterior (ALD) and fast posterior (PLD), were investigated with intact muscles incubated in ^{32}P-containing physiological salt solution for 4 hours. Several proteins were found to be phosphorylated in both types of muscles. The only protein which showed a major difference in ^{32}P-phosphate incorporation between slow and fast muscles was localized to the 200,000 x g supernatant fraction. A heat soluble protein of 25,000 apparent molecular weight was essentially carrying all the label in this fraction of the ALD muscle. This protein was present in the same fraction of the PLD muscle but it was not labeled. The phosphorylated 25,000-dalton ALD protein was purified to such an extent that 100 µg of phosphoprotein migrated as a single radioactive band on SDS-urea gels. With the same purification procedure a 25,000-dalton heat soluble PLD protein was purified and amino acid analysis of the two pure proteins showed identical composition. Analysis of alkaline labile phosphate revealed that both the ALD and PLD proteins contain approximately one mole of phosphate per mole of protein, but only in the ALD will approximately half of the phosphate exchange in 4 hours with the terminal ^{32}P-labeled phosphate of ATP in the live muscle. The rate of incorporation of ^{32}P-phosphate into the ALD protein was not changed upon treatment of the intact muscle with isoproterenol, epinephrine, or insulin. Similarly, tetanic contraction of the muscle had no effect. The very low incorporation of ^{32}P into the PLD protein was not increased by any of these treatments. (Supported by NS-12712 from NIH).

W-AM-C7 COMPARATIVE STUDIES ON PROTEIN PHOSPHORYLATION IN ARTERIAL AND UTERINE SMOOTH MUSCLES. K. Bárány, R.A. Janis*, J.T. Barron*, M. Bárány, D.D. Doyle* and J.G. Sarmiento*. Univ. of Illinois Med. Ctr., Chicago, IL 60612 and Northwestern Univ. Med. Ctr., Chicago, 60611

Helical strips from porcine carotid arteries and myometrial strips from rat uteri were incubated in physiological salt solution containing ^{32}P-orthophosphate while mounted in muscle chambers for tension measurements. Phosphoprotein profiles of the two classes of smooth muscle were compared utilizing one- and two-dimensional gel electrophoresis. In arterial muscle the following molecular weight protein zones were labeled: 240 K, 200 K, 140 K, 125 K, 108 K, 93 K, 30 K, and the 20 K myosin light chain (LC). In uterus the same proteins as well as an additional 45 K-dalton protein were labeled. Resting arterial strips, under passive tension, contained 0.4-0.5 mole ^{32}P-P/mole LC, while resting but spontaneously contracting myometrial strips, freeze-clamped in the relaxed phase, also contained 0.4-0.5 mole ^{32}P-P/mole LC. Maximal contraction of arterial and myometrial strips phosphorylated the LC to 0.7-0.9 mole in both. Whereas EGTA or theophylline decreased the passive tension and the ^{32}P-P content of LC to 0.2-0.3 mole/mole in arterial muscle, similar treatment did not change the resting level of ^{32}P-P content of LC in uterus. Addition of EGTA, isoproterenol or lowering the temperature did, however, stop spontaneous myometrial contractions. Contracted arterial strips were relaxed by theophylline, and contracted uteri by isoproterenol, or 3-isobutyl-1-methylxanthine, and both classes of smooth muscle were also relaxed by inhibitors of calmodulin. Under these conditions, the LC was found to be dephosphorylated to the level of that in resting muscle. Re-addition of contractile agents resulted in maximal tension and maximal rephosphorylation of LC in both muscles. Thus, myosin light chain phosphorylation seems to be an integral part of the contraction cycle of arterial and uterine smooth muscles. (Supported by CHA, BRSG 79904 and NIH).

W-AM-C8 CHARACTERIZATION OF MYOSIN PHOSPHATASE I FROM SMOOTH MUSCLE. Mary D. Pato and Robert S. Adelstein, National Heart, Lung, and Blood Institute, NIH, Bethesda, Md. 20205

Myosin phosphatase I (MP-I) has a molecular weight of 165,000 as determined by sedimentation equilibrium and is composed of three subunits (M_r = 60,000; 55,000; 38,000) in equimolar ratios. Unlike MP-II which has also been purified from smooth muscle, MP-I is not activated by Mg^{2+} (Pato, M.D. and Adelstein R.S., J. Biol. Chem. 255, 6535-6538, 1980). In an effort to understand how MP-I might be regulated, the enzyme was characterized as follows: Using phosphorylated 20,000 dalton myosin light chains as substrate, MP-I was found to have a K_m = 9.5 μM and a V_{max} = 7.7 μmol/min/mg. Both products of dephosphorylation, (i.e., phosphate and the dephosphorylated light chain) act as competitive inhibitors. Other factors inhibiting MP-I activity include a high concentration of KCl (50% inhibition = 43mM), pyrophosphate (50% inhibition = 0.3 mM); ATP (1.0 mM); ADP (1.2 mM) and AMP (6.2 mM).

Preliminary experiments were carried out to determine which of the three subunits of MP-I might be the catalytic subunit for phosphorylated myosin and myosin kinase. MP-I was dissociated following freezing in 0.2 M β-mercaptoethanol and the 38,000 dalton subunit separated from the 60,000 and 55,000 dalton subunits by gel filtration. The isolated 38,000 dalton subunit of MP-I catalyzed the dephosphorylation of smooth muscle myosin previously phosphorylated with myosin kinase. Dephosphorylation resulted in a marked decrease in the actin-activated MgATPase activity of myosin. This subunit was relatively inactive in dephosphorylating myosin kinase that had been phosphorylated with cAMP-dependent protein kinase. On the other hand, the holoenzyme of MP-1 rapidly catalyzed dephosphorylation of myosin kinase resulting in an increase in kinase activity.

W-AM-C9 REVERSIBLE REGULATION OF THE ACTIN-ACTIVATED MgATPase ACTIVITY OF SMOOTH MUSCLE MYOSIN. Janes R. Sellers, Mary D. Pato and Robert S. Adelstein, NHLBI, Bethesda, Md. 20205

The 20,000 dalton light chain of smooth muscle myosin can be phosphorylated by a Ca^{2+}-calmodulin-dependent myosin kinase and dephosphorylated by smooth muscle myosin phosphatases. This phosphorylation-dephosphorylation is thought to play a major role in regulating the actin-activated MgATPase activity of smooth muscle myosin. We have investigated the effect of phosphorylation-dephosphorylation on the MgATPase activity of smooth muscle myosin using the following purified proteins: myosin or heavy meromyosin (HMM); myosin kinase purified on a calmodulin-Sepharose 4B column; myosin phosphatase purified on a thiophosphorylated myosin light chain-Sepharose 4B column; purified skeletal muscle actin. Myosin and actin were free of kinase and phosphatase activities.

Myosin	Phosphate Content (mol P_i/mol myosin)	Actin-activated MgATPase Activity (nmol/mg/min at 25°)
As isolated	0-0.1	6
Phosphorylated	2.0	70
Dephosphorylated	0	4
Rephosphorylated	1.8	78

Phosphorylation of myosin had no significant effect on MgATPase activity in the absence of actin, or on the K^+-EDTA ATPase activity measured at high ionic strength. Experiments with similar results were obtained using HMM in place of myosin. This reversible regulation of the actin-activated MgATPase activity of myosin suggests that phosphorylation alone is sufficient to play a major role in the regulation of smooth muscle contraction. It does not rule out the co-existence of other regulatory systems. (JRS is a fellow of Musc. Dyst. Assoc.).

W-AM-C10 PHOSPHORYLATION OF SMOOTH MUSCLE MYOSIN KINASE IN THE PRESENCE AND ABSENCE OF BOUND CALMODULIN BY cAMP-DEPENDENT PROTEIN KINASE. Mary Anne Conti and Robert S. Adelstein
National Heart, Lung, and Blood Institute, NIH, Bethesda, Md. 20205

Smooth muscle myosin light chain kinase, a calmodulin-dependent enzyme, binds one mole of calmodulin per mole of kinase in the presence of Ca^{2+}. This enzyme is a substrate for cAMP-dependent protein kinase whether or not calmodulin is bound, however, both the extent and effect of phosphorylation are affected by the binding of calmodulin. When myosin kinase is phosphorylated in the presence of bound calmodulin 0.5-0.9 mole of phosphate is incorporated per mole of myosin kinase. Extensive tryptic digestion of the phosphorylated kinase yields a single peptide containing phosphate. Phosphorylation in the presence of bound calmodulin has no effect on myosin kinase activity. In contrast, phosphorylation of myosin kinase in the absence of bound calmodulin results in the incorporation of 1.3-2.0 moles of phosphate per mole of kinase. Extensive tryptic digestion of this enzyme results in the identification of two phosphate containing peptides, one of which appears to be the same as that phosphorylated when calmodulin is bound. Phosphorylation of myosin kinase in the absence of bound calmodulin decreases myosin kinase activity. This decrease is due to a 10-20-fold decrease in the calmodulin concentration required for 50% activation of myosin kinase and a 36% decrease in the maximal rate of enzyme activity at infinite calmodulin concentration. This effect can be reversed by dephosphorylation of myosin kinase by smooth muscle myosin phosphatase I.

W-AM-C11 LOCATION OF REGULATORY LIGHT CHAINS IN SCALLOP MYOSIN. Paula Flicker, Theo Wallimann, Peter Vibert (intro. by C. Cohen), Graduate Program in Biophysics, Dept. of Biology & Rosenstiel Center, Brandeis University, Waltham, Ma. 02254.

Electron microscopy of individual scallop myosin molecules using rotary shadowing reveals the location of the regulatory light chains. The heads of intact myosin appear "pear-shaped": they are widest near the end remote from the tail and taper to a narrower "neck" near the junction with the tail. The heads of desensitized myosin (regulatory light chain removed) appear more globular often lacking a "neck" region. The shape of Ca-Mg S-1 appears similar to that of the head of intact myosin, whereas EDTA S-1 (lacking regulatory light chain) appears rounder. The dimensions of these S-1s are comparable to those of the myosin heads. Shadowed images also show that antibodies (Fab) specific for regulatory light chains bind preferentially to the "neck" region of intact heads at or near the junction with the tail. Fab specific for the "essential" (-SH) light chain appears to bind in the same region. These findings imply that the region of the myosin head near its junction with the tail may comprise parts of three polypeptide chains (the heavy chain and two light chains). Our structural studies confirm previous biochemical evidence which suggested that the "neck" region of the molecule may be a critical site in Ca^{++}-regulation.

Supported by grants (to C. Cohen & A.G. Szent-Györgyi) from NIH, NSF, and MDA. Peter Vibert is an Established Investigator of AHA; Theo Wallimann held a Fellowship from MDA.

W-AM-C12 PROXIMITY OF THE REGULATORY AND ESSENTIAL LIGHT CHAINS IN SCALLOP MYOSIN. Peter M. D. Hardwicke, Theo Wallimann & Andrew G. Szent-Györgyi, Dept. Biol., Brandeis U., Waltham, MA. 02254.

The thiol groups of the essential light chains of scallop myosin are protected by the regulatory light chains. Thiol groups are readily alkylated by iodoacetate (IAA) provided regulatory light chains had been previously removed by EDTA treatment at 23°C. About 1-2 thiol groups/essential light chain react overnight at 4°C with a 5-10 fold excess IAA over myosin-SH. Thiol groups of heavy chains, corresponding to a total of about two moles are also modified. Alkylation of the essential light chains but not of the heavy chains is reduced cca. 10 fold by regulatory light chains, i.e. in intact or reconsituted myosins. Dansyl chloride at pH 6.7 or 1,5 IAEDANS also react preferentially with essential light chains in the absence of regulatory light chains. EDTA/K, Ca and Mg-ATPase activities are not altered by the modification of the essential light chain thiol groups. Regulatory and essential light chains can be cross-linked with the bifunctional photosensitive reagent, N-hydroxy-succinimidyl-4-azidobenzoate (HSAB). Isolated regulatory light chains modified with 4-6 moles HSAB and recombined with myofibrils in the dark cross-link with essential light chains and heavy chains upon illumination. The presence of both regulatory and essential light chains are detected by specific antibodies at positions corresponding to dimers (35K), trimers (50K) and heavy chains cross-linked with light chains (220K). Myofibrils containing modified regulatory light chains retain ATPase activities and Ca sensitivity before but not after photolysis. These indications of proximity of the two light chain types in scallop myosin agree with structural studies (Flicker et al. this volume) and support the suggestion that the essential light chains are also components of myosin linked regulation (Wallimann & Szent-Györgyi, Biochemistry, in Press.) Supported by grants from NIH (GM14675) and MDA.

W-AM-D1 DIVALENT CATIONS, MOBILE GATING CHARGE AND FIXED SURFACE CHARGE IN SQUID AXON.

Wm. F. Gilly and Clay M. Armstrong. Dept. of Physiology, Univ. of PA, Phila., PA.

Effects of divalent cations on excitable membranes are conventionally explained in terms of the fixed surface charge theory. This holds that divalent cations neutralize negative external surface charge in the vicinity of ionic channels, thereby changing the electric field within the membrane and effectively hyperpolarizing the channels. The theory predicts that all parameters of channel gating (forward and reverse rate constants as well as equilibrium constant) should sense the same bias voltage, but these predictions have seldom been rigorously tested. We find that divalent cations of the IIb transition metal group -- Zn, Cd, Hg -- can markedly slow kinetics of channel opening, have a much smaller effect on the equilibrium constant, and show very little if any effect on the rate of channel closing. Thus, 30 mM $ZnCl_2$ leads to an apparent shift of 20-30 mV in Na channel ON kinetics, an ~5 mV shift in the g_{Na}-V relation, and no detectable effect on OFF kinetics. Na channel gating current is altered in a parallel manner. K channels are also affected in the same way, but at much lower concentrations; 2 mM $ZnCl_2$ is roughly equivalent to 30 mM on the g_{Na}.

We suggest that these divalent cations, and perhaps others, can interact with mobile gating charges of Na and K channels. Specifically, a negative charge is exposed at the membrane's outer surface when the channel is in the resting, closed configuration. This gating charge is driven inward by depolarization. The resting state can be electrostatically stabilized by a nearby divalent cation, and inward movement of gating charge is therefore hindered. Many transition metal ions are very polarizable and readily react with uncharged residues of proteins. In particular, the above IIb ions favor the imidazole nitrogen of histidine. Fixed negative surface charge need not be involved at all in the action of the group IIb divalent metal ions.

W-AM-D2 A POPULATION OF SLOWLY ACTIVATING Na CHANNELS AT LOW TEMPERATURE.

Donald R. Matteson and Clay M. Armstrong. Dept. Physiology, Univ. of PA, Phila. PA

We have examined the effects of temperature changes on Na currents and gating currents in squid axons. Temperature decreases in the range 12° to 1° C decreased peak Na current with a Q_{10} of more than 2. Steady state Na current was either unaffected by changes in temperature or increased slightly as the temperature went down. The steady state current was TTX sensitive and had the same reversal potential as peak current. After removal of inactivation by pronase treatment the steady state current had a Q_{10} of about 2.

At large positive voltages Na currents were sometimes found to have both a fast and a slow activation phase. The fast component activated and partially inactivated normally, but was followed by a slow current increase that lasted many milliseconds. Peak Na current amplitudes could be potentiated by delivering large positive prepulses, and this potentiation effect was more pronounced at low temperatures. After a prepulse the slow activation phase was eliminated. Gating currents were potentiated by prepulses to about the same extent as peak Na currents.

These results are consistent with the hypotheses that (1) there are two populations of Na channels; (a) rapidly activating channels which completely inactivate and (b) slowly activating channels which do not inactivate. (2) As temperature is lowered, some fast channels are converted to slow ones, possibly because of a phase transition in the membrane. (3) Slow channel activation is faster for approximately 100 ms after the termination of a large positive prepulse: the slow channels temporarily have rapid activation kinetics and contribute to peak Na current.

W-AM-D3 CRAYFISH GATING CURRENTS SUPPORT A COUPLED MODEL OF SODIUM ACTIVATION AND INACTIVATION.

R.P. Swenson, Jr., Dept. of Physiology, University of Pennsylvania, Philadelphia, PA

Non-linear charge movements associated with Na channel gating well-known in squid, *Myxicola*, and myelinated nerves have been measured in voltage clamped, internally perfused axons of the crayfish, *Procamburus clarki*.* After subtraction of linear capacitive and leakage currents using the standard P/4 technique, it was found that Q_{on} equalled Q_{off} for brief depolarizations ($\leq$ 0.2ms), suggesting a conservation of charge typical of capacitance elements. The sigmoidal Q-V curve saturated at potentials more positive than 0 mV verifying a finite number of polarizable charges, ~2000e-/um^2. The midpoint of the normalized Q-V curve was -35 to -40 mV. Charge movement correlated with sodium current in two regards: 1) the maximum Q_{on} increased when the fibers were held at more negative potentials commensurate with relief from slow inactivation, and 2) Q_{off} diminished as depolarizing pulse length was increased paralleling fast inactivation.

As a result of the rapid inactivation present in crayfish axons, calculations based on Hodgkin and Huxley's independent model of sodium channel gating predict crayfish axons should produce a readily visible inactivation charge movement. No evidence of an h gating current was observed. Rather, experiments support a coupled model of activation and inactivation. The rate of sodium current inactivation and gating charge immobilization was the same when the two were measured in several ways. Inactivation was measured from the falling phase of sodium currents, from the reduction in sodium tail currents, and with a double pulse procedure; immobilization was measured as Q_{off}/Q_{on} for a single pulse or by the reduction of Q_{on} with the double pulse procedure.

* Experiments were performed at 8°C with 1/3 normal Na with and without TTX outside the fiber and a Cs_3Citrate internal perfusate from holding potentials of -80 to -90 mV.

W-AM-D4 GATING CURRENT FROM CRAYFISH GIANT AXON. J.G. Starkus, B.D. Fellmeth and M.D. Rayner. Dept. of Physiol., Univ. of Hawaii, Hon., HI 96822.

Following suppression of the Na and K ionic currents with tetrodotoxin and 4-amino-pyridine, and following subtraction of leakage and linear capacity currents, gating current in the crayfish axon becomes clearly visible in both single sweep records and in records utilizing a 12-bit signal averager. Saturation of charge movement appears to occur near 0mV and -100 mV. Maximal gating current (Ig) occurs at a hold potential of -100 mV (Peak Ig may be as high as 500 $\mu A/cm^2$ for a 100 mV depolarizing step). Ig decreases substantially following lowering hold potential to -70 mV and is completely immobilized at -65 mV. At -70 mV hold potential recovery of both INa and Ig occurs by interposing a hyperpolarizing prepulse to -120 mV for 350 ms. Depolarizing prepulses reduce both INa and Ig, whereas recovery occurs by increasing the interpulse interval (between prepulse and test pulse). Inactivation of INa and low holding potential both affect Ig by immobilizing charge movement. Our results suggest that the large gating currents observed in crayfish axons can be accounted for in part by the faster sodium kinetics, and in part by a greater asymmetry charge per unit area. (Supported in part by BRSG Grant No. RR05599-13 and NIH Grant No. GM29263-01).

W-AM-D5 GATING CURRENTS IN THE FREQUENCY DOMAIN. J.M. Fernández*, R.E. Taylor, F. Bezanilla
Dept. of Physiology, UCLA, CA 90024; Biophysics, NINCDS, NIH, Bethesda, MD 20205.

The admittance of the membrane of squid giant axon under voltage clamp was studied in the absence of ionic conductances in the range of 0 to 10 KHz for membrane potential (V) between -120 mV and +70 mV. A 2 mV peak-to-peak Pseudo Random Binary Noise Signal was superimposed on either a variable command pulse (ca. 400 ms duration) from a given holding potential or a variable holding potential (HP). Standard P/4 procedure was used to study gating currents in the same axons. We found that the real part of the complex capacitance (C*) calculated as the imaginary part of the admittance divided by the angular frequency ($\omega=2\pi f$) is voltage as well as frequency dependent. For any given V, C* has a maximum as f approaches zero and decreases as f increases requiring at least two time constants to be fitted. $C^*(f\to 0)$ has an absolute maximum of about 1.5 $\mu F/cm^2$ approaching about .9 $\mu F/cm^2$ at f=3KHz. When V is varied with the holding potential, $C^*(f\to 0)$ as a function of V, is bell-shaped with a maximum at about V=-60mV and decreasing by about .15 $\mu F/cm^2$ for potentials of V=-120 mV or V=+10 mV. When HP=-70 and V is varied by pulsing, $C^*(f\to 0)$ still is a bell-shaped function of voltage with its maximum at -40 mV. However when HP=0 the maximum of C* occurs at about -70 mV. The shift in the maximum C* is in agreement with the shift of the charge (Q) vs. V curve observed in our experiments with regular P/4 procedure (see also, Bezanilla & Taylor, Biophys. J. 25:193a, 1979) when the HP is varied. A model with four states in which a charged gating particle can move within the field and interacts with another particle not affected by the field predicts the above results. At very positive potentials in which the gating charge is saturated, C* still decreases with increasing frequency showing that the membrane capacitance is lossy, this can be fitted with a distribution of time constants.
Supported by MDA, PHS AM25201 and E.I. duPont de Nemours & Co.

W-AM-D6 NO CAPACITANCE INCREASE IN SQUID AXON ADMITTANCE WHEN "INACTIVATION" OF "GATING CHARGE" IS INSIGNIFICANT. H.M. Fishman, L.E. Moore, D. Poussart, H.R. Leuchtag and J. Sanchez, Department of Physiology & Biophysics, University of Texas Medical Branch, Galveston, Texas 77550.

Previous measurements of squid axon admittance, $Y(j\omega)$, under "gating current" conditions showed no changes in $Y(j\omega)$ that could be interpreted as a membrane capacitance increase during step voltage-clamp depolarizations from a steady hyperpolarized holding potential (Fishman et al, 1977, B.J. 19:177). However, those $Y(j\omega)$ measurements were made 250 ms after step changes of potential, during which "gating charge" is presumed to have "inactivated". The present $Y(j\omega)$ measurements confirm the previous findings, but under conditions in which the possibility of significant "gating charge inactivation" during the measurements is very unlikely. $Y(j\omega)$ was measured by rapid transfer function analysis under two different conditions: (1) 4 ms after step changes to depolarized voltages from a 70 ms prepulse of -120 mV in the frequency range 125 Hz to 50 kHz and (2) 25 ms after step changes to depolarized voltages from a holding potential of -70 mV in the frequency range 5 to 2000 Hz and with Na conductance inactivation removed by internal perfusion with pronase. The fact that no apparent capacitance increase (to within 1%) is measured in the frequency range where a large increase is indicated in asymmetry current under these conditions must now be considered a serious difficulty in interpreting the asymmetry current as "gating current".

(Aided by NIH Grants NS-11764, NS-13778 and NS-13520.)

W-AM-D7 Effects of Local Anesthetics on Na and Gating Currents in Squid Axon Membranes. J.Z. Yeh and H. Vijverberg*. Dept. of Pharmacol., Northwestern Univ., Chicago, Il., and Dept. of Veterinary Pharmacol. and Toxicol., Univ. of Utrecht, Utrecht, Nederland.

QX-572 and QX-314, quaternary derivatives of local anesthetic lidocaine, exhibit resting and conditioned block of Na currents in many excitable membranes. In squid axons, QX-572 was found to block Na currents with the following characteristics which were not shared by QX-314: First, the resting block by QX-572 was enhanced by holding the membrane at less negative potentials. Second, the frequency-and voltage-dependent block of Na channels by QX-572 was independent of the intactness of Na inactivation mechanism, and third, the voltage dependence of contioned block was similar whether it was determined in 0, 33.3 or 100% normal Na sea water, suggesting that the direction of current flow had little effect on the voltage dependence measured. Gating current (Ig) was recorded in internally perfused and voltage clamped axons with P/4 method of Bezanilla and Armstrong (1975). In the presence of 200 μM QX-572, the rising phase of Ig became indiscernible and the declining phase was accelerated. The total charge movement associated transient ON Ig (Qon) was decreased to 40 and 25% of the control for step depolarization to +20mV from Eh= -80 and -70 mV, respectively. The transient ON Ig was completely suppressed when Eh= -60 mV. The OFF Ig upon returning to -70 mV was almost completely abolished. This is in sharp contrast to QX-314 which has little or no effect on the immobilization-resistent component of OFF gating currents (Cahalan and Almers, 1979). Thus, QX-572 affected all components of gating currents as slow inactivation did (Meves and Vogel, 1977). These differential effect on Ig between QX-572 and QX-314 is in general expected from their remarkable different action on Na currents. (Supported by GM 24866 and NS 14144).

W-AM-D8 CHANGES IN MICROVISCOSITY AFFECT SQUID AXON CHANNEL GATING. J.J. Shoukimas, R.J. French, P. Belamarich, M.S. Brodwick, D.C. Eaton. Lab. of Biophysics, NINCDS, MBL, Woods Hole, MA 02543; University of Texas Med. Br., Dept. Physiol. and Biophysics, Galveston, TX 77550.

Voltage clamped, perfused squid axons have been examined under conditions of altered, macroscopic solution viscosity. When sucrose was added internally or on both sides of the membrane sodium and potassium conductance showed a slowing of kinetics and decrease in peak or steady state amplitude. Addition of 1.5M sucrose internally increased the value of τ_m and τ_h (Hodgkin-Huxley model) for a pulse to +20mV by 1.29 and 1.99 respectively. $\bar{g}_{Na}$ was reduced to 0.43 of the control level. Addition of 1.5M sucrose on both sides of the membrane led to an increase in τ_m and τ_h by factors of 3.9 and 3.8 respectively while $\bar{g}_{Na}$ was reduced to 0.1 of the control value. Sucrose effects on sodium ionic currents are paralleled by effects on sodium gating currents. With 1M sucrose present internally total "on" charge movement was reduced by 26% while the time constant of the on gating current decay was increased by a factor of 1.9 (pulses to +120, +150, +180mV). Similar viscosity effects were seen for the potassium ionic currents. With 1M sucrose added to both sides of the membrane τ_n increased by a factor of 1.67 while g_K decreased to 0.25 of the control value when tested by a pulse to +100mV. In contrast, addition of 12.5% Ficoll (MW=400K) (macroscopic viscosity equivalent to 1.5M sucrose) to the internal solution had little effect on g_{Na} and addition to both sides of the axon led to a 1.35 fold increase in τ_m with no change in τ_h. Conductivity measurements showed that Ficoll had little effect on microscopic viscosity. This differential effect of sucrose and Ficoll suggests that changes in microscopic viscosity reflected by changes in ionic mobility, and water activity may have a direct effect on channel gating behavior.

W-AM-D9 SODIUM CHANNEL GATING CURRENTS IN FROG SKELETAL MUSCLE. Donald T. Campbell, Department of Physiology and Biophysics, University of Iowa, Iowa City, IA 52242.

Asymmetric charge movements have been studied in frog skeletal muscle using the Vaseline-gap voltage clamp method. Ionic currents were blocked by an external solution containing 1 μM TTX, 115 mM TEA Br, 5 CsCl and by cutting the ends of the fibers in 120 CsF. In agreement with Vergara and Cahalan (Biophys. J. 21:167a) two temporally distinct components of asymmetric current were resolved: 1) a fast current peaking in 30-120 μsecs with characteristics of Na channel gating current (I_g) (Armstrong and Bezanilla, J. Gen. Physiol. 63: 533); and 2) a smaller, much slower current with characteristics of the putative E-C coupling current (Chandler, et al., J. Physiol., 254:245). In a representative fiber, the total charge moved for a step to 0 mV from -90 mV, was 215 nC/cm^2 (28.1 nC/uF), of which 27.7 nC/cm^2 (3.62 nC/μF) was Na channel gating charge (Q_g) that moved in the first 1.5 msec.

Q_g was measured at 4°C for V=-150 to +60 mV. Peak Q_g averaged 25.8 nC/cm^2 (range, 13.1 to 37.7). The plot of Q_g vs V rises slowly from -150 to -75 mV (∿15% at -90 mV); rises steeply between -45 and -15 mV; and then saturates beyond 0 mV. Below -15 mV, the gating current rises in 30 to 50 μsecs and then decays exponentially with time constant of 200 to 400 μsecs. For steps beyond 0 mV an initial fast rise of current is usually followed by an additional ∿20 percent rise to a peak 50 to 70 μsecs later. For pulses shorter than 300 μsecs, Q_{off}/Q_{on} approaches unity. For longer pulses, charge immobilization occurs, with Q_{off}/Q_{on} dropping to about .3 in 1 msec (+30 mV) to 5 msec (-30 mV). In two experiments I_{Na}(tail) and I_g(off) were measured at -90 mV following 1.5 msec pulses to -30, 0 and +30 mV. The time constant of I_{Na}(tail) was between 1.5 and 2 times faster than I_g(off). Supported by MDA and NS 15400.

W-AM-D10 ASYMMETRIC CHANGES IN THE BIREFRINGENCE OF VOLTAGE CLAMPED INTERNALLY PERFUSED SQUID GIANT AXONS. David Landowne & Virginia Scruggs. University of Miami School of Medicine Miami, Florida 33101

Axon birefringence is the amount of light passing through an axon mounted at 45° between crossed polars. Depolarizing the membrane from -70 mV to 0 mV produces a decrease in axon birefringence by about one part in 10^4. A symmetrical hyperpolarizing pulse to -140 mV produces an asymmetrical increase in birefringence. For a depolarization the birefringence response is slower and smaller compared to the response to hyperpolarization.

Pairs of pulses were used to compare the birefringence response to a test pulse to 0 mV with and without sodium inactivation. Records with conditioning pulses to -140 or 0 mV were made to coincide at the start of the test pulse. After the first 100 microseconds the responses diverge. The response corresponding to inactivated sodium current (with the 0 mV conditioning pulse) has a smaller slope than the fully activated case.

These asymmetrical responses were also seen with symmetrical pulses beyond the sodium equilibrium potential and also in the presence of tetrodotoxin indicating they are not simple artifacts produced by the flow of sodium ions. Deteriorated axons which lost their sodium currents also lost their asymmetry of the birefringence response.

The data suggest the birefringence response is a measure of the molecular motion which underlies the asymmetric 'gating' current.

Supported by NIH grant NS 13789

W-AM-D11 STOCHASTIC FLUCTUATION THEORY OF MEMBRANE SENSITIVITY: RESULTANT CURRENT NOISE. Franklin F. Offner and C.R. Hill*, Technological Institute, Northwestern University, Evanston, IL 60201.

Ion channel gates opening and closing times as to be expected for molecular deformations or adsorbed cations (e.g. Ca^{++}), in the range from micro- to nanoseconds, combined with relaxation times for the electric field within the channel of the order of 10^{-5} to 10^{-4}sec, can result in membrane sensitivity far higher than predicted by the usual application of Boltzmann's principle, e.g. 270 Debye Units (Meves, J. Physiol. 243, 847 (1974)); (Offner, Biophys. J. 21, 84a (1978); Offner, J. Phys. Chem. 84, 2652 (1980)).

The current noise to be expected from this process has been computed using the fluctuation - dissipation theorem (D.K.C. MacDonald, "Noise and Fluctuation," John Wiley, 1962) and found to be consistent with that found experimentally. The assumption of stochastic gate closings orders of magnitude more rapid than Hodgkin-Huxley kinetics is very different from that of Hill and Chen (Biophys. J. 12, 948 (1972)) and similar analyses in which calculations of axon noise are based on gate dynamics following the H-H equations. In our theory the local electric field approximately follows the H-H equations, and the fractional -time open of the gates is determined by the local electric field.

Supported under USPHS Grant No. NS 08137.
*Now at Northern Illinois University, Normal, IL. 61761.

W-AM-D12 TNBS MODIFIES SURFACE CHARGES NEAR SODIUM CHANNELS. P. Pappone and M.D. Cahalan, Dept. of Physiology and Biophysics, University of California, Irvine, CA 92717.

We have examined the effects of the amino group reagent trinitrobenzene sulfonic acid (TNBS) on the sodium currents of voltage clamped bullfrog myelinated nerve and skeletal muscle fibers. TNBS is membrane impermeant and reacts rapidly and specifically with primary amino groups to form a neutral trinitrophenylated derivative. Externally applied TNBS shifts the voltage dependence of sodium current activation and inactivation to more hyperpolarized potentials. The reaction is complete within 2-3 min following application of 10 mM TNBS at pH's above 9. 10 mM TNBS caused a shift in the midpoint of the steady-state inactivation-voltage relation of the sodium current ($\bar{V}_h$) of -14 mV $\pm$ 1 mV ($\pm$ S.E. of mean, n = 11) in nerve fibers and -18 mV $\pm$ 1 mV (n = 8) in muscle fibers. The potential for half-maximal activation of the peak sodium current was shifted to a lesser extent, averaging -9 mV $\pm$ 2 mV (n = 9) in muscle fibers. External TNBS increased the rate of development of sodium current inactivation during depolarizing pulses to potentials in the threshold range, but had no effect on the completeness of inactivation. In muscle, the effects of TNBS are largely irreversible. $\bar{V}_h$ remains shifted for up to 50 min following washout of the reagent. In nerve, however, $\bar{V}_h$ returns to nearly its control value within a minute of removing TNBS after a short exposure to the reagent. A possible explanation of the difference in recovery in the two fiber types is that TNBS modifies a membrane component which is free to diffuse in the plane of the membrane. In myelinated nerve fibers, only the ~1 μm node of Ranvier is exposed to the reagent, and the diffusion of membrane components with the mobility of phospholipids in bilayers could occur over this distance with a half time of seconds. (Supported by NIH Grant NS14609 and a postdoctoral fellowship from the Muscular Dystrophy Association of America.)

W-AM-E1 LASER SCATTERING FLUCTUATIONS IN NON-BEATING RAT MYOCARDIUM RELATED TO SPONTANEOUS MYOPLASMIC CALCIUM OSCILLATIONS. Michael D. Stern, Arthur A. Kort, Gopal M. Bhatnagar, and Edward G. Lakatta, Gerontology Research Center, NIA and the Johns Hopkins Medical Institutions, Baltimore, MD (Intr. by. Mordecai P. Blaustein).

In passing through non-beating rat cardiac muscle, a laser beam is modulated, giving rise to intensity fluctuations in the scattered light (SLIF); both resting force and the frequency of SLIF are Ca^{2+}-dependent (Science 207: 1369, 1980). To determine whether SLIF reflect an intrinsic property of activated myofilaments, we quantitated them by photon-counting autocorrelation, both in right ventricular papillary muscles skinned with Triton X100 (1%) and in muscles with intact membrances under conditions that alter cellular Ca^{2+} fluxes. In skinned muscles activated over a full range of $[Ca^{2+}]$, no SLIF were observed. In intact muscles, the frequency of SLIF was markedly enhanced by substituting K^+, Li^+ or sucrose for Na^+ in the bathing fluid. Caffeine (8 mM or greater) abolished SLIF. These features suggest that SLIF are not an intrinsic property of Ca^{2+}-activated myofilaments but rather reflect oscillations of $[Ca^{2+}]$ in the myofilament space of the type attributed to Ca^{2+}-dependent Ca^{2+} release from SR (J. Physiol. 249: 469, 1975). A statistical model assuming periodic asynchronous contractions of cells predicts both the features of the scattered light spectrum and the occurrence of Ca^{2+}-dependent resting force, and in addition, predicts post-twitch "hyperrelaxation" and periodic aftercontractions observed in rat muscle routinely and in other species during Ca^{2+} loading. Phase contrast microscopy and cinematography revealed cellular motions which are enhanced by Na^+ removal and abolished by caffeine simultaneously with the changes in SLIF. We conclude that SLIF are caused by spontaneous cellular oscillations occuring in intact rat myocardium and, by inference, that "resting" myoplasmic $[Ca^{2+}]$ in individual cells is not in a steady state.

W-AM-E2 SARCOPLASMIC Ca ION ACTIVITY IN CANINE CARDIAC PURKINJE FIBERS MEASURED WITH Ca^{2+}-SELECTIVE MICROELECTRODES. C.O. Lee and M.R. Dagostino*. Department of Physiology, Cornell University Medical College, New York, N.Y. 10021

Ca^{2+}-selective microelectrodes (tip diameter of about 1 μm) made employing the neutral ligand (W. Simon) were calibrated with the following solution: 10^{-3}, $10^{-4}$and 10^{-5}M Ca^{2+} solutions without EGTA (Sol. I); 10^{-5}, 10^{-6}, 10^{-7} and 10^{-8}M Ca^{2+} solutions with EGTA using Schwarzenbach's apparent stability constant, 4.83×10^6 M^{-1} (Sol. II), and Allen and Blinks' constant, 2.5×10^6 M^{-1}(Sol. III). All the solutions had 150 mM K^+, 1 mM Mg^{2+} and a pH of 7.00. At Ca^{2+} concentrations $> 10^{-6}$M, the electrode calibration showed Nernstian slope (about 30 mV). The slopes between 10^{-6} and 10^{-7}M Ca^{2+} of Sol. II varied from one electrode to another, from 10 to 25 mV, while the slopes between 10^{-6} and 10^{-7}M Ca^{2+} of Sol. III varied from 7 to 15 mV. The slopes (5-10 mV) between 10^{-7} and 10^{-8}M Ca^{2+} of Sol. II were also greater than the slopes (3-7 m V) between 10^{-7} and 10^{-8}M Ca^{2+} of Sol. III. The electrode potentials measured at 10^{-5}M Ca^{2+} of Sol. I were closer to those at 10^{-5}M Ca^{2+} of Sol. III than to those at 10^{-5}M Ca^{2+} of Sol. II. This suggests that Allen and Blinks' constant is more likely to be closer to the true value. To determine sarcoplasmic Ca^{2+} activity (a^i_{Ca}) in the fibers, the potential of each electrode was plotted against Ca^{2+} activity in Sol. I, Sol. II and Sol. III (0.32 was used for the Ca^{2+} activity coefficient in the solutions). From the calibrations with Sol. II, the a^i_{Ca} in resting state was found to be 46±19 nM(S.D., n=6). From the calibrations with Sol. III, the a^i_{Ca} was found to be 86±53 nM(S.D., n=6). The difference between the two values are expected from the difference between the two apparent stability constants. Brief exposures (3-5 min) of spontaneously beating fibers to 10^{-6}M strophanthidin led to about 2-3 fold increase in a^i_{Ca}. (Supported by USPHS HL 21136).

W-AM-E3 CAN TRANSPORT OF CALCIUM AND DEVELOPMENT OF TENSION OCCUR IN SODIUM DEPLETED FROG VENTRICULAR MUSCLE? Teruyuki Yanagisawa, Leslie Tung, and Martin Morad. Department of Physiology, University of Pennsylvania, Philadelphia, PA, 19104.

Internal sodium concentration was reduced in frog ventricular strips (D=0,3-0,5mm) by bathing them either in $Tris^+$ or Li^+ Ringer's for 1-2 hours. In these solutions action potential markedly shortened, the time to peak of contraction increased, and the rate of relaxation slowed as muscle started to develop contracture tension. Following complete replacement of Na^+ in 50μM Ca^{2+}-containing solution, the ventricular strips generated transient contractures which lasted 10-20 min. One hour after complete relaxation of the "zero-Na^+" contractures, depolarizations of the preparation with 120 mM KCl produced transient contractures lasting 1-1.5 min. The KCl-induced contractures in Na^+-depleted strips were consistently and reproducibly measured for 2-3 hours. D600 (10^{-6}M) suppressed the KCl-induced contractures in Na^+-depleted strips. Elevation of Ca^{2+} to 1-3 mM not only produced elevated baseline tensions but also increased the amplitude of KCl-induced contractures. Voltage clamps using the single sucrose gap technique showed a qualitative change in the tension-voltage relationship in Na^+-depleted strips. The voltage-tension relation changed from a monotonically increasing relation between -40 to +60 mV to one which peaked around 0 mV and decreased back to baseline tension around +60 to +80 mV. The depolarization-induced peak tension in zero-Na^+ solutions was much larger than the tension generated at the same potential in normal Ringer's solution. The voltage-dependence of development of tension in Na^+-depleted strips seemed to be quite similar to that measured for the slow TTX-insensitive inward current. These results indicate that the frog ventricle can generate significant amounts of tension when $[Na]_i$ and $[Na]_o$ are maximally reduced, suggesting the presence of a Ca^{2+} transport system which does not require a significant transmembrane Na^+ gradient.

W-AM-E4 A PHOTOMETRIC METHOD FOR DETERMINING ACTIVE AND PASSIVE UPTAKE AND RELEASE OF Ca FROM SINGLE SKINNED FIBERS. G. M. Katz, C. Goblet, J. P. Reuben, Muscle Physiology Lab, Dept. Neurology, Columbia University, New York 10032.

Chemically skinned rabbit psoas fibers (60-110 μm dia.) threaded through capillary tubes (200-400 μm dia., 4 mm length) and subsequently mounted in an optical set up (dual wavelength recording) provides a means for monitoring Ca distribution between fiber and perfusing solutions containing Ca indicators. The fiber ends, folded back over the fire polished edges of the glass capillary, are held by sleeves of polyethylene tubing. The latter also forms part of a plumbing systemfor flow of solution through the capillary. The flow is controlled by a micrometer driven syringe. Light from a quartz iodide source is delivered to the capillary by a fiberglass bundle. Solutions containing Ca indicators are moved into the capillary preceded by an air bubble which marks exchange of the capillary solution. By limiting the recording field to 70 μm near the midportion of the capillary (either of the fiber or solution), the readout of calcium concentration (within less than 5 min) is not modified by longitudinal diffusion, i.e., a concentration space clamp is achieved. This procedure allows for a quantitative assay of Ca removed from, or delivered to the solution by the muscle fibers. Very large signals are generated when Ca sequestered by the SR (+Mg-ATP, pCa 6.6) is released upon removal of MgATP. However our initial study has focused on passive Ca uptake (binding) by fibers in rigor (-MgATP). These results will be compared to those obtained by conventional isotopic measurements. Supported by MDA and NIH.

W-AM-E5 REDUCTION OF THE SUCROSE-RINGER INTERDIFFUSION IN THE SUCROSE GAP TECHNIQUE BY CONTROLLED COMPRESSION OF THE EXTRACELLULAR SPACE. M. Suenson, Dept. of Biophysics, The Panum Institute, University of Copenhagen, DK-2200 Denmark, L. Cleemann, Department of Physiology, School of Dental Medicine, University of Pennsylvania, Philadelphia, Pa. 19104.

Frog ventricular strips (0.5-1.2 mm in diameter) were placed in a single sucrose gap chamber with three pools. The strip passed through holes in two rubber partitions which could be stretched producing variations in the diameter of the holes from 0.3 to 1.2 mm. With Ringer solution in all three pools the intracellular and extracellular conductances (g_i and g_e respectively) were estimated from measurements of the total resistance and extra- and intracellular action potentials. Compression reduced g_e 10 to 20 times to a value which was 50-100% of the nearly constant g_i. The rubber partitions were adjusted to produce different values of g_e at the two ends of the strip and the sucrose gap was established by admitting sucrose solution to the middle pool. The more constricted end had the lower threshold and the healthier action potential. With ^{14}C-sucrose in the middle pool the fluxes to the pools at the ends were monitored for ½ to 2 hours. The steady state flux consistently was smaller through the more compressed end of the strip. Finally the strip was frozen in the chamber and the longitudinal distribution was measured by counting the isotope contentof ½ mm thick slices. The parts of the strip outside the sucrose compartment had a ^{14}C-sucrose content which was up to 20 times smaller than expected if the sucrose had diffused through a uniform extracellular space. The measurements of g_e, the steady state ^{14}C-sucrose flux and the ^{14}C-sucrose distribution indicate that compression reduces the width of the extracellular diffusion pathway and minimizes the interdiffusion of Ringer and sucrose. (Supported by the Danish National Science Research Council and HL 24667).

W-AM-E6 WHITE NOISE ANALYSIS OF VOLTAGE DEPENDENT ION CONDUCTION IN VOLTAGE CLAMPED SKELETAL MUSCLE FIBERS. Lee E. Moore, Department of Physiology and Biophysics, University of Texas Medical Branch, Galveston, TX, U.S.A., 77550

A vaseline-gap voltage clamp of single skeletal muscle fibers combined with a "white" noise admittance technique showed that a moderate membrane depolarization, which activated the voltage-dependent ionic conductances, had pronounced effects on the complex admittance. A linear frequency analysis was done at different membrane potentials by superimposing a 1 mV noise source with the step clamp command signal. The effects of the specific ionic conductances were separated by ion substitution and by partially blocking the potassium conductance with tetraethylammonium ions. It is shown that the negative sodium conductance is reflected in the admittance by a decrease in the low frequency magnitude when the fibers are moderately depolarized. The analysis was done during a 1600 msec voltage clamp pulse, thus showing that the sodium system does not completely inactivate with long pulses. Larger depolarizations show an anti-resonance in the admittance, characteristic of voltage dependent ion conductance processes. The form of the magnitude and phase functions are shown to be entirely consistent with the general behavior of the linearized Hodgkin-Huxley equations, which can be represented as specific equivalent circuits for the kinetic phenomena.

This work was partially supported by NIH Grant NS-13520.

W-AM-E7 INTRACELLULAR POTASSIUM AND INWARD-GOING RECTIFICATION IN VOLTAGE-CLAMPED FROG VENTRICULAR MUSCLE. L. Cleemann, Department of Physiology, School of Dental Medicine, University of Pennsylvania, Philadelphia, Pennsylvania 19104. Intr. by M. Civan.

Strips of frog ventricular muscle are voltage-clamped using the single sucrose gap technique. ^{42}K is used to obtain a simultaneous record of the cellular K content. The strip is equilibrated for 3 hours after adding the isotope. A Geiger counter under the setup detects the β-radiation from the strip (0.1 mm^3) and the surrounding perfusion chamber (1 mm^3). The K content of the slowly exchangeable cellular compartment (ca. 10 nM) is obtained from the measured record by subtracting the K content of the rapidly exchangeable extracellular compartment (ca. 3 nM). The cellular K content is assumed to be roughly proportional to the intracellular K concentration (K_i). The cellular K content may be lowered up to 50% by lowering the extracellular K concentration (K_o) or by adding 10^{-4} M strophanthidin to the perfusate. Cellular loss of K is accompanied by a decrease in the rate of rapid repolarization of the action potential and an increase in the time constant of the resting membrane. Voltage-clamp experiments relate these changes to suppression of an inward rectifying K current. The mechanism for inward-going rectification is elucidated by comparing the effects of K_o and K_i. The membrane conductance at rest is proportional to $K_i^{1.7} \cdot K_o^{0.3}$ i.e. it is much more sensitive to K_i than to K_o. Current-voltage relations measured before and after changing K_o cross each other. This violation of the independence principle has suggested that extracellular K ions are required to open the rectifier channel. Decreasing the cellular K content decreases the outward membrane current at all membrane potentials by an amount which is consistent with the independence principle. This suggests that intracellular K ions pass through the rectifier channel without being involved in the gating process. (HL 24667).

W-AM-E8 RESPONSE OF CARDIAC PURKINJE FIBER E_M TO VARYING $(K)_o$ AND $(Cl)_o$ WITH AND WITHOUT OUABAIN. J. L. Walker and N. L. Shearin. Department of Physiology, College of Medicine, University of Utah, Salt Lake City, UT 84108

It has been reported (Walker, 1978) that the ouabain induced depolarization of sheep cardiac Purkinje fibers is not due to a decrease in intracellular K^+ activity, $a_i(K)$. We have extended this finding to canine cardiac Purkinje fibers. Under control conditions E_M and E_K were -99.4 mv and -102.0 mv respectively while during ouabain intoxication (2.5×10^{-8} M) E_M and E_K were -46.9 mv and -99.3 mv respectively. In an attempt to determine the cause of the depolarization, E_M was measured while either $a_o(K)$ or $a_o(Cl)$ was varied. Under control conditions the slope of E_M vs log $a_o(K)$ was 53.4 mv while during ouabain intoxication it decreased to 34.6 mv. The dependence of E_M on log $a_o(Cl)$ changed from the control value of -3.3 mv to -9.3 mv during ouabain intoxication. The implications of these observations as they relate to the depolarization of ouabain intoxication are discussed.

Supported by NIH grants HL 18053 and NS 07938

W-AM-E9 EFFECTS OF SODIUM PENTOBARBITAL ON FUNCTIONALLY SKINNED MYOCARDIAL CELLS FROM RABBITS. J.Y. Su, Dept. of Anesthesiology, Univ. of Wash., Seattle, WA 98195.

The mechanism(s) by which pentobarbital (PB) decreases myocardial contractility was studied. Functionally skinned myocardial cells prepared by homogenization (J. Appl. Physiol. 39:1052, 1975) of right ventricular papillary muscle from rabbits were used to study the effects of PB on Ca^{2+} activation of the contractile proteins (CP) and Ca^{2+} uptake and release from the sarcoplasmic reticulum (SR). The bathing solutions contained [Mg^{2+}], 1 (for CP), 0.1 (for SR); [K^+], 70; [$MgATP^{2-}$], 2; [creatine $phosphate^{2-}$], 15; [$EGTA_{total}$], 7 (for CP), 0.05 or 7 (for SR) (in mM); imidazole; major anion, propionate (for CP), methanesulfonate (for SR); and [Ca^{2+}], 10^{-9} to $10^{-3.8}$ M. Ionic strength was adjusted to 0.15 and pH 7.00 ± 0.02 at 23°C (±1).

Effects on the CP: The fiber bundle was activated with various Ca^{2+} concentrations and steady-state tension development was measured. PB (0.5-5 mM) decreased the maximal Ca^{2+}-activated tension by 5-20% and in general did not significantly change the [Ca^{2+}]-tension relationship, expressed the maximal tensions as 100%.

Effects on the SR: The fiber bundle was loaded with Ca^{2+} (uptake) and the Ca^{2+} was released from the SR with 25 mM caffeine and a tension transient was generated. The area of the tension transient was analyzed. PB (0.5-5mM) decreased Ca^{2+} uptake by 7-73% and Ca^{2+} release by 4-32% from the SR. The effects of PB on the above parameters were dose-dependent and the percentage decrease in Ca^{2+} uptake was comparable to that observed with isolated intact cardiac muscle preparations (Am. J. Physiol. 222:339, 1972). The results suggest that PB decreases myocardial contractility mainly by decreasing the Ca^{2+} uptake by the SR and in part by decreasing the maximal Ca^{2+}-activated tension and Ca^{2+} release from the SR. (Supported by NIH HL 20754).

W-AM-E10 IMPEDANCE OF SHEEP CARDIAC PURKINJE STRANDS. R.F. Valdiosera and B. Mendiola*. CINVESTAV-IPN. México 14, D. F. México.

The impedance of sheep cardiac Purkinje strands has been measured in the frequency range 1-10000 Hz using the methods developed by Valdiosera et al (1974). At frequencies above 100 Hz the effect of the resistance of the connective tissue sheath around the strand becomes important and must be taken into account. The effect of this resistance is more pronounced in larger strands with lower input impedances. Phase results of 24 Purkinje strands have been measured. The phase angle at 10000 Hz was around -45° in 14 strands and more negative than -45° in 10 of them. Serial transverse sections of each Purkinje strand were analyzed by light microscopic methods looking for branching of the main cell aggregate. These studies suggest that variability in the phase results may be caused by structural variability.
(Supported by research grant PNCB-1622 from CONACYT).
R. Valdiosera, C. Clausen, and R.S. Eisenberg (1974). Biophys. J. 14-295.

W-AM-Po1 INHIBITORS AS PROBES OF THE MECHANISM OF ACTION OF EPIDERMAL GROWTH FACTOR. Rolf R. Freter and Manjursi Das. Biochemistry and Biophysics, Univ. of Pennsylvania Sch. Med., Philadelphia, Pa. 19104

Epidermal growth factor (EGF), a mitogenic pol peptide of M_r 6045 interacts with responsive cells through high affinity surface receptors. Interaction of EGF with this receptor has been shown to lead to the intracellular generation of an activator of DNA replication. As with many other polypeptide ligands, binding of EFG to the surface receptor has been shown to be followed by endocytic uptake of the hormone-receptor complex leading to subswquent proteolytic degradation of both EGF and the receptor within lysosomes. Earlier studies had indicated that the phenomenon of EGF-induced receptor internalization may play an essential role in the induction of the message necessary for the mitogenic response. We are therefore interested in using various inhibitory compounds which block one or more of the steps in the cascade of cellular reactions that follow hormone-receptor binding, and in studying their effect on the induction of the mitogenic message and the earlier biological effects of EGF.

Among the various inhibitors tested, two have been found to be particularly effective. Chlorpromazine (.056mM) has been found to selectively inhibit degradation of EGF. Phenylglyoxal (1.2mM) is a potent inhibitor of internalisation of surface-bound EGF. Some early cellular responses to EGF have been shown to be inhibited by these compounds. This suggests the involvement of internalization/degradation of hormone/receptor in these message-transmission pathways.

[Supported by NIH Grants (AM-25724 and AM-25819) and a Research Career Development Award (AM-00693)]

W-AM-Po2 EFFECTS OF LIGHT AND cGMP ON CALCIUM MOVEMENTS IN ROD OUTER SEGMENT DISKS. J.S.George AND W.A.Hagins, LABORATORY OF CHEMICAL PHYSICS, NIAMDD, THE NATIONAL INSTITUTES OF HEALTH, BETHESDA, MD. 20205

Frog rod outer segments with a few mitochondria and nuclei were rapidly isolated from dark adapted retinas, broken by centrifugal packing and resuspended in 70 mM K Isethionate, 40 mM NaCl containing 5 mM ATP and GTP and 20 mM Creatine Phosphate. Rhodopsin concentrations in the suspensions were 15-60 μm. Ca++ activity was monitored with a miniature Ca++ sensitive electrode containing ETH 1001.

In darkness, Aca fell from >6 to 2-3 μM over 20 minutes. A light flash (1-10 photons/disk) usually caused an increase of 20-100 nm in suspension Aca, beginning with the flash and continuing 20-40 seconds. By calibrating Ca++ buffering of the medium by injection of known quantities of calcium, it is calculated that 1000-2000 Ca++ ions are released per absorbed photon. Preliminary experiments with similar disk suspensions incubated with 45Ca suggest that larger light flashes may cause 5-10% of the exchangeable calcium in rod disks to be released into the suspending medium.

Cyclic GMP,but not GMP, causes Aca in rod suspensions to decrease by 100-400 nM in 2-5 minutes by increasing the rate of Ca++ uptake by some component of the suspension.

W-AM-Po3 SODIUM-CALCIUM EXCHANGE AND THE KINETICS OF THE ROD RESPONSE. S. YOSHIKAMI AND W.A. HAGINS, LABORATORY OF CHEMICAL PHYSICS, NIAMDD, THE NATIONAL INSTITUTES OF HEALTH, BETHESDA, MD. 20205.

Intracellular release of calcium by light appears to control the dark current in retinal phototransduction. Does Ca^{++} extrusion by Na:Ca exchange affect the steady state dark current and the kinetics of the light response?

The dark current is fully suppressed by reducing the $[Na^+]_o$ from 136mM to 10mM in the presence of 1.36mM Ca, but not when the calcium is lowered to 0.1μM. The dark current stopped by the application of 40μM ouabain to the retina in the presence of 1,36mM Ca is restored in less than 10s upon the reduction of $[Ca^{++}]$ to 10μM.

When the rod membrane potential is suddenly reduced by increasing external $[K^+]$ from 2.5 to 25mM with a fluid jet, the kinetics of recovery of both the Ca^{++} efflux and the dark current from a test flash are slowed within 2s. These results suggest that Na:Ca exchange strongly shapes the kinetics of the light responses of retinal rods. A simple model in which the Na^+ dark current enters the outer segments on the same carrier that mediates Na:Ca exchange explains most of the observations.

W-AM-Po4 AN ELECTRON MICROPROBE STUDY OF CHANGES IN IONIC COMPOSITION OF RETINAL RODS. Margaret C. Foster and W.A. Hagins. Laboratory of Chemical Physics, NIAMDD, National Institutes of Health, Bethesda, Md. 20205.

After incubation in a Ringers containing 0.5 mM Ca++, live frog retinas were frozen by clamping between sapphire blocks at 77K. The frozen tissue was freeze dried at -76 to -60C and the rod layers were analyzed by electron-excited x-ray microanalysis in a scanning electron microscope. The EDTA complex of scandium was added to the incubating solutions to act as a marker for extracellular fluid.

Na, Mg, P, S, Cl, K, Ca, and Sc could be detected at concentrations large enough to analyse in the outer segment layer. The preparations were stable under a 100 pA, 20 kV electron beam for several hours.

Ouabain (.05 mM) caused rods to lose about 30% of their K and gain both Na and Cl. After 10 min. - a time sufficient to abolish the dark current in live frog retinas - the rods contained more than tenfold more K than did the bathing fluid. Thus the driving force for the dark current was still present, suggesting that the Na conductance of the plasma membrane was suppressed.

Exposure of the retinas to 1 min of white light that bleached most of their rhodopsin caused loss of about half of the 2mM Ca++ in the outer segment layer.

W-AM-Po5 TRACE ELEMENT ANALYSIS OF BOVINE RETINAL DISC MEMBRANES UTILIZING PARTICLE INDUCED X-RAY EMISSION. Larry D. McCormick, University of Florida, Gainsville, FL 32611*

Trace element content of bovine retinal disc membranes was determined using a new multi-elemental technique, particle induced X-ray emission (PIXE). PIXE samples were prepared from intact disc membranes obtained from previously frozen bovine retinas. The trace element content of each sample was related to the rhodopsin content using the sulfur content of rhodopsin. Since all detectable elements are determined simultaneously, a separate rhodopsin assay is not required. The amount of chlorine, calcium, iron, copper, and zinc per rhodopsin was .903 ± .455, .492 ± .153, .0243 ± .0075, .132 ± .060, and .0577 ± .010 respectively. Upper limits for manganese, molybdenum, and nickel were determined to be .007, .006, and .0333 per rhodopsin. Comparison of samples which had been previously exposed to light and samples which were maintained in the dark disclosed no significant differences in detected trace element content. This study demonstrates that PIXE has the potential to be a valuable analytical technique for numerous biological problems. It can be particularly useful for studies which require comparison of amounts of materials present in a sample. Examples of potential problems for PIXE analysis are protein content of membranes (if the protein contains a detectable element, e.g. sulfur), stoichiometry of a trace element and a protein, and changes in trace element or protein content.

*Present address: U.S. Bureau of Mines, Avondale, MD 20782

W-AM-Po6 RESOLUTION AND RECONSTITUTION OF BOVINE RETINAL OUTER SEGMENT 3',5'-CYCLIC-GMP PHOSPHODIESTERASE COMPLEX. Russell E. Kohnken, Deborah M. Eadie and David G. Mc Connell, Michigan State University Department of Biochemistry, E. Lansing, MI 48824. Mammalian cyclic nucleotide phosphodiesterases (CNPDE) are frequently multi-subunit enzyme complexes. Resolution of bovine retinal outer segment (ROS) PDE suggests that it too is a multi-subunit complex. Purification of the catalytic subunits (P) in the presence of β-mercaptoethanol (BME) and ethylenediaminetetraacetate (EDTA) destabilizes soluble PDE activity though the protein apparently remains intact. Purified P exhibits a single band on both SDS and native polyacrylamide gels with MW 170,000 by sucrose velocity and 250,000 by gel filtration. If purification is attempted in the absence of BME and EDTA, another component (G protein - a dimer with MWs 37,000 and 41,000)is incompletely resolved from P. SDS gels then show 3 bands, whereas the native gel has the same single band and the MW estimates are unchanged from the pure P values. The unresolved PG complex retains stable activity during purification by gel filtration or sucrose velocity.

In samples which retain some stable activity, 50-fold reactivation of GTP- and light-dependent PDE can be accomplished. Both membrane pellet and G protein are essential. Both P and G proteins apparently have deactivated forms which block reconstitution. Reconstituted activity is linear with respect to P and also G up to a 20-fold molar excess of P. Optimal GTP concentration is between 20 and 100 μM for both native and reconstituted activities. Unless all components are present and in an active form, PDE activity is inhibited. Research was supported in part by USPHS Grant RO1-EY01574 to DM.

W-AM-Po7 FURTHER EXAMINATION OF THE RESPONSE OF SKATE PHOTORECEPTORS TO EXTERNALLY APPLIED GTP AND ANALOGS. James W. Clack and David R. Pepperberg (Intr. by Burks Oakley II). Dept. of Biological Sciences, Purdue Univ., W. Lafayette, IN 47907.

We recently reported (Fed. Proc. 39:1815, 1980) that treatments of the strongly light-adapted, isolated skate retina with GTP and certain related compounds (4 mM) promote sustained decreases in the threshold of the (aspartate-isolated) PIII response associated with photoreceptor activity. Because nucleoside triphosphates and related substances exhibit (variable) affinity for Ca^{++}, we further examined whether the effects induced by these compounds are distinct from any effects linked merely to the chelation of Ca^{++} in solutions applied to the retina. Levels of Ca^{++}(free) in the test solutions were measured with the use of an ion selective electrode; Ca^{++}(free) in the standard, unsupplemented Ringer's solution was 2.5 mM.

(1) Treatment of the light-adapted retina with Ca^{++}-deficient Ringer's solution (Ca^{++}(free)=0.9 mM) induces only a transient decrease in photoreceptor threshold; by contrast (as previously reported), solutions containing 4 mM GTP (or 4 mM β,γ methylene GTP) + 0.9-1.2 mM Ca^{++}(free) induce permanent decreases of 0.7-1.3 log units. (2) At 0.2 mM, β,γ methylene GTP and β,γ imido GTP induce sustained threshold decreases of 0.4-0.9 log unit. (3) Solutions containing 4 mM GTP or 1 mM β,γ methylene GTP in the presence of 2.5 mM Ca^{++}(free) (readjusted by addition of $CaCl_2$) induce sustained threshold decreases of 0.5-0.8 log unit. (4) A solution containing 1 mM GMP, 1 mM pyrophosphate, and 2.5 mM Ca^{++} (free) exhibits relatively little activity (sustained threshold decrease $\leq$0.1 log unit). The threshold-lowering activities of GTP and certain analogs therefore appear not to arise merely by the chelation of Ca^{++} in the applied solutions. (Supported by NIH Grant EY-02103.)

W-AM-Po8 ACTIVATION OF BOVINE GTPase BY PHOTOINTERMEDIATES OF RHODOPSIN. R.D. Calhoon, T.G. Ebrey, and M. Tsuda, Department of Physiology and Biophysics, University of Illinois, Urbana, Illinois 61801 USA.

After light absorption, rhodopsin can activate a GTPase in bovine ROS. This GTPase as well as an inhibitor protein is required to activate the ROS phosphodiesterase. The conformational intermediate of rhodopsin which activates GTPase may be associated with one or more photointermediates. We are trying to block the photointermediate transitions of bovine rhodopsin in order to find which of them can activate the GTPase. In DMPC vesicles, the meta I→meta II transition is much slower below the phase transition of DMPC (24°C) than in native membrane but it is not much affected at 30°C. The activation of GTPase at 30° is the same whether initiated by bleaching rhodopsin in DMPC vesicles or by rhodopsin in disc membranes. At 4°C and 10°C activation by bleaching rhodopsin in disc membranes is unaffected. However, the GTPase is not activated by rhodopsin in DMPC vesicles at 4°C. The activation is reduced by half at 10°C. This experiment suggests that meta I cannot activate GTPase, but that meta II or meta III can. Hydroxylamine attacks meta II, so in the presence of hydroxylamine, meta III is not formed. GTPase activity in the light in the presence of rhodopsin is the same with or without hydroxylamine. Thus meta III does not appear to be necessary for activation of GTPase.

W-AM-Po9 LIGHT INDUCED METHYLATION OF ROD OUTER SEGMENT PROTEINS
Richard Swanson and Meredithe Applebury, Department of Biochemical Sciences, Princeton University, Princeton, New Jersey 08544

In the last few years it has become apparent that several protein activities in the vertebrate rod outer segment are activated by light. Among these are the cGMP phosphodiesterase, the guanyl nucleotide binding protein, and one (or more) kinase activities. In the course of our studies we have also found a light induced methylation of three bovine rod outer segment proteins. These methyl accepting proteins have apparent molecular weights (by SDS-PAGE) of approximately 21,000, 26,000, and 88,000. There is a small basal level of methylation in the dark. Methylation is seen in isolated rod outer segments as well as in intact retina. S-adenosyl-L-methionine is the methyl group donor in these reactions. The identities of the methyl accepting proteins and the possible functions of the methylation process are discussed.

W-AM-Po10 PHOTOACOUSTIC SPECTROSCOPY OF CATTLE VISUAL PIGMENT. François Boucher and Roger M. Leblanc. Groupe de recherche en biophysique, Université du Québec, Trois-Rivières Qué. Canada. G9A 5H7.

Among dissipative processes which could allow the excited rhodopsin's chromophore to return to ground state, internal conversion remains the most probable. Such non-radiative transitions can be directly probed by photoacoustic spectroscopy. We measured the photoacoustic spectra of cattle rhodopsin, rod outer segments and retina at temperature ranging from 77 K to 300 K. Rhodopsin, iso-, batho-, lumi- and metarhodopsin show photoacoustic signals amplitudes comparable to other non-fluorescent and non-photosensitive biological molecules, thus providing direct experimental evidence for the importance of the thermal decay in the early intermediates of rhodopsin's bleaching cycle. When measurements are performed on whole retinae, the spectra show, in addition to rhodopsin's band, photoacoustic signals arising from other cellular components. The amplitude of the non-rhodopsin photoacoustic signals depends on the depth probed into the sample (acoustic modulation frequency used). It reveals a layer by layer retinal spectrum.

Supported by the NSERC of Canada and the Ministry of Education of Quebec.

W-AM-Po11 OCTOPUS HYPSORHODOPSIN, Ajay Pande, Robert H. Callender, Physics Dept., City College of New York, N.Y., N.Y. 10031; M. Tsuda, Physics Dept., Sapporo Medical College, Sapporo 060, Japan and Thomas G. Ebrey, Dept. of Physiology and Biophysics, Univ. of Ill., Urbana, Ill. 61801.

Primary photochemical event in visual pigments is generally believed to be the formation of a red-shifted intermediate called bathorhodopsin. However, there are reports suggesting the formation of a blue-shifted intermediate, hypsorhodopsin, as a primary photochemical event around 4°K. Tsuda et al. (1) have recently shown, by their low temperature absorption studies that Octopus (Misudako, Paroctopus defleini) rhodopsin can be selectively enriched with the hypso intermediate in a photostationary state upon illumination with 530 nm light. Under these conditions we observe a dramatic increase in the intensity of the Raman line at 1564 cm^{-1} with a parallel increase in the 1664 cm^{-1} line. Since the 1664 cm^{-1} line moves to 1637 cm^{-1} upon deuteration, it must be the line corresponding to $C{=}NH^{+}$ vibration of the protonated Schiff base. Our preliminary studies thus indicate that hypsorhodopsin may be a protonated Schiff base. However, because of the blue shifted absorption spectrum of the hypsorhodopsin, it has generally been believed to be an unprotonated Schiff base. Our observations, therefore, raise the question regarding the origin of the blue shift in the absorption spectrum of hypsorhodopsin. Deuteration of octopus rhodopsin results in an alteration of the photostationary state composition as well. We are presently continuing these investigations of various photostationary states of known composition at several different temperatures on the one hand, and of the primary pigment and pure intermediates by rapid flow techniques, on the other.

(1) Tsuda, M., Tokunaga, F., Ebrey, T. G., Yeu, K. T., Marque, J. and Eisenstein, L. Nature, (in press).

W-AM-Po12 CONFORMATION OF THE RETINAL CHROMOPHORE IN BATHORHODOPSIN. Bo Curry, Gregory Eyring and Richard Mathies, Chemistry Dept., University of California, Berkeley, CA 94720

Bathorhodopsin, the first photochemical intermediate in vision, exhibits distinctive resonance Raman (RR) lines at 854, 875 and 922 cm^{-1}. We have used selective deuteration and normal coordinate analysis to assign these lines to hydrogen out-of-plane (HOOP) vibrations of $C_{14}H$, $C_{10}H$, and $HC_{11} = C_{12}H$, respectively (G. Eyring, B. Curry, R. Mathies, A. Broek and J. Lugtenburg, J.A.C.S., 102, 5390 (1980)). The large RR intensities of all three lines and the unusually low frequency for the $HC_{11} = C_{12}H$ vibration are not observed in model compounds, and thus are caused by perturbations of the chromophore by the protein. The RR intensities of the $C_{10}H$, $HC_{11} = C_{12}H$, and $C_{14}H$ HOOP vibrations indicate that the chromophore of bathorhodopsin is twisted differently in the ground and excited states between C_9 and C_{15}. Such differential twists can arise if the motion of the methyl group on C_{13} in the course of isomerization is impeded by a protein residue. We have computationally modeled this protein interaction by allowing the chromophore to relax to its minimum energy in the presence of a non-bonding barrier which holds the C_{13} methyl group out of plane. The anomalously low frequency of the $HC_{11} = C_{12}H$ HOOP vibration can be explained by the presence of a charged opsin residue near $C_{11} = C_{12}$, which may be mechanistically important in the isomerization pathway. This combination of non-bonding and electrostatic interactions with opsin is the minimum perturbation capable of explaining the RR spectrum of bathorhodopsin.

Supported by USPHS grant EY 02051

W-AM-Po13 THE KINETICS OF CONFORMATIONAL CHANGES IN A REGION OF THE RHODOPSIN MOLECULE AWAY FROM THE RETINYLIDENE BINDING SITE. A.S. Waggoner, P.L. Jenkins, J.P. Carpenter and R. Gupta. Chemistry Department, Amherst College, Amherst, MA 01002.

The reactive sulfhydryl group on the F1 region of cattle rhodopsin has been covalently labeled with a cyanine dye. The absorbance of this dye at 660nm is sensitive to conformational changes of rhodopsin that occur following a short and intense light flash. With disc membranes and digitonin extracts at 15°C, the kinetics of the conformational changes at the labeled site are similar to the kinetics of the meta rhodopsin I to meta rhodopsin II transition. On the other hand, octyl glucoside, ammonyx LO, Triton, cholate, and CTAB detergent solutions of rhodopsin at 15°C show strikingly different kinetics at the labeled site. Furthermore these conformational changes do not follow the kinetics of the Meta I to Meta II transition. The relevance and time scale of these conformational changes in connection with the enzyme cascade mechanism for visual excitation will be discussed.

W-AM-Po14 MODELING THE BIREFRINGENCE CHANGE IN ROD OUTER SEGMENTS ASSOCIATED WITH METARHODOPSIN II FORMATION. Michael W. Kaplan, Neurological Sciences Institute, Good Samaritan Hospital & Medical Center, Portland, Oregon 97210.

The birefringence (Δn) loss associated with metarhodopsin II (MII) formation in flash-bleached *Rana pipiens* retinal rod photoreceptor cells ($\delta(\Delta n)_{MII}$) has been studied using a microretardometer that concurrently measures Δn changes and forward light-scattering changes in single, osmotically intact rod outer segments (ROS). The static form Δn component was reduced by perfusing ROS with isotonic glycerol-containing solutions. The $\delta(\Delta n)_{MII}$ signal, normalized for the amount of rhodopsin bleached, is constant (0.0018 ±0.0005/absorbance unit) for perfusate refractive indices in the range n_p = 1.335 → 1.390 (0-40% glycerol). No light-scattering change (0.5% resolution) was detected for any of the n_p values used. ROS were modeled as two-dielectric and three-dielectric lamellar systems. Various putative structural perturbations leading to changes in the form Δn component were then tested to see if they could account for $\delta(\Delta n)_{MII}$. None of the attempted perturbations using the two-dielectric model could account for the experimental results. Using a three-dielectric model, however, changes in form Δn caused by disk volume shrinkage and concurrent cytoplasmic volume expansion were independent of n_p. Models involving changes in disk membrane refractive index were unsuccessful in predicting experimental results. The $\delta(\Delta n)_{MII}$ signal can therefore be either a change in form Δn caused by disk shrinkage, or a change in intrinsic Δn caused by reorientation of dielectrically anisotropic membrane components.
Supported by USPHS grant EY01779 and the Oregon Lions Sight and Hearing Foundation.

W-AM-Po15 FLUORESCENCE OF METARHODOPSIN IN CRAYFISH PHOTORECEPTORS. **Thomas W. Cronin and Timothy H. Goldsmith, Dept. of Biology, Yale University, New Haven, CT 06511.**

Photoreceptor microvilli (rhabdoms) were isolated from dark-adapted crayfish (Procambarus, Orconectes) and individual organelles studied on a microscope equipped for quantitative measurements of fluorescence. The rhabdoms are initially nonfluorescent, but become weakly fluorescent following exposure to light. Several lines of evidence suggest that this fluorescence originates from metarhodopsin:

i) The photogeneration of fluorescence proceeds with first-order kinetics, as does the photoconversion of rhodopsin to metarhodopsin. The rate constants for both processes are equal and are directly proportional to irradiance over the 30-fold range of intensities studied.

ii) In the rhabdoms the absorption spectrum of metarhodopsin is dependent on pH, shifting from 515nm at values of pH above 7.5 to 460nm at pH 1.9. The fluorescence excitation spectrum matches the absorption spectrum of metarhodopsin and shows the same dependence on pH. The fluorescence emission spectrum peaks at 670nm (pH 7.5) and 650nm (pH 1.9).

iii) If rhabdoms are photoequilibrated to long wavelength light, most of the rhodopsin is converted to metarhodopsin. If fluorescence is then excited with blue light, the fluorescence intensity falls with time as the proportion of metarhodopsin decreases to a new photosteady state.

W-AM-Po16 TWO-DIMENSIONAL CRYSTALS IN DETERGENT-EXTRACTED DISK MEMBRANES FROM FROG ROD OUTER SEGMENTS (ROS). B.L. Scott, D.R. McCaslin and J.M. Corless*. Depts. of Anatomy, Physiology and Ophthalmology, Duke Univ. Medical Center, Durham, NC 27710 USA.

Earlier observations of small 2-dimensional crystalline domains in the disk membranes of intact frog ROSs with freeze-fracture methods provided an impetus for efforts to produce more extensive arrays for low-dose image analysis. We have detergent-extracted purified photoreceptor disk membranes from Rana catesbeiana. Electron microscopic examination of suspensions stained with uranyl acetate reveals non-crystalline vesicular structures and crystalline areas, about 0.5μm in diameter, which have a distinctive "herring bone" appearance. Optical diffraction of the micrographs reveals an orthorhombic unit cell, approximately 5nm x 16nm (a x b), with mm symmetry in the diffraction pattern to a resolution of 2nm. Absence of odd-ordered reflections along the reciprocal unit cell axes suggests pgg plane group symmetry for the projection. We tentatively identify the protein component of these lattices to be rhodopsin. Optical and computer reconstructions of the projected structure reveal elongated protein dimers at the corners and center of the unit cell, and dense accumulations of stain, about 2-3nm in diameter, centered on the remaining four 2-fold axes. Each protein dimer measures 1.5 -2.0nm in width and 7 - 8 nm in length, with the longer axis forming an angle of $\pm$ 16 - 17° with the b-axis of the unit cell. The dimer has a slight but definite sigmoidal shape. Individual crystalline sheets are often observed to roll up or fold over, in which cases the angle between the fold line and the b-axis is 31-33°. Two-dimensional lattices have also been obtained from bovine ROS disk membranes. Supported by USPHS Grants RO1-EY01659 and KO4-EY-00016 to J.M.C., a Duke Univ. Graduate Fellowship to B.L.S., and a Dr. Chaim Weizmann Fellowship for Scientific Research to D.McC.

W-AM-Po17 PHOTOCHEMICAL REACTIONS OF DRIED PHOTORECEPTOR MEMBRANES AT 77 K. C.N. Rafferty & H. Shichi. Laboratory of Vision Research, National Eye Institute, NIH, Bethesda, MD 20205

Rod outer segment membranes from bovine retinas were dried to form thin films on glass plates. Dehydration of these films relative to room humidity (40 to 60%) induces a major hypsochromic shift of the α-band of rhodopsin from 498 to 390 nm, indicative of deprotonation of the Schiff base nitrogen [Rafferty, C.N. and Shichi, H., Photochem. Photobiol., in press, 1980]. On cooling dehydrated films to 77 K, the α-band of rhodopsin shifts from 390 to 410 nm. These films remain optically clear. Illumination of dehydrated films at 77 K with narrow band UV light (intensity maximum at 385 nm) induces a large photoreversible bathochromic shift of the α-band of rhodopsin to 460-480 nm, analogous in magnitude and direction to the changes observed on the formation of bathorhodopsin in aqueous preparations and hydrated films. We interpret these results as suggesting that a water molecule in the form of a hydronium ion, possibly stabilized by an adjacent anionic group of the protein, is the means by which the retinylidene Schiff base nitrogen is protonated in both rhodopsin and bathorhodopsin. Furthermore, the occurrence of large photochemically induced bathochromic shifts at 77 K which are independent of the state of hydration of the membrane suggests that a proton may be translocated in a region of the protein different from but next to the original Schiff base protonation site. By inference, a different side group (or groups) of the protein may be involved. According to this view, the 543 nm absorption maximum of bathorhodopsin is attributed both to protonation of the Schiff base nitrogen with a hydronium ion and to the localization nearby of an additional proton.

W-AM-Po18 THEORETICAL STUDY OF THE PHOTOISOMERIZATION RATE OF RHODOPSIN. T. Kakitani, A. Sarai and H. Kakitani, Department of Physiology and Biophysics, University of Illinois, Urbana, IL 61801.

The photoisomerization rate of rhodopsin R to bathorhodopsin B is theoretically investigated using the thermally barrierless common excited state C. For this, we present some evidence for the fact that the thermal equilibrium is almost attained before the non-radiative transition from the common state. We develop a general theory of the non-adiabatic multi-phonon decay process, including the interference effect among promoting modes. The non-adiabatic coupling parameter is evaluated using the self-consistent HMO theory. In the numerical calculations, we considered typical two types of the chromophores of R and B: torsion model and plane model. As a result, it is found that the transition rate from C to D which is a possible quasi-stable state around the top of the ground state energy surface is 10^{10} s^{-1} - 10^{12} s^{-1} for both the models, in agreement with the experimental result. The direct transition rates for C → B and C → R calculated by the torsion model are comparable with that of C → D. The large value of the transition rate in the case of the torsion model is due to the matching between the energy gap and the residual vibrational energy after the transition. The interference effect among promoting modes is considerable and important for the C → B and C → R transitions in which the conformational rearrangements accompanying the transition are large. As a conclusion it is theoretically demonstrated that the very fast photoisomerization of the chromophore of rhodopsin is possible when one considers the thermally barrierless common excited state which corresponds to an intermediate with twisting of the 11-12 double bond by 70°-90°.

W-AM-Po19 OUTWARD RECTIFICATION OF LIGHT INDUCED K^+ CURRENT IN SCALLOP PHOTORECEPTORS STUDIED WITH SINGLE ELECTRODE VOLTAGE CLAMP. M. Carter Cornwall and A. L. F. Gorman, Dept. of Physiology, Boston University School of Medicine, Boston, Mass. 02118

Single electrode voltage clamp and current clamp techniques were used to assess the behavior of the light induced current in distal photoreceptor cells in the retina of the bay scallop, Pecten irradians. Membrane currents during light and darkness were measured following step changes in the membrane voltage in the range between -20 mV and -90 mV during perfusion of the retina with solutions of different ionic composition. Our data indicate that a conductance increase, almost exclusively to K^+ ions, underlies the hyperpolarizing light response in these cells. The reversal potential of the light response is found to change by about 58 mV per 10 fold change in potassium concentration (between 5 mM and 100 mM). It is unaffected by complete substitution of Na^+ by choline and the complete removal of Ca^{2+} (with the addition of 2.0 mM La^{3+}). The light induced current displays a marked outward rectification (e-fold change in light induced membrane conductance / 25 mV change in membrane potential) as the membrane potential is shifted from values more negative than to those more positive than the reversal potential. The solution in which these measurements were made was free of Na^+ and Ca^{2+} and contained 2.0 mM La^{3+} suggesting that this rectification is a property of the light sensitive K^+ channel alone. The voltage dependence of the light induced conductance-voltage relation can be prediced by a model which incorporates a channel with a single energy barrier located near the external side of the membrane. Supported by NIH grant EY01157

W-AM-Po20 SYSTEM IDENTIFICATION OF *PHYCOMYCES* LIGHT RESPONSE CHANNEL. E.D. Lipson, R.C. Poe, and J.A. Pollock, Department of Physics, Syracuse University, Syracuse, NY 13210.

The Wiener theory of nonlinear system identification is being applied further to the light growth response of the *Phycomyces* sporangiophore (Biophys. J. 15:989, 1975). In this response the elongation rate of the sporangiophore varies transiently in response to changes in light intensity. The light growth response is fundamental to phototropism. Together these photoresponses serve as a model for the processes of photosensory transduction in primary receptor cells. Experiments are performed on the *Phycomyces* tracking machine. Two types of test stimuli are employed, one stochastic and the other deterministic. The former, gaussian white noise, is standard in applications of the Wiener theory. The latter, a sum of sinusoids, has been shown recently by Victor to be superior in a neural system (PNAS 76: 996, 1979). The addition of a new microcomputer system to the tracking machine has permitted the implementation of the sum-of-sinusoids method (Biophys. J. 29:459, 1980) with favorable results. The experiments are being performed on a collection of single and double mutant strains affected in the seven known genes for the photoresponse channel. In addition, a new family of hypertropic mutants is being examined. The results are obtained in the form of Wiener kernels and their Fourier transforms. The interpretation of the results is performed by system analysis methods primarily in the frequency domain. These methods are being employed to test models for the dynamics of photosensory transduction. (Supported by grants GM24367 from NIH and PCM8003915 from NSF)

W-AM-Po21 THE PRINCIPLES OF VISION AND TECHNIQUE OF NARROW SPECTRUM AND PULSE. Lei Shizu, Hauzhong Institute of Technology, Wuhan, People's Republic of China.

The eye is an organ of the human body of very high sensitivity. Can this property of the eye be used to renovate some technology for the benefit of man?

In this paper, a new technique of narrow spectrum and pulse has been proposed for application to two important problems. Namely, the microminiaturization of the motion pictures projector and minimization of the consumption of electrical energy for illumination.

W-AM-Po22 EVIDENCE FOR AN ESSENTIAL HISTIDINE RESIDUE AT THE CATALYTIC CENTER OF THE (H^++K^+) ATPase. Gaetano Saccomani, Maria Luisa Barcellona, Alberto Spisni and George Sachs, Laboratory of Membrane Biology, and Laboratory of Molecular Biophysics, University Station, University of Alabama in Birmingham, Birmingham, Alabama 35294

Exposure of highly purified gastric membrane suspensions at neutral pH to the histidine specific reagent diethylpyrocarbonate (DEPC) led to concentration and time-dependent inhibitions of K^+-ATPase as well as H^+ transport activities, while the K^+ stimulated pNPPase is not affected by this treatment. Evidence that DEPC reacts with histidine residues is provided by spectrophotemetric studies following the increase in absorbance at 242 nm, of the N-carboethoxy histidyl groups formed and by the fact that K^+-ATPase activity is regenerated by treatment with hydroxylamine. Although several ethoxyformyl groups are introduced into the enzyme molecule, inactivation can be correlated with modification at a single group as indicated by spectral analysis and binding with [^{14}C] DEPC. The loss of the K^+-ATPase activity is prevented only by ATP addition before DEPC treatment and this protective effect is independent of the presence of Mg^{2+}. Circular dichroism measurements show that native and DEPC-treated enzyme have similar or overlapping CD spectra indicating that loss of K^+-ATPase activity is not due to structural alteration of the protein. These data suggest that: (1) a single histidine residue is essential for the catalytic activity of the gastric ATPase and this residue is located at or near the ATP-binding center of the enzyme: (2) the pNPP site is not identical to the ATP site although residing on the same enzyme molecule. (supported by NIH, NSF)

W-AM-Po23 PHOTOAFFINITY LABELING OF DNA-DEPENDENT RNA POLYMERASE FROM E. coli WITH 8-AZIDO-ADENOSINE 5' - TRIPHOSPHATE A-Young M. Woody, Connie R. Vader, Richard R. Reisbig, and Robert W. Woody, Department of Biochemistry, Colorado State University, Fort Collins, CO 80525 Boyd E. Haley, Department of Biochemistry, University of Wyoming, Laramie, Wyo. 82071

A photoaffinity analog of ATp, 8-Azido-ATp, has been used to elucidate the role of the various subunits involved in forming the active site of DNA-dependent RNA polymerase from E. coli. 8-Azido-ATp is found to be a competitive inhibitor of the enzyme in the elongation phase of transcription with K_I = 41 μM. A Hill plot analysis of the inhibition data shows n to be 0.95, indicating that 8-Azido-ATp is bound to the enzyme in a molar ratio close to 1:1. UV irradiation of the reaction mixture containing RNA polymerase and (γ-^{32}p)8-Azido-ATp induced covalent incorporation of radio active label into the enzyme. Analysis by gel filtration and nitrocellulose filter binding indicates specific binding. Subunit analysis by SDS gel electrophoresis and autoradiography of the labeled enzyme shows that the subunits are labeled in the order $\beta > \sigma > \beta' > \alpha$, with the same pattern observed both in the presence and absence of poly[d(A-T)]. 400 μM ATp reduces the incorporation of radio active label in all bands by about 30-40% both in the presence and absence of poly[d(A-T]. Our results thus far strongly suggest that all of the subunits of DNA-dependent RNA polymerase participate in forming the active site of the enzyme. (Supported by USPH GM 23697 at Colorado State University and USPH GM 21998 at University of Wyoming).

W-AM-Po24 SITE OF SUBSTRATE MONOOXYGENATION IN THE REACTION CATALYZED BY PSEUDOMONAS CEPACIA SALICYLATE HYDROXYLASE. R.Y. Hamzah* and S.-C. Tu. Department of Biophysical Sciences, University of Houston, Houston, TX 77004.

Salicylate hydroxylase, classed as a flavoprotein external monooxygenase, catalyzes the decarboxylation and hydroxylation (or monooxygenation) of salicylate to yield catechol as a product. In such a reaction, the site of hydroxylation could be at position either 1 or 3 of the salicylate ring. The determination of the substrate hydroxylation site is important for an understanding of the reaction mechanism. In the present study, [3,5-^{2}H]salicylate was obtained by heating a salicylate sample in ^2H_2O at 100°C. The hydrogen/deuterium exchange occurred specifically at positions 3 and 5, and reached ~97% completion after 40 days. Using the deuterated salicylate as a substrate for Pseudomonas cepacia salicylate hydroxylase, the product catechol was isolated and characterized with respect to the positions of deuterium retention. Based on nuclear magnetic resonance and mass spectroscopy analyses, the product was identified as [3,5-^{2}H]catechol. It is thus unequivocally demonstrated that salicylate is decarboxylated and hydroxylated at the same position in the ring. Also consistent with this conclusion is the lack of a kinetic isotope effect for the deuterated salicylate substrate.

W-AM-Po25 FLAVIN MONONUCLEOTIDE COMPLEXATION WITH DIHYDROXYANTHRAQUINONE, A NEW ANTINEOPLASTIC AGENT. Evan D. Kharasch and Raymond F. Novak, Department of Pharmacology, Northwestern University Medical and Dental Schools, Chicago, IL 60611.

Proton FT NMR and UV-Vis spectroscopy were used to characterize the interaction of FMN with dihydroxyanthraquinone (DHAQ) (1,4-dihydroxy-5,8-bis[[2-(hydroxyethyl)amino]ethyl]amino-9,10-anthracenedione), which is less cardiotoxic than the antineoplastic anthracycline antibiotic Adriamycin (ADM). DHAQ (0.1 - 3 mM) addition to 1 mM FMN in 100 mM phosphate buffer pH_{obs} 7.5 produced an upfield shift of the proton NMR signals of FMN in a saturable, concentration dependent manner, reflective of a π-π ring stacking interaction. The shift of the aromatic FMN H-6,9 signal was approximately twofold greater than that of the 7α and 8α methyl signals (0.43 vs 0.22 ppm at 1 mM DHAQ, respectively). Variable temperature studies showed downfield shifts with increasing temperature suggesting disruption of the FMN-DHAQ complex. The linear double-reciprocal plot of chemical shift vs. concentration indicates formation of a complex with 1:1 stoichiometry and an apparent association constant of approximately 960 M^{-1}. UV-Vis studies showed a bathochromic shift of the FMN and DHAQ absorbances with complexation, further supporting a stacking interaction between the anthracenedione and isoalloxazine rings of DHAQ and FMN. We have previously shown that ADM also interacts with FMN via ring stacking, however the interaction of FMN with DHAQ is approximately twofold greater than with ADM as evidenced by the magnitude of chemical shift changes of the H-6,9 proton signal (0.48 vs 0.27 ppm at 1 mM) and apparent association constants (960 vs 530 M^{-1}). The greater affinity of FMN for DHAQ appears to be the result of structural differences between the two drugs (anthracenedione and anthracycline-sugar) and may be related to differences in their cardiotoxicity. (Supported by American Cancer Society Grant 80-46 and NIH Grant GM 27836 to RFN and NIH Training Grant GM 07236 to the Department of Pharmacology.)

W-AM-Po26 COFACTOR INTERACTIONS IN NATIVE AND "REDUCED" DIAMINE OXIDASE. Michael D. Kluetz, Department of Chemistry, University of Idaho, Moscow, Idaho 83843.

Pea seedling diamine oxidase (DAO; diamine: O_2 oxidoreductase [deaminating]; EC 1.4.3.6) operates according to a ping-pong kinetic mechanism, and thus can exist in one of two stable free-enzyme forms - the native, oxidized (E) form and the intermediate, "reduced" (E') form obtained after the anaerobic conversion of amine to aldehyde. The enzyme's Cu(II) remains in the divalent state throughout the catalytic cycle. We have attempted to elucidate the nature of the as yet unidentified organic cofactor (originally believed to be PLP), which is required in addition to Cu(II), by observing DAO in both its E and E' forms. The visible spectrum of native E has a single band at 525 nm (pink), while that of E' has bands at 360, 432, 455 and 463 nm (yellow). Cryoenzymologic studies indicate that this intermediate E' form is generated via several other intermediates, is independent of substrate used, and is identical to that formed upon the anaerobic addition of amine at room temperature. The spectrum of the enzyme reacting under steady-state conditions is a hybrid of those of the E and E' forms, the relative contributions of the two being dependent on the O_2 level; the O_2-requiring stage of the reaction appears to be rate-limiting at most O_2 concentrations. The chromophores giving rise to the spectra of both forms appear to involve divalent copper, as both spectra are bleached by dithionite (that of E' disappears instantaneously, that of E much more slowly). Our suggestion that Cu(II) is directly coordinated by the organic moiety in the E' form of DAO is supported by the fact that when one removes Cu(II) from this form, the resulting protein spectrum is featureless, while the spectrum of the Cu(II)-carbamate complex contains new bands, presumably representative of the organic group. Finally, water proton relaxation measurements indicate that water ligands are lost upon the conversion of E to E', which could result from ligand displacement by the organic group.

W-AM-Po27 HYDROXYL FREE RADICAL FORMATION FROM HYDROGEN PEROXIDE AS CATALYZED BY METAL CHELATES. A SPIN-TRAPPING STUDY. Robert A. Floyd, Ph.D., Oklahoma Medical Research Foundation, Oklahoma City, Oklahoma 73104.

Hydroxyl free radicals are implicated in several pathological conditions. Their formation from hydrogen peroxide in biological systems is poorly understood. I have utilized the spin-trap, 5,5-dimethyl-1-pyrroline-1-oxide (DMPO) which reacts with OH· at nearly diffusion controlled rate, to investigate radical formation from hydrogen peroxide as influenced by various metal ions, chelators and buffers commonly utilized in biological chemistry studies. The oxidation state of the metal ion, the type of buffer and the type of chelator utilized influences the amount of OH· spin-trapped by as much as 100 times. Fe (II) as compared to Fe (III) is highly effective in catalyzing OH· formation when chelated with diethylenetriamine penta-acetate or ehtylenediamine tetra-acetate but not when chelated with deferoxamine. The effectiveness of either Cu (I) or Cu (II), in catalyzing OH· formation with any of the buffer systems tested, was decreased by the chelators tested. Of more direct biological implication, Fe (II) complexed with DNA accelerated OH· formation from H_2O_2, and, also, human blood plasma collected in the presence of a chelator, is effective in catalyzing OH· formation from H_2O_2.

W-AM-Po28 FORMATION OF NITROXYL FREE RADICALS VIA COVALENT ADDITION OF AROMATIC NITROSO COMPOUNDS TO STEROIDAL OLEFINS. R. Sridhar and R. A. Floyd, Oklahoma Medical Research Foundation, Oklahoma City, Oklahoma 73104.

Nitrosoaromatic compounds such as nitrosobenzene, 2-nitrosotoluene and 2-nitrosofluorene were found to react with steroidal olefins in an Alder-ene manner to form hydroxylamino derivatives which underwent easy oxidation to the corresponding nitroxyl derivatives as judged by electron spin resonance spectroscopy. The formation of nitroxyl free radicals was observed in reactions of nitrosoaromatic compounds with several olefinic steroids such as cholesterol, lanosterol, ergosterol, stigmasterol and progesterone. The reaction of nitrosobenzene with cholesterol yields two different nitroxyls depending on the reaction conditions and the proof of the structure of one of these nitroxyls has been obtained by comparison of ESR spectrum with a model compound. Investigations are under way to assess the importance of these reactions in relation to the cytotoxic and mutagenic properties of nitrosoaromatic compounds and their precursors. For example, the carcinogen 2-nitrosofluorene underwent addition to cholesterol at room temperature to yield a hydroxylamino derivative. This hydroxylamine underwent oxidation in air to yield a fairly stable nitroxyl radical. Preliminary studies indicate that this free radical derived from the addition of nitrosofluorene to cholesterol can be incorporated into artificial liposomes prepared by sonication of type V-E egg phosphatidyl choline. The ESR spectrum of these liposomes showed a highly immobilized nitroxyl signal at room temperature. Increase in mobility of this nitroxyl was observed when spectra were recorded at higher temperatures.

W-AM-Po29 METALLOPORPHYRIN CHARGE-TRANSFER COMPLEXES IN CATALYSIS, MEDICINE, AND BIOLOGY.* J. A. Shelnutt, Sandia National Laboratories†, Albuquerque, NM 87185

Charge-Transfer (CT) complexes of more than 20 small molecules with copper (II) and iron (III) porphyrins in aqueous solution have been studied with Raman difference spectroscopy (RDS). The RDS technique allows small frequency shifts in the vibrational spectrum of the porphyrin moiety to be detected. The shifts are the result of complexation of an addend to the porphyrin and the magnitude and direction of the changes in vibrational frequencies provide information about the structure of the CT complex. The addends chosen are of interest in catalysis, malaria-drug binding to hemoglobin-based pigments, and artificial photosynthesis systems. Copper uroporphyrin I (CuURO) was chosen because of its water solubility and its weak attraction for axial ligands. Addends generally result in shifts in most of the high frequency Raman lines to either higher or lower frequency, consistent with a general strengthening or weakening of the porphyrin macrocycle. In iron porphyrins this pattern of frequency shifts has been interpreted as a change in the π-electron density in the ring. Studies of complexes with derivatives of phenanthroline, in which increases in frequencies are from 0.2 to 2.0 cm^{-1}, demonstrate that π-π interactions are important, not interactions with the Cu ion. The implications of this study for the CT model[1] of cooperative O_2 binding in hemoglobin will be discussed. Methyl viologen (MV) binds to CuURO to give the largest decreases in the porphyrin vibrational frequencies of any CT complex. The structure of this complex is proposed and a mechanism is suggested for initial charge separation in artificial photosynthetic systems using MV as the acceptor and a metalloporphyrin as photosensitizer.

1.J.A.Shelnutt,D.L.Rousseau,J.M.Friedman,S.R.Simon, Proc. Natl. Acad. Sci. USA 76, 4409(1979).

*This work sponsored by the U.S.Department of Energy(D.O.E.) under contract DE-AC04-76-DP00789
†A U.S. Department of Energy facility

W-AM-Po30 CONFIGURATION OF A SPIN-LABEL SUBSTRATE IN THE ACTIVE SITE OF CARBOXYPEPTIDASE A. Lawrence C. Kuo, Dept. of Biophys. & Theor. Biol., University of Chicago, Chicago, IL 60637

The conformation of a spin-label ester substrate in the active site of Co(II)-substituted carboxypeptidase A (CoCPA) is determined. Water proton relaxation enhancement studies at 24.3, 100, and 270 MHz indicate that the metal-bound water molecule in CoCPA is in fast chemical exchange; the spin lattice relaxation time (T_{1s}) of the metal ion is estimated to be 1.7×10^{-12} sec in the 20°C to -35°C range. With the spin-label nitroxide substrate shown below, an acylenzyme intermediate is stablized at -70°C in fluid cryosolvents. The dipolar interaction between the high spin Co(II) ion and the nitroxide group results in a 28% quenching of the EPR signal amplitude of the spin-label. This observation together with the value of T_{1s} leads to a calculated distance of 6.0 ± 0.5 Å between the spin centers. With the carbonyl oxygen of the substrate's scissle bond coordinated to the Co(II), this distance requires that the substrate is altered from a *trans* to a *cis* configuration upon formation of the acylenzyme. This configuration is compatible with the steric constraints in the active site of the enzyme by model building studies. Hitherto only the scissle bond of a substrate is known to be distorted in the catalytic site of the enzyme. These findings along with model building studies suggest that long range steric hindrance imposed by the enzyme in regions distal to the immediate vicinity of bond cleavage is responsible for the configuration change observed for the substrate and may be important in the hydrolytic mechanism of carboxypeptidase A. (NIH GM 21900)

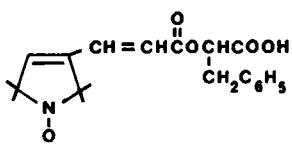

W-AM-Po31 AN APPARENT SUPEROXIDE OXIDASE ACTIVITY OF CONCANAVILIN A. Paul D. Levin and D. W. Kupke, Dept. of Biochemistry, Univ. of Virginia, Charlottesville, Va. 22908.

The metal-binding site of Concanavalin A (Con A) has a metal specificity and structure analogous to the general class of superoxide dismutases (SOD). We have assayed Con A for SOD-like activity using tetranitroblue tetrazolium (TNBT) as the electron acceptor dye, and riboflavin/methionine/visible light as the superoxide ($O_2^{\cdot}$) generating system [Beauchamp, C. & Fridovich, I., *Anal. Biochem. 44;* 276, (1971)]. Unlike typical SOD activity, Con A enhances the rate of TNBT reduction up to a mean enhancement of ∿60% over control conditions at a Con A monomer to TNBT molar ratio of 0.24 (0.05% protein). Increasing the protein concentration led to a decrease in the apparent enhancement; little enhancement remained above [Con A]/[TNBT] = 0.71. Bovine serum albumin and bovine pancreatic ribonuclease were similarly assayed to determine non-specific protein effects; both proteins exhibited a net decrease in dye reduction with concentration relative to control conditions following a small or marginal apparent enhancement at low molecular ratios (∿0.07). The Con A specific ligand, α-methyl mannopyranoside, at 100-fold excess over Con A monomer had no effect on the Con A mediated enhancement of dye reduction. Whereas riboflavin and light were both required for the observed enhancement in the presence of Con A, a significant although reduced enhancement was still obtained in the absence of methionine. These results suggest that Con A has an enzymatic activity which may be useful to the plant, possibly as protection for acid polysaccharides, membranes and photosynthetic pigments from $O_2^{\cdot}$ destruction and/or via a role in the cyanide-resistant electron transport system in certain plant storage tissues.

Supported by: NIH grant GM-07294 and U. Va. Biomed. Res. Grant 5-S07-RR05431-18.

W-AM-Po32 ^{13}C NMR STUDY OF TRANSAMINATION DURING ACETATE UTILIZATION BY S. CEREVISIAE J.A. den Hollander and K.L. Behar, intro by R.G. Gillies. Yale University; Dept. of MB&B; P.O. Box 6666, New Haven, CT 06511

^{13}C Nuclear Magnetic Resonance was used to follow the metabolism of [2 - ^{13}C] acetate and [1 - ^{13}C] acetate on aerobic suspension of S. cerevisiae. In the experiment with [2 - ^{13}C] acetate the ^{13}C label first appeared in glutamate $-C_4$, and with lower intensity in glutamate $-C_2$ and $-C_3$. After exhaustion of the acetate the glutamate signals diminished, while aspartate $-C_2$ and $-C_3$ increased in intensity. During a subsequent chase experiment with unlabelled acetate the aspartate peaks decreased, while glutamate $-C_2$ and $-C_3$ increased in intensity. These observations have been interpreted in terms of an interplay between the glutamic - oxalacetic transaminase and TCA cycle activity. This interpretation was confirmed by an experiment with the transaminase inhibitor amino oxacetate. During all these experiments we observed the formation of trehalose. The NMR gives a direct measurement of the label distribution, and from that information it followed that the flow through the glyoxylate cycle and the TCA cycle are comparable in magnitude. The intermediates citrate, succinate, fumarate, malate, PEP, 3PGA and G6P were identified in a ^{13}C NMR spectrum of a perchloric acid extract taken during the metabolism of [2 - ^{13}C] acetate. Enrichment of glutamate $-C_5$ shows the existence of a futile cycle in which PEP, formed from oxaloacetate, returns to the TCA cycle through pyruvate and acetyl CoA.

W-AM-Po33 CHEMICAL MODIFICATIONS OF CYTOCHROME c OXIDASE : EFFECT OF SULFHYDRYL REAGENTS. E. Keyhani and J. Keyhani, Inst. Biochem. Biophys., Univ. of Tehran, P.O. Box 314-1700, Tehran, Iran and Johnson Research Foundation, Univ. of Pennsylvania, School of Medicine, Philadelphia, Pa 19104, U.S.A.

The aerobic interaction of dithiothreitol (DTT), a sulfhydryl reagent, and purified beef heart cytochrome c oxidase was studied in vitro in the absence or presence of added ligand. Chemical studies indicate that dithiothreitol reduced disulfide bonds in the protein. Polarographic studies showed that the addition of DTT was accompanied by a decrease in the cytochrome c oxidase activity (90% inactivation in the presence of 160 mM DTT). Spectrophotometric studies showed that in the presence of formate as a ligand, addition of DTT produced a reduction of cytochrome a and copper, while cytochrome a_3-formate remained essentially oxidized. In the absence of ligand, addition of DTT to cytochrome c oxidase produced a reduction of hemes a and a_3 and copper. The cytochromes a and a_3 exhibited, however, a distinct pattern of reduction, presumably due to substrate accessibility induced by change in the sulfhydryl groups and subsequent modification in the configuration of the enzyme from a compact to a more elongated structure. The reoxidation of DTT-reduced cytochrome c oxidase under aerobic conditions was found to be accelerated by a mixture of reduced and oxidized glutathione. Disulfide bond formation was found to take place in two phases : a fast phase in which 50% of the cytochrome c oxidase activity was restored, and a slower phase. 85% of the cytochrome c oxidase activity was restored after one hour of incubation in 100 μM reduced and oxidized gluthathione.

These observations suggest the involvement of disulfide bonds in cytochrome c oxidase activity.

W-AM-Po34 THE CALCIUM-STIMULATED HYDROLYSIS OF ATP BY A GOLGI-ENRICHED MEMBRANE FRACTION FROM MURINE MAMMARY TISSUE. Christopher D. Watters and Margaret C. Neville, Department of Physiology, University of Colorado Health Sciences Center, Denver, CO 80262.

As previously reported (Neville, et al, J Supramol. Struct. suppl. 4:101, 1980), a membrane fraction from lactating mouse mammary gland, enriched for galactosyl transferase activity and substantially free of succinate dehydrogenase activity, exhibited ATP-dependent and A-23187-releasable uptake of calcium. This fraction also showed calcium-stimulated and hydroxylamine-sensitive phosphorylation of a 100K dalton protein. We now report the presence in this fraction of calcium-stimulated hydrolysis of ATP (Ca-ATPase). This activity was detected reproducibly in the presence of micromolar concentrations of Mg^{2+} and ATP, a condition which drastically reduced the large "basal" ATPase activity associated with the fraction. If the fraction was rapidly frozen and stored at -60 °C, the Ca-ATPase retained substantial activity for at least a month. In the presence of 20 μM free Mg^{2+} and 2.5 μM Mg-ATP, the Ca-ATPase exhibited an apparent K_m for Ca^{2+} of approximately 2 μM. In the presence of 2 μM free Mg^{2+} and 10 μM free Ca^{2+}, the apparent K_m for ATP was approximately 1 μM. The Ca-ATPase was also activated by millimolar concentrations of K^+. It was insensitive to oligomycin at a concentration that is reported to inhibit the mitochondrial ATPase, to dibucaine between 1 and 50 μM, to quercetin between 6 and 300 μM, and to 20 μM CCCP. It was partially inhibited, however, by 200 μM CCCP. These kinetic properties identify this Ca-ATPase as being similar to those responsible for calcium transport in other membranes, such as the sarcoplasmic reticulum and the plasma membranes of red cells and adipocytes. (Supported by NIH grant HD 14013)

W-AM-Po35 AGE-DEPENDENT CHANGES IN KIDNEY BRUSH BORDER MEMBRANE MALTASE. Uzi Reiss and Bertram Sacktor (Intr. by Gunther Eichhorn). National Institutes of Health, National Institute on Aging, Gerontology Research Center, Baltimore, MD 21224.

The specific activity of maltase in kidney cortex homogenates of aged rats (24 mo) is decreased about 30-40% compared to the activity in young (6 mo) rats. Similar age-decrement was observed for the pure enzymes - 46.1 and 32.5 units/mg protein for "young" and "old" maltase, respectively. Maltase was purified from kidneys of young and old rats using a new affinity chromatography procedure in which Tris, an inhibitor of maltase, served as the ligand. Recovery of enzyme activity and fold-purification were similar for "young" and "old" enzymes - 38 and 44%, 1150- and 1200-fold, respectively. Pure enzymes from the two age groups do not differ in K_m, molecular weight, electrophoretic mobility, amino acid composition and antigenicity. The loss of enzymatic activity does not appear to result from higher proteolytic activity in "old" homogenates. The rate of enzymatic inactivition at 4°C, was similar in both homogenates of "young" and "old" with or without antiproteolytic reagents. The conformational structure of the two enzymes differed as determined by Circular Dichroism spectra. Both enzymes contain β- and random coil structure, with no α-helix. However, while "young" enzyme is estimated to include equal proportions of β-structure and random coil, "old" enzyme consists of about 58% β-structure and 42% random coil.

W-AM-Po36 HYDROGEN SELENIDE OXIDATION AND ITS IMPLICATIONS IN SELENITE METABOLISM, Kern Nuttall and Fritz S. Allen, Department of Chemistry, University of New Mexico, NM 87131.

The essential trace element selenium, as selenite (SeO_3^{-2}), is rapidly taken up in the blood stream by the red blood cells and released in an altered form which is strongly associated with the plasma proteins. This altered form has been shown to be hydrogen selenide (H_2Se) which is notoriously prone to oxidation via the following reaction:

$$H_2Se + \frac{1}{2} O_2 \longrightarrow Se + H_2O.$$

We have studied the kinetics of this reaction and have found it takes place readily under physiological conditions; on this basis we postulate that elemental selenium is formed in the normal course of selenite metabolism in vivo.

W-AM-Po37 EXPERIMENTAL AND THEORETICAL INVESTIGATION OF SPIN-TUNNELING IN CO RECOMBINATION TO HEMOGLOBIN Bernard S. Gerstman, Robert Austin, J.J. Hopfield (Princeton University and California Institute of Technology)

Experimental evidence for the spin-orbit coupling model to explain the S=2 to S=0 spin state change of the Fe in hemoglobin upon recombination of CO has been obtained. Using a 10 tesla magnet at the M.I.T. Magnet Lab we have seen an optical anisotropy produced by the magnet field. This is due to a magnet field dependence on the recombination rate due to the dependence of Fe spin sublevel upon orientation of the heme in the external field. The experiment is done at liquid helium temperatures to keep the Boltzman population of higher spin sublevels to a minimum. We find a polarization at high field and low temperature of $\sim(8\pm2)\times10^{-3}$. A polarization dependence on field strength and temperature has also been investigated. The data is compared with theoretical calculations employing the crystal field splitting and spin-hamiltonian for deriving the states of the system.

Work supported by NSF BMR 78-05916

W-AM-Po38 QUENCHING OF Hb^{desFe} FLUORESCENCE BY OXYGEN, D. M. Jameson, M. Coppey, B. Alpert, and G. Weber (Biochemistry Department, University of Illinois, Urbana, Illinois 61801 and Faculte de Medecine, 45 Rue des St. Peres, Paris 75270, France).

We have investigated the quenching of the fluorescence of protoporphyrin IX and its complex with apohemoglobin (Hb^{desFe}), at 20°C, by oxygen at concentrations of 1 to 140 mM obtained by oxygen pressures of 1 to 100 atmospheres. The unquenched lifetime of Hb^{desFe}, τ_o, is 19.6 ns, measured either by phase (τ_ϕ) or modulation (τ_M). Stern-Volmer plots of relative fluorescence efficiency (F_o/F) were markedly convex towards the [O_2] axis. At [O_2] = 140 mM, $F_o/F = 6.5$; $\tau_o/\tau_\phi = 3.3$ and $\tau_o/\tau_M = 2.5$. The considerable difference between F_o/F and τ_o/τ stand in contrast to the usual equivalence of these quantities in the quenching of tryptophan fluorescence by oxygen, as also does the departure of F_o/F from the linear law. The apparent rate of oxygen quenching, calculated from the values of τ_o/τ_ϕ, is $7.10^8 s^{-1}$ for Hb^{desFe} and $1.3\ 10^{10}\ s^{-1}$ for protoporphyrin IX. All these observations are explained qualitatively and nearly quantitatively under two simple assumptions: 1. The quenching is due to oxygen molecules already within the protein structure at the time of the excitation, 2. The distribution of oxygen molecules among the protein molecules follows a Poisson distribution with a partition coefficient of nearly two in favor of the protein. The results indicate that retention of oxygen within the protein structure must be taken into account in explaining the kinetics of many Hb-oxygen reactions. (Supported in part by NIH Grant No. GM 11223 and INSERM Grant No. 78.1.1059.5.)

W-AM-Po39 DETECTION OF QUATERNARY STRUCTURE DEPENDENT CHANGES AT THE HEME IN HEMOGLOBIN. M. R. Ondrias and D. L. Rousseau of Bell Labs, Murray Hill, NJ 07974 and S. R. Simon, State University of New York, Stony Brook, NY 11790.

We have probed the low frequency region of the Raman spectrum in deoxyhemoglobins by using the highly sensitive technique of Raman Difference Spectroscopy. Several hemoglobins were studied in which quaternary structure changes could be induced. These include carp hemoglobin, and valency hybrid, chemically modified, and mutant human hemoglobins. The R to T comparisons among these proteins display a series of concerted frequency and intensity changes in the 50 to 500 cm^{-1} region, including a large change in the band at 215 cm^{-1} which has been assigned to the iron-histidine stretching frequency. Similar changes are detected in this region when isolated α and β chains are compared to tetrameric T state hemoglobin. The quantitative differences between the various R/T comparisons may reflect chain heterogeneity or tertiary structure effects. The changes detected in the oxidation state marker line (1357 cm^{-1}) have also been examined and found to be consistent with previous results obtained with chemically modified hemoglobins. However, the magnitude of the systematic changes in this high frequency line and those in the low frequency region do not linearly correlate. These data imply that the influence on the heme of the protein quaternary structure change is not restricted to a single interaction.

W-AM-Po40 INVERSE FARADAY EFFECT IN HEMOGLOBIN DETECTED BY RAMAN SPECTROSCOPY: AN EXAMPLE OF MAGNETIC RESONANCE RAMAN ACTIVITY T.W. Barrett, University of Tennessee Center for the Health Sciences, Memphis, TN 38163.

A complete polarization study of human oxy- and carbonmonoxy-hemoglobin is reported for backscattered light in the resonance Raman light scattering situation with excitations in the long wavelength region, λ = 5682 Å and 5815 Å, and excitations in the short wavelength region, λ = 4579 Å and 4880 Å, as comparison. All four polarization components of the scattered light with respect to the two polarization conditions of linearly and circularly polarization of the incident light were measured. These were: (1) parallel; (2) perpendicular; (3) corotating; and (4) contrarotating.

This method has been used to characterize the three invariants of the nonsymmetric Raman tensor for randomly oriented molecules. These invariants are based on a model in which the scattered light is dependent on only an induced electric dipole. With no higher moments involved in the scattering process, the amplitude of any band measured under the four conditions should satisfy the relation: (1) + (2) = (3) + (4). As an apparatus test, this relation was seen to hold for the bands of carbon tetrachloride and benzene.

We report that although this relation is satisfied for short wavelength [4579 Å and 4880 Å] excitation, it is not satisfied for long wavelength [5682 Å and 5815 Å] excitation, for which (1) + (2) < (3) + (4) holds.

The inequality is due to magnetic resonance Raman activity by porphyrin ring-metal electron charge transfer coupling, involving an inverse Faraday effect which is induced by circularly polarized light.

W-AM-Po41 REVERSIBLE HEMICHROME FORMATION IN MYO- AND HEMOGLOBIN. MODULATION OF HEMEBOUND WATER IN CONCENTRATED IONIC SOLUTIONS Blake Schlaeppi and Bo Hedlund, Univ. of Minnesota, Minneapolis, Minn.

Methemoglobin and metmyoglobin exist as aquometderivatives at neutral acidic pH. A water molecule occupies the space between the ferric heme and the distal histidine and this water molecule presumably exists in equilibrium between the heme binding site and bulk water, possibly mediated by protein associated water in the heme pocket. It is known that this heme-associated water can be removed when human hemoglobin is treated with compounds such as benzoate ion and aspirin at fairly high concentrations (ca. 0.5M) to form a derivative referred to as hemichrome. In this form of hemoglobin the distal histidine interacts directly with the ferric heme. In this study we report further investigations of the aquomet-hemichrome equilibrium using human methemoglobin and sperm whale metmyoglobin and employing concentrated solutions of salts. Certain ions perturb this equilibrium in a well defined and reversible fashion. Both anions and cations can be used to form the hemichrome. Perchlorate ion is an efficient anion, while calcium ion causes the same effect at higher concentration. The latter effect must be cation mediated since sodium and lithium chloride cannot be used to obtain the effect observed in calcium chloride at identical chloride concentrations. Aromatic carboxylic acids do not produce hemichrome in metmyoglobin, suggesting that this reaction differs from the effect observed in the concentrated salt solutions. It seems likely that the interaction between salicylate and hemoglobin is mediated by direct binding to the protein, while the hemichrome formation observed in the salt solutions may be due to change in water activity, thus, allowing spectral analysis of water as a ligand as a function of water activity. Supported by the VIKINGS' CHILDREN FUND.

W-AM-Po42 CONCENTRATION DEPENDENCE OF O_2 BINDING TO HEMOGLOBIN ALPHA CHAINS. William T. Windsor and Todd M. Schuster, Biological Sciences Group, University of Connecticut, Storrs, CT 06268.

Temperature jump relaxation kinetics have been performed on human hemoglobin alpha chains over a range of oxygen saturations and protein concentrations. The experiments were done under conditions in which alpha chain dimerization equilibrium constants have been obtained previously by gel chromatography (1). The results show that a single relaxation is observed for low protein concentrations (2 μM - 10 μM heme) and the rates are similar to those observed previously (2). At higher protein concentrations (10 μM - 140 μM) two phases are resolved. The faster phase is due to ligand binding and analysis of this phase indicates differences in monomer and dimer O_2 affinity. In contrast to the beta chains, the associated form of the alpha chains appears to have a decreased affinity for O_2. The slower phase is proposed to result from coupling of the monomer-dimer reaction to the ligand binding reactions. These preliminary results suggest that the individual monomer and dimer O_2 binding rates can be obtained as well as the dimerization rates.

(1) Valdes and Ackers, J. Biol. Chem. 252, 74 (1977)

(2) Brunori and Schuster, J. Biol. Chem. 244, 4046 (1969)

Supported by NIH grant HL 24644 and NSF grant PCM 7903964

W-AM-Po43 LASER PHOTOLYSIS STUDIES OF MERMAID (CARP-HUMAN HYBRID) HEMOGLOBINS.
Dixie J. Goss and Lawrence J. Parkhurst, Dept. of Chemistry and School of Life Sciences, University of Nebraska, Lincoln, NE 68588.

Laser photolysis studies of hybrid hemoglobins were undertaken to assess the contributions of the individual chains to the Root effect. Hybrid hemoglobins were prepared from isolated alpha and beta chains of carp (Cyprinus carpio) and human hemoglobins. Dye laser photolysis measurements were carried out on the CO mermaid hemoglobins. Measurements of the fraction rapid phase in the CO recombination reaction as a function of laser intensity were used to assess the presence of the R and T states for the hybrid hemoglobins. At pH 6.0 in the presence of 1 mM inositol hexaphosphate, carp hemoglobin is assumed to be in the T state since the recombination reaction is entirely slow even at very low fractional photolysis. Human hemoglobin shows no detectable slow component at pH 6.0 (+IHP) for 4% photolysis. Preliminary measurements of CO recombination reactions under the same conditions for the two hybrids suggest that the alpha(carp)beta(human) hybrid assumes a T state conformation, since there was no rapid component even at 10% photolysis. The alpha(human)beta(carp) hybrid, however, shows bi-phasic kinetics. The recombination reaction has about 50% rapid phase with a rate characteristic of isolated human alpha chains, but disc gel electrophoresis shows only the one band for a hybrid hemoglobin, and the slow phase is much slower than that of isolated carp beta chains. These results suggest that in the latter hybrid, the human alpha chains remain in the R state whereas the carp beta chains assume a T state conformation. Grant Support: NIH HL 15284-08, NSF PCM-8003655.

W-AM-Po44 AGGREGATION OF DEOXYGENATED BULLFROG HEMOGLOBIN. L.-T. Tam and A.F. Riggs, Dept. of Zoology, University of Texas, Austin, TX 78712.

The hemoglobin of the bullfrog, Rana catesbeiana, forms aggregates larger than tetramers in two ways. The first, which results from intermolecular disulfide links, can be prevented by treatment with iodoacetamide. Araki et al. (Biochim. Biophys. Acta, 351: 427, 1974) showed that iodoacetamide-treated hemolysates would form 7 S aggregates rapidly and reversibly upon deoxygenation. We find that neither of the purified major components B or C forms 7 S aggregates by itself when deoxygenated at pH 7.5 in 0.05 M Tris-HCl buffer with 0.1 M NaCl and 1 mM EDTA at 20°C and a total protein concentration of 0.28 mM (heme). The formation of 7 S aggregates requires the presence of both components. Although the stoichiometry has not been determined, the sedimentation data are not consistent with the formation of a simple 1:1 complex between components B and C. A 2:1 mixture of components B and C gives a single, highly asymmetric sedimentation peak of 7 S which is skewed towards lighter material. However, a 1:2 mixture of components B and C gives two peaks, one at approximately 4.5 S and one near 7 S. One possibility is the presence of aggregates of the form BCB. Oxygen equilibrium measurements of the unfractionated mixture at a high concentration, 16 mM (heme), give Hill plots with slopes greater than 4 above 60% oxygenation. Such a Hill plot is similar to that found by Gill et al. (Science 201: 362, 1978) for human hemoglobin S. Since the B and C components appear to share common β chains, the B-C aggregation behavior probably requires two different kinds of α chains. (Supported by Robert A. Welch Foundation grant F-213 and NSF grant PCM 79-04053).

W-AM-Po45 INTERACTION OF LIGANDS WITH DISTAL GLUTAMINE IN ELEPHANT MYOGLOBIN.
D. E. Bartnicki, H. Mizukami, and A. E. Romero-Herrera, Dept. of Biological Sciences and Dept. of Anatomy, Wayne State University, Detroit, Michigan 48202

The role of glutamine as a distal amino acid to the heme is examined by comparing the temperature dependent esr spectra of elephant nitrosyl myoglobin (MbNO) with those of whale or human MbNO and the pKa for the acid-alkaline equilibrium of ferric elephant Mb.

Distal histidines of hemoproteins are evolutionarily conserved and their replacement with other amino acids often produces impaired molecular function. However, recent analysis reveals that glutamine could be a successful replacement for distal histidine. The distal histidine of Asian elephant Mb is replaced with glutamine, yet its interaction with oxygen is similar to that of human or whale Mb. Furthermore, kinetic studies show a strong interaction between the distal glutamine and polar ligands, such as carbon monoxide, together with reduced heme auto-oxidation rates. In opposum hemoglobin, which contains distal glutamine in the alpha-chains, a weakened interaction between nitric oxide ligand and glutamine has been observed using esr and spectrophotometric methods.

Our esr study shows that the binary spectral equilibrium found with most nitrosyl hemoproteins is shifted toward a higher temperature in elephant Mb, suggesting a weakened glutamine-NO interaction. However, the pKa for the acid-alkaline equilibrium was found to be 0.40 pH units lower than that of human or whale Mb, indicating a strong glutamine-OH^- interaction. (Supported in parts by grants from NSF DEB 7619924 and PCM 7717644, and NIH HL 16008)

W-AM-Po46 T_1 RELAXATION RATE STUDIES ON THE EFFECT OF IMIDAZOLE ON THE INTERACTIONS OF ANILINE, ACETANILIDE, AND N,N-DIMETHYLANILINE WITH HEMOGLOBIN AND MYOGLOBIN. Karen Kaul Hajek and Raymond F. Novak. Dept. of Pharmacology, Northwestern Univ. Medical and Dental Schools, Chicago, IL 60611.

^{1}H FT NMR relaxation rate studies have previously shown that imidazole (IM) inhibits the interaction of acetanilide (AC) with the purified hemeproteins cytochrome P-450$_{LM_2}$ and LM_4. The T_1 relaxation rates of the phenyl and methyl protons of AC in solution with LM_2 or LM_4 were decreased by IM to values virtually identical to those obtained with the diamagnetic ferrous carbonyl form of the enzyme indicating that IM displaces or limits the accessibility of AC to the paramagnetic heme iron atom [K.L.Kaul *et al*, *Fed. Proc. 39*, 661 (1980)]. In the present study, the effect of IM on the interactions of AC, aniline (AN), and N,N-dimethylaniline (DMA) with ferrihemoglobin (Hb) and ferrimyoglobin (Mb) was examined. Hb or Mb produce an increase in the T_1 relaxation rates of the phenyl and methyl protons of AC and DMA and the phenyl protons of AN, indicating that each compound interacts with Hb or Mb at a site near the paramagnetic heme iron atom. In each case, evaluation of the paramagnetic contribution to the observed relaxation rate change was performed using the ferrous carbonyl form of the hemeprotein as a diamagnetic control. Addition of IM (25 mM) to a solution of AC (4.25 mM), AN (18.9 mM), or DMA (3.2 mM) containing Hb (50 μM) or Mb (100 μM) in 0.02 M phosphate buffer in D_2O, pH 7.5, resulted in a decrease in the T_1 relaxation rates of approximately 10-50% with Hb and 30-80% with Mb suggesting that IM acts to displace or limit the accessibility of AC, AN, and DMA to the heme iron atom of Hb or Mb. These results support the role of IM as a competitive inhibitor of interactions between certain substrates and hemeproteins. (Supported in part by NIH Training Grant 07263 to the Department of Pharmacology and by NIH Grant 27836 and Chicago Heart Grant C80-13 to RFN).

W-AM-Po47 A ^{1}H NUCLEAR RELAXATION STUDY OF THE ANILINE-BINDING SITE IN HUMAN HEMOGLOBIN. Robert P. Sheridan and Raj K. Gupta. Inst. for Cancer Research, Philadelphia, PA 19111.

Hemoglobin-catalyzed hydroxylation of aniline to para-aminophenol may be taken as a model for similar reactions catalyzed by cytochrome P-450. This reaction involves the degradation of oxyferrohemoglobin to methemoglobin plus peroxide or superoxide, which attacks the substrate. The substrate-hemoglobin complex for methemoglobin presumably resembles the complex for the active oxyferrous form or some intermediate along the reaction pathway. We have examined the paramagnetic effects of high-spin Fe^{3+} in methemoglobin and fluoromethemoglobin on the nuclear relaxation rates of bound aniline protons. From the magnitude of these effects, using accurately measured correlation times for methemoglobin and fluoromethemoglobin from magnetic field-dependence of water proton relaxation, we calculate the Fe^{3+} to aniline proton distances as 8.5±0.7 Å. It is well known that aniline binding perturbs the optical spectrum of methemoglobin. No such effect is seen on fluoromethemoglobin, although our relaxation studies show the aniline also binds to this form with a comparable affinity. From our calculated distance and the observations from optical spectroscopy, we propose a mode of binding, wherein the amino group of aniline hydrogen bonds to the distal histidine of hemoglobin. In methemoglobin, but not in fluoromethemoglobin, aniline binding could perturb the optical spectrum by affecting the hydrogen bond between the iron ligand and the histidine. Given this mode of binding, the aniline carbon opposite the amino group, which is hydroxylated in the active oxyferrohemoglobin complex, is rather far from the reactive radicals presumably generated at the iron and so a diffusable intermediate is required. (Supported by NIH Grants CA-09035 and AM-19454.)

W-AM-Po48 A STUDY OF THE APPARENT POLARITY OF THE HEME BINDING SITES OF APOMYOGLOBIN AND APOHEMOGLOBIN UTILIZING 6-PROPIONYL-2-(DIMETHYLAMINO)NAPHTHALENE, A. A. Kasprzak, B. Alpert, D. M. Jameson, R. D. Hall, and G. Weber (University of Illinois, Biochemistry Department, Urbana, Illinois 61801).

Previous investigations on the interaction of fluorescent probes with apomyoglobin and apohemoglobin have purported to demonstrate that heme-binding sites are highly non-polar (Stryer, L. (1965), J. Mol. Biol., 13, 482) or non-relaxing (Gafni, A. et al. (1977), Biophys. J., 17, 155). These studies have utilized N-arylaminonaphthalenesulfonates such as ANS or TNS whose fluorescence spectra and quantum yields are sensitive to the polarity of the environment. A new fluorophor synthesized in our laboratory, 6-propionyl-2(dimethylamino)-naphthalene (PRODAN) has fluorescence maxima ranging from 401 nm in cyclohexane (orientational polarizability $\Delta f = 0.001$) to 531 nm in water ($\Delta f = 0.320$) (Weber, G. and Farris, F.J. (1979), Biochemistry 18, 3075). An advantage of PRODAN over ANS in polarity studies is that PRODAN is soluble in appreciable amounts in both polar and totally apolar solvents, whereas ANS solubility in the latter solvents is negligible. We have shown that PRODAN binds to apomyoglobin and apohemoglobin with K_d's of 4.10^{-5}M and 1.10^{-4}M, respectively. The dye exhibits characteristic emission spectra in each complex with maxima at 452 nm for apomyoglobin and 464 nm for apohemoglobin. These emissions correspond to Stokes shifts of 6780 cm^{-1} and 7350 cm^{-1} and hence $\Delta f \sim 0.25 - 0.27$, indicating a site of appreciable polarizability. This finding is not unexpected since even if all contacts are non-polar the amide groups of the protein would still interact strongly with the fluorophore across this non-polar medium. (Supported in part by NIH Grant No. GM 11223.)

W-AM-Po49 COMPARISON OF THE MOTIONAL BEHAVIORS OF DEOXYGENATED NORMAL AND SICKLE HEMOGLOBIN AT HIGH CONCENTRATION: A SPIN LABEL STUDY. P. Thiyagarajan, W. Wong, B. Bates, B. Currie and M.E. Johnson, Medicinal Chemistry Department, University of Illinois Medical Center, Chicago, Illinois 60680.

Extensive EPR and saturation transfer EPR (ST-EPR) studies have been carried out on deoxygenated Mal-6 spin labeled sickle (dHbS) and normal (dHbA) hemoglobins over the concentration range 16 to 30 gm/dL. The hyperfine extremal linewidths differ little between dHbA and dHbS, and show only a small concentration dependence. The hyperfine separations, however, have higher values for dHbS than for dHbA. The slope of the concentration dependence curve for this parameter is less for dHbA than dHbA. In contrast, the lineheight ratio ST-EPR parameters for dHbS and dHbA differ significantly in their values, as well as in their dependence on temperature and concentration. The temperature behavior of these ratios for dHbS goes asymptotically to large values, in contrast to the existence of small values with a linear dependence for dHbA. An oxygen permeable sample holder and the ST-EPR displays were used to monitor the oxy to deoxy conformational transition and resulting aggregation behavior at high temperature. The results appear to relate to the nucleation process which is hypothesized to precede gelation. Studies utilizing the perdeuterated Mal-6 spin label are being utilized to obtain a higher resolution of the motional behavior occurring during gel formation. The results of these studies will be discussed in terms of the different motional behaviors of dHbA and dHbS under various conditions.
(Supported in part by grants from the Research Corporation, Chicago Heart Association and NIH; MEJ is an Established Investigator of the American Heart Association.)

W-AM-Po50 OSMOTIC STRESS STUDY OF PHASE TRANSITIONS OF DEOXYGENATED SICKLE CELL HEMOGLOBIN. M. S. Prouty, V. A. Parsegian, A. N. Schechter, National Institutes of Health, Bethesda, MD 20205

In order to test theories of solution-gel-crystal phase transitions and to determine protein chemical potentials in deoxygenated sickle cell hemoglobin (HbS), we are using the osmotic stress technique previously used to investigate intermolecular forces in phospholipid bilayers (Parsegian et al., PNAS 76, 2750 (1979)) and muscle (Millman and Nickel, Biophys. J. 32, 49 (1980)). Hemoglobin solutions are equilibrated with large inert Dextran T500 suspensions across a semi-permeable membrane. We determine HbS concentration and macroscopic state as a function of increasing dextran osmotic pressure (and consequently of water activity and of HbS activity). At low concentrations this procedure gives the osmotic pressure of HbS solutions. Osmotic stress above a critical level causes transition to a highly viscous "gel" phase. This transition occurs at a hemoglobin solution concentration equal to its solubility determined by centrifugation. Above this first transition, there is a region of relatively rapid increase in HbS concentration with applied pressure, followed by a region of progressively stiffer gels and gradually increasing HbS concentration (finally exceeding 60 g/dL). These findings are in qualitative agreement with the models of Minton (J. Mol. Biol. 82, 483 (1974)) and Briehl and Herzfeld (PNAS 76, 2740 (1979)) who envisage formation of non-aligned HbS polymers from monomeric solution then progressive alignment and growth of polymer to create an anisotropic phase of ordered fibres.

W-AM-Po51 THE REACTION OF c-TYPE CYTOCHROMES WITH THE IRON HEXACYANIDES: MECHANISTIC IMPLICATIONS. M.A. Cusanovich and N. Ohno, University of Arizona, Department of Biochemistry, Tucson, AZ 85721.

The iron hexacyanides are unique among the nonphysiological oxidants and reductants used to study electron transfer by c-type cytochromes as they form a kinetically detectable complex with c-type cytochromes prior to electron transfer. This mechanism is similar to that observed for the interaction of c-type cytochromes with physiological oxidants and reductants. Generally the iron hexacyanide-cytochrome reaction has been analyzed using assumptions to allow graphical solutions to obtain the rate constants. Recently we have reanalyzed available kinetic data for the reaction of eleven different c-type cytochromes with the iron hexacyanides. These cytochromes which have isoelectric points ranging from 4.5 to 10.4 and oxidation potentials of 260 to 380 mV are resolvable in terms of identical complex kinetic mechanism. Using numerical integration with no a priori assumptions we can resolve six rate constants which describe the reaction mechanism. Based on our analysis we conclude that 1) The usual study-state approximations are not valid. 2) The ratio of rate limiting first-order processes for oxidation and reduction is approximately 1.0 and 3) It is the ratio of the apparent binding rate constants for oxidation and reduction which control the oxidation-reduction potential of a particular cytochrome. The ramifications of these findings will be discussed (Supported by NIH Grant GM21277).

W-AM-Po52 HIGH RESOLUTION FLUORESCENCE EMISSION OF IRON-FREE CYTOCHROME C. P.J. Angiolillo, S.N. Dixit, J.M. Vanderkooi, Department of Biochemistry & Biophysics, University of Pennsylvania, Philadelphia, PA 19104.

High resolution Shpol'skii spectra of metallo and non-metallo porphines in various organic matrices have been known for sometime (1). However, comparable resolution in biological porphyrin molecules remained unattainable. The porphyrin of Fe-free cytochrome c at room-temperature and at liquid nitrogen temperatures exhibits a broad ($\geq$ 20 nm linewidth) structureless emission spectrum independent of excitation wavelength. Under conditions of narrow -band ($\sim$ 1 cm^{-1}) laser excitation ($\sim$ 100 mW) of the Q_x electronic transition at 4.2 K, 10μM samples in a glycerol glass matrix exhibited vibronic fine-structure reminiscent of a Franck -Condon intensity progression. Upon tuning through the Q_x band from higher to lower energy (17,450 cm^{-1} to 16,840 cm^{-1}) a continuous simplification of the fine-structure is observed until 16,920 cm^{-1} at which time essentially a single emission at 16,280 cm^{-1} is obtained with a linewidth on the order of 10 cm^{-1} (0.4 nm at 620 nm). These results can be interpreted via an energy selection model whereby one excites a small fraction of the total ensemble of inhomogeneously broadened states that comprise the Q_x and Q_y electronic transitions. As one tunes through the Q_x band from higher to lower excitation energy, less excess energy is supplied to the chromophore resulting in a lower vibrational temperature of the first excited state, thus lowering the probability for intramolecular radiationless transitions and hence broadening. (1) Personov, R.I. Opt. Spectrosc. 15, 30 (1963) (Supported by National Institutes of Health Grant GM12202)

W-AM-Po53 X-RAY FLUORESCENCE STUDIES ON CYTOCHROMES C [+]Z.R. Korszun, [*]M.A. Cusanovich and [T]K. Moffat, [+]Section of Biochemistry, Molecular & Cell Biology, Cornell University, Ithaca, New York 14853, and [*]Department of Chemistry, University of Arizona, Tucson, Arizona 85721.

Extended X-ray absorption fine structure (EXAFS) spectra were obtained at CHESS, the Cornell High-Energy Synchrotron Source, on various cytochromes c differing in midpoint potential, for both oxidation states of the proteins. The cytochromes studied are C. thiosulfatophilum c-555 ($E_{m,7}$ = +145 mV), cytochrome c from tuna heart (+260 mV), R. rubrum cytochrome c_2 (+320 mV), and E. gracilis c-552 (+370 mV). Preliminary analysis of these spectra shows that no average Fe - ligand bond length changes greater than 0.03A are observed. The average Fe - ligand bond length does not vary with change in oxidation state, nor does it vary in any systematic way as a function of midpoint potential. K-edge spectra nevertheless reveal an approximately 1.5 eV difference in the position of the 1s - 4p transitions as a function of oxidation state ; the value for the reduced state is lower than that for the oxidized state. These results are consistent with an interpretation which places the reducing electron in an orbital which is primarily metallic in character, but which does not point directly at the ligand positions. Although stereochemical regulation of cytochrome midpoint potential may exist, it is evidently not of a nature which requires changes in the lengths of the (average) Fe - ligand bonds. Instead, non-bonded heme - protein interactions which differ among this class of cytochromes are thought to be responsible for regulating their midpoint potentials. These studies are currently being expanded to other heme proteins and inorganic heme complexes, in order to examine the basis for midpoint potential regulation in iron-containing biomolecules.

W-AM-Po54 THE SITES OF INTERACTION OF REDUCTANTS WITH CYTOCHROME aa_3. KINETIC SCHEMES OBTAINED FROM SCANNING STOPPED-FLOW STUDIES. F. G. Halaka*, G. T. Babcock, and J. L. Dye*. Dept. of Chemistry, Michigan State University, East Lansing, MI 48824.

The site of interaction of cytochrome aa_3 with reducing agents appears to depend on the charge type of the reductant. With 5,10-dihydro-5-methyl phenazine (reduced PMS), anaerobic rapid-scanning stopped-flow experiments in the Soret region showed that this reductant reacts primarily with the component of the oxidase that has its maximum absorption near 430 nm in the oxidized protein. This initial phase (second-order rate constant k_1 = 1.8±0.03 x $10^5 M^{-1}s^{-1}$) is followed by a slower phase. Study of the dependence of the "slow phase" on the enzyme concentration showed that this phase can be described by two first order processes, k_2 = 0.19±0.03 s^{-1} and k_3 = 0.0206±0.0008 s^{-1}. These slow processes may describe the intramolecular electron redistribution within the protein molecule. The reduction by sodium dithionite, apparently as SO_2^-, on the other hand, was found to be primarily with the component of the oxidase that absorbs at around 410 nm. The kinetics can be described by a scheme similar to that used with PMS reduction. Based on spectral assignments of Vanneste (Biochemistry 5, 838 (1966)), these data show that reduced PMS, an uncharged molecule, reacts more rapidly with cytochrome a than it does with cytochrome a_3, while the negatively charged radical anion SO_2^- appears to have more direct access to cytochrome a_3.

This research was supported by NIH grant GM-25480 (to GTB) and by NSF grant PCM 78-15750 (to JLD).

W-AM-Po55 EPR AND ELECTRON NUCLEAR DOUBLE RESONANCE OF THE NO-LIGATED CYTOCHROME a_3 CENTER IN CYTOCHROME *c* OXIDASE. R. LoBrutto*, Y. H. Wei, C. P. Scholes, and Tsoo E. King, Dept. of Physics and Lab of Bioenergetics, SUNY at Albany, Albany, NY 12222.

The a_3 center binds O_2 and catalytically converts it to H_2O. ENDOR is useful for finding unpaired electronic distribution at paramagnetic centers like the NO-ligated a_3. Best resolved ENDOR was obtained at extremal electronic g-values of 1.98 and 2.09. At g = 2.09 hyperfine couplings were 30.6 MHz for ^{14}NO and 16.5 MHz for $^{14}N_\epsilon$ of histidine; the quadrupole coupling to ^{14}NO was 2.2 MHz. Proton ENDOR was obtained from histidine and heme. The variation of heme mesoproton couplings predicts that the 1.98 and 2.09 g-tensor components point at the mesoprotons. ^{14}NO couplings measured by ENDOR in NO-myoglobin are about 15% smaller than in cytochrome oxidase, and ENDOR of NO-ligated a_3 is better resolved overall than in NO-myoglobin, implying a better ordered site for NO binding to a_3.

In complementary EPR studies, NO rebinding to a_3 after photolysis was followed at low temperatures. No detectable NO rebinding occurred at T<45°K, while the rebinding rate increased dramatically in the 50-65°K range. Non-exponential rebinding was observed, and its time dependence was empirically fit by $(1 + t/t_o)^{-n}$, where n and t_o are temperature dependent. Austin, Frauenfelder *et. al* [Biochem. 14 (1975) 5355] observed similar rebinding of CO and O_2 to myoglobin, and the rebinding kinetics were related to a thermal activation energy distribution for recombination over a barrier near the heme. The temperature dependence of n/t_o yields the activation energy and entropy at the peak of this distribution. The activation energy for NO rebinding to a_3 is comparable to that for CO or O_2 rebinding to myoglobin, while the entropy of rebinding is much more negative, implying a more ordered environment for NO rebinding to the a_3 center. (This work is supported by NIH Grants: AM 17884, HL 12576, and GM-16767.)

W-AM-Po56 THE CHARACTERIZATION OF OXIDIZED AND REDUCED CYTOCHROMES *a* and a_3 BY HEME *a* MODEL COMPOUND STUDIES. I. Salmeen†, P. M. Callahan*, J. Frentrup* and G. T. Babcock. †Ford Motor Company, Dearborn, MI 48121 and Department of Chemistry, Michigan State University, East Lansing, MI 48824

Optical and resonance Raman spectroscopic studies on a full complement of heme *a* model compounds have been carried out. These species were characterized as a function of the following experimental variables: (1) redox state of the iron, (2) coordination state of the iron, (3) polarity and hydrogen-bonding capability of the solvent and (4) spin state of the iron. The spectroscopic properties of the models were compared to analogous features of oxidized and reduced cytochromes *a* and a_3 which had been determined in previous work (Salmeen *et al*, Biochemistry 17, 800 and Babcock *et al*, Biochemistry, in press). The results indicate that cytochrome a_3 is six coordinate, high-spin in the oxidized enzyme and five coordinate, high-spin in the reduced enzyme. In both valence states a_3 appears to be in a hydrophobic environment. Cytochrome *a* is shown to be six coordinate low-spin in both valence states of the enzyme. However, the vibrational properties of the heme *a* formyl group in cytochrome a^{3+} are not reproduced by low-spin, oxidized model compounds. We are exploring the involvement of Schiff's base formation *in vivo* as a possible explanation for this observation. (Research at Michigan State University was supported by NIH grant GM 25480.)

W-AM-Po57 INHIBITION OF CYTOCHROME P-450scc BY BENZIDINE DERIVATIVES. J.J. Sheets, J.F. Duval and L.E. Vickery, Dept. of Physiology and Biophysics, Univ. of Calif., Irvine, CA 92717.

Cytochrome P-450scc catalyzes the initial and rate-limiting step in steroid biosynthesis, the side chain cleavage of cholesterol to pregnenolone (CSCC). Like many other P-450 enzymes, P-450scc is inhibited by certain nitrogen base compounds, but the structural requirements which determine inhibitor binding specificity and affinity are poorly understood. We have found that for benzidine (Bz) inhibition of P-450scc, substitution of a methoxy group *ortho* to the arylamine results in a dramatic increase in potency. CSCC was measured in a reconstituted system of purified enzymes from bovine adrenocortical mitochondria, using excess adrenodoxin (Adx) and adrenodoxin reductase (AR) so that the concentration of P-450scc was rate-determining. Using 70 μM cholesterol in the presence of 0.3% Tween-20, a specific activity of 10-11 moles pregnenolone/mole P-450/min at 37° was observed. Dose response curves for inhibition by Bz, 3-methoxy-Bz and 3,3'-dimethoxy-Bz are shown in Fig. 1; the curves drawn through the data were calculated assuming a non-cooperative reversible binding of inhibitor to enzyme and K_d = 40, 8, and 1.5 μM, respectively. Control studies showed no effects on Adx or AR, and inhibition was relieved by dilution or dialysis. Addition of 3,3'-DMBz to the cholesterol complex of ferri-P-450scc also caused a shift in the Soret absorption spectrum, indicative of a high (S = 5/2) to low (S = 1/2) spin state transition (Fig. 2). These results suggest reversible binding to P-450scc as the origin of inhibition. (Supported by NIH Grant AM 21792.)

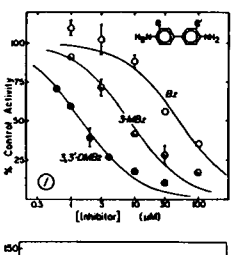

W-AM-Po58 A THERMODYNAMIC MODEL FOR CODON BIAS IN GENES Glenn W. Rowe and L.E.H. Trainor, Dept. of Physics, University of Toronto, Toronto, Ontario M5S 1A7 Canada.

This work is concerned with explanation of the bias observed in many gene structures, from sources as varied as bacteriophages and rabbits, for given bases to select preferred sites in the codon, e.g. G prefers the first site, T the third, A and C the second. Several statistical tests for randomness indicate that the observed results are consistent with a random distribution of codons once the relative numbers of each codon are known. We display these biases in a novel way and show that they can be accounted for in a thermodynamic model relating to primordial development. The interaction energies between neighboring nucleotides required in the model to account for the observations are of the same magnitude as those calculated from various molecular orbital models. However, the different molecular orbital calculations give results that vary widely so that a direct comparison is difficult.

This work is supported by a grant from the Natural Sciences and Engineering Research Council of Canada.

W-AM-Po59 LOOP FORMATION IN POLYNUCLEOTIDES: INTERNAL LOOPS AND BULGES. N. L. Marky and W. K. Olson, Department of Chemistry, Rutgers University, New Brunswick, N.J. 08903.

As part of a continuing study of polynucleotide flexibility, a theoretical model, based upon an elaborated form of the Jacobson-Stockmayer theory of polymer cyclization equilibria, has been developed to determine the probability of occurrence of internal loops and bulges in regular double helical structures. The probability $Q_{nm}(\underset{\sim}{r},\gamma)$ of such irregularities is dependent upon the positioning of a single-stranded oligonucleotide of chain length m in a particular loop closure volume V centered at vector location $\underset{\sim}{q}$ relative to a coordinate frame fixed in the complementary, but nonassociated single strand of length n. In order to maintain acceptable Watson-Crick base pairs in the adjacent helical stems, the terminal bonds of the m-mers are also required to align at an angle $\Delta\theta = \cos^{-1}(\gamma)$ relative to the initial bonds of the bulged n-mers. These conditions are estimated by the product of the three-dimensional spatial density distribution function $W_{nm}(\underset{\sim}{r})$ associated with all possible arrangements of the two interconnected oligonucleotide segments n and m times the angular correlation factor $\Gamma_{nm,\underset{\sim}{r}}(\gamma)$ related to the angular orientation of terminal bonds. Using randomly coiling models of flexibility in the two single strands, bulge formation is maximized with chains of length 1-2. (Supported by N.I.H. grants GM-20861 and CA-25981 and PRF grant AC-11586).

W-AM-Po60 A MODEL-FREE APPROACH TO THE INTERPRETATION OF NMR RELAXATION IN MACROMOLECULES. G. Lipari and Attila Szabo, Laboratory of Chemical Physics, NIAMDD, National Institutes of Health, Bethesda, MD 20205.

The usual approach to the extraction of motional information from NMR relaxation measurements involves the use of dynamical models which are based on physical intuition and/or the ease of formulation. While such analyses can be useful, there is the danger of over-interpretation of limited data and the possibility of the lack of uniqueness of the resulting physical picture of the motion. Here we present a complementary, model-free approach to this problem. After factoring out the contribution due to the overall motion of the macromolecule, we represent the appropriate correlation function for internal motion using only two parameters: (1) an effective correlation time (τ) which is a measure of the rate of motion and (2) a generalized order parameter (S) which is a measure only of the spatial restriction of the motion. S is expressed in terms of the equilibrium orientational distribution. To study the validity of our approach, we first analyze NMR relaxation data generated using a variety of sophisticated dynamical models for which the exact S and τ are known. Using a fitting procedure, we extract S and τ that not only accurately reproduce the NMR data but also agree with their exact values, when the internal motion is considerably faster than the overall motion. Finally, we analyze a variety of experimental results. Special emphasis is placed on recent proton and phosphorous NMR studies of DNA. Considering the simplicity of our method, it is remarkable how well it works.

W-AM-Po61 DIFFUSION-CONTROLLED LIGAND BINDING TO PROTEINS: THE EFFECT OF ROTATIONAL DIFFUSION AND ORIENTATION CONSTRAINTS. D. Shoup, G. Lipari, and Attila Szabo. Laboratory of Chemical Physics. National Institute of Arthritis, Metabolism and Digestive Diseases, National Institute of Health, Bethesda, MD 20205.

The calculation of the diffusion-limited rate constant for reactions between asymmetric species (e.g. the ligand binding site of a macromolecule covers only a portion of its surface) is almost always analytically intractable. In the usual formulation of the above example, a differential equation must be solved subject to the boundary conditions that (1) the ligand concentration vanishes over the reactive part of the macromolecular surface and (2) the flux vanishes over the remainder. We show that if boundary condition (1) is replaced by the less stringent requirement that the ligand concentration vanishes only on the average over the reactive part of the macromolecular surface, a whole class of problems can be solved analytically. We establish the accuracy of our approach by studying a simple model using both the usual and our boundary conditions. We take into account both the translational and rotational diffusion of the reactants and treat partially diffusion-controlled reactions using the so-called radiation boundary condition. As an illustration of the power and general applicability of our method, we explicitly consider two different models studied numerically by Schmitz and Schurr[1] and by Solc and Stockmayer[2].

[1]K.S. Schmitz and J.M. Schurr, J. Phys. Chem. 76, 534 (1972).
[2]K. Solc and W. H. Stockmayer, Int. J. Chem. Kinetics 5, 733 (1973).

W-AM-Po62 SPATIAL DENSITY DISTRIBUTIONS: AN ALTERNATIVE PROBE OF BIOPOLYMER STRUCTURE. A. R. Srinivasan and W. K. Olson. Chemistry Dept., Rutgers, The State University, New Brunswick, N.J. 08903

A novel method is presented to analyze the three-dimensional features of crystalline biopolymers in terms of the spatial density distributions of their constituent atoms. The structures are visualized as clusters of coordinate vectors radiating from their molecular centers of mass rather than complex sequences of concatenated chemical moieties. The computed chain moments and the principal axes associated with such vector distributions are employed as useful indexes to compare the tertiary structures of similar molecules. The utility of this procedure is demonstrated for the crystal structures of yeast phenylalanine transfer RNA and bovine pancreatic trypsin inhibitor. Conformational changes barely perceptible in molecular models are identified by the large differences in chain moments and angular parameters. While the various domains and subdomains in the molecule are located from the extremes of the radial displacements, the molecular secondary structure is evident from the sequential fluctuations of distances. (Supported by USPHS Grant GM-20861).

W-AM-Po63 APPLICATION OF CONTINUOUS OPTICAL SCANNING IN PAGE: SEPARATION OF RAGWEED POLLEN ANTIGENS. B. L. Chen, ERRB, NICHD, NIH, Bethesda, MD. 20205

Application of continuous optical scanning has permitted the estimation of protein diffusion coefficient during gel electrophoresis. The method has been extended to study the stack of a protein mixture, native or SDS-derivative, as it is about to diffuse into separated zones in the resolving gel. Simultaneously, diffusion and migration took place and governed the resolution. The study was aimed at developing a suitable buffer system which could provide a better resolution during protein separation. Prior to the protein analysis, electrophoretic properties of SDS in the buffer system of GABA-BICINE-AMMEDIOL, pH 9-11, were investigated using a gel (5%T 15%C, 10%T 2%C). Since both SDS micelles and anions at the moving boundary were able to be detected optically, the relative electrophoretic mobility, R_f, of SDS and the effect of SDS upon anion transport in gel were elucidated. In separating a native protein mixture, pigmented zones were detected in the vicinity of the moving boundary, while the remaining proteins migrated randomly behind the moving boundary. For separating an SDS protein mixture, mixed micelles of pigments and SDS migrated at the leading edge of the moving boundary, and SDS proteins were resolved into discrete zones (4-5). In addition, pigmented zones found in PAGE and SDS-PAGE were dependent on the pH of the gel buffer. These results suggested that ragweed pollen antigens were protein-pigment complexes. Overall, the separation of an SDS-protein mixture at pH below 10 seemed to provide a better resolution. The R_f values calculated on the basis of the resolved SDS-protein zones by the optical method were in agreement with those estimated by the manual staining method. The present study serves as a prototype for the automated analysis of protein samples by PAGE.

W-AM-Po64 KINETICALLY ACTIVE SPECIES OF ATP AND ADP IN THE ADENYLATE KINASE REACTION. Raj K. Gupta and Richard D. Moore; Institute for Cancer Research, Philadelphia, PA 19111, and Biophysics Laboratory, SUNY, Plattsburgh, NY 12901.

Since the cell interior contains approximately 150 mM K^+, it is important to know whether KATP and KADP can substitute for free ATP and ADP in the adenylate kinase reaction. If the K^+ forms of the substrates do not substitute in the reaction, changes in intracellular K^+ would affect the equilibrium of the reaction. Whether the K^+ forms can substitute may be tested by determining if K^+ affects the equilibrium in vitro using ^{31}P NMR to determine the concentrations of ATP and ADP. The concentrations of these nucleotides were determined by measuring the peak areas of ATP and ADP in the NMR spectra. Adenylate kinase was present in the NMR tube to ensure equilibrium of the system. All measurements were made when sufficient time had been allowed for equilibrium to be reached and were at 25 °C. When K^+ was added, no change in the concentrations of either ATP or ADP was observed, demonstrating that the equilibrium was not affected. Therefore, it may be concluded that the K^+ forms are equivalantly active to the free molecular species of ATP and ADP. (Supported in part by NIH Grants AM19454, AM17531, and AM21059.)

W-AM-Po65 INTEGRATION AND RESTRICTION-MODIFICATION OF MYCOPLASMA VIRUS L2. K. Dybvig and J. Maniloff. Dept. of Radiation Biology and Biophysics and Dept. of Microbiology, Univ. of Rochester Medical Center, Rochester, N.Y. 14642

Mycoplasma virus L2 is an enveloped, nonlytic virus of the wall-less prokaryote Acholeplasma laidlawii. Viral DNA is a double-stranded superhelical molecule of 7.8×10^6 daltons. DNA/DNA hybridization was used to demonstrate the integration of L2 DNA into the host chromosome of persistently infected cells. The site of integration was found to be unique, and a prophage map was determined. Restriction-modification of L2 has also been studied using host strains 1305 and JA1. DNA from 1305 cells and DNA from L2 virus grown on 1305 are resistant to restriction endonucleases BglII (AGATCT) and BamHI (GGATCC). This resistance is absent in JA1 cells. L2 DNA from a 1305 host has three BclI sites (TGATCA) while L2 DNA from a JA1 host has two BcI sites. Therefore, strain 1305 modifies these restriction endonuclease sites. Sucrose gradient analysis of parental L2 DNA in infected cells indicates that mycoplasma restriction does involve a nuclease activity.

W-AM-Po66 LASER LIGHT SCATTERING STUDIES ON HIGHER ORDER CHROMATIN STRUCTURES WHICH ARE SOLUBLE AT PHYSIOLOGICAL IONIC STRENGTHS. A. W. Fulmer and V. A. Bloomfield. Dept. of Biochemistry, Univ. of Minnesota, St. Paul, MN 55108

Inactive chromatin of the chicken erythrocyte nucleus was shown to consist of two distinct classes (I and S). I chromatin (~60% of total genome) is insoluble above 0.1 M ionic strength whereas S chromatin (~40% of total genome) is soluble at all ionic strengths studied (0.01 to 0.3 M). These chromatins were released from nuclei upon digestion with micrococcal nucleus by two separate processes which do not represent a precursor-product relationship. Isolated I chromatin fragments displayed a progressive reduction in size from >250 to ~10 nucleosome equivalents with increasing digestion times at temperatures below 15°C. Prolonged digestion of nuclei at temperatures above 15°C resulted in conversion of I chromatin to mononucleosomes which were insoluble above 30 mM NaCl. Isolated S chromatin fragments displayed a constant size distribution with increasing digestion times which peaked around 35 nucleosome equivalents. Prolonged digestion of nuclei at temperatures above 0-2°C resulted in the conversion of S chromatin to mononucleosomes which were soluble at physiological ionic strengths. Both I and S chromatins contain a full complement of histones. Quasi-elastic and Rayleigh light scattering measurements were employed to determine molecular weight, hydrodynamic radius and radius of gyration of S chromatin which was fractionated by gel filtration chromatography. S chromatin structures underwent an ionic strength dependent contraction in molecular dimensions which plateaued between 0.15 and 0.25 M NaCl. Variations of hydrodynamic parameters across elution profiles have led to a model for the packing of higher order chromatin structures in solutions of physiological ionic strengths.

W-AM-Po67 REGULATION OF THE INITIATION OF DNA REPLICATION AND OF THE SYNTHESIS OF THE *dnaA* PRODUCT IN *E. coli*. H. Eberle, N. Forrest, C. Stillman, University of Rochester School of Medicine and Dentistry, Rochester, NY 14642.

The *dnaA* product is necessary for the initiation of DNA synthesis in *E. coli* and is thought to also regulate its own synthesis. Our laboratory has isolated a phenotypic revertant of a *dnaA* temperature sensitive mutant which may have lost the ability to regulate its own synthesis. This phenotypic revertant, PR1, can initiate DNA replication at 42°C and grows more slowly and poorly at 32°C than does the *dnaA* parent strain or *dnaA*$^+$ strains. It also appears to overinitiate DNA synthesis at 32°C. The PR1 mutation has been mapped in the *dnaA* region of the chromosome, and appears to overproduce a protein of 50-53 KD, which is the approximate size of the *dnaA* product. DNA from the *dnaA* region of strain PR1 is being cloned and this mutant will be used to try to elucidate the mechanisms whereby the *dnaA* product is regulated. This work was supported by contract No. DE-AC02-76EV03490 with the US/DOE.

W-AM-Po68 DEPRIMERONES (LOW MOLECULAR WEIGHT PEPTIDES) ASSOCIATED WITH NUCLEAR RNA, DNA AND POLYSOMAL POLY(A)-mRNA IN NORMAL AND CANCER CELLS. M. Hillar, Z. Stolzman, J. Wagle, S. Allen, Department of Biology, Texas Southern University, Houston, TX 77004

Low molecular weight peptides (deprimerones) (M. Hillar and J. Przyjemski, Biochim. Biophys. Acta. 564, 246-263, 1979) were extracted with 80% ethanol at pH 9.5 from nuclear RNA, DNA and polysomal poly(A)-mRNA. They can also be isolated from intact cell nuclei.

These peptidic preparations were further purified and fractionated on Sephadex G-25 column, thin layer chromatography on cellulose plates and by HPLC on uBondapak C_{18}. They were characterized with respect to their amino acid composition, molecular weight. Isolated peptides control transcription and initiation of translation in reconstituted cell-free systems and stabilize double stranded structure of DNA. Peptide levels are decreased when extracted from neoplastic tissue preparations (Novikoff hepatoma, mouse lymphosarcoma, mouse fibrosarcoma) by about 40% in deproteinized DNA, by 66% in isolated nuclei and by 70% in deproteinized polysomal poly(A)-mRNA. Extraction of deprimerones from deproteinized DNA from normal cells amplifies several times its template activity for transcription. Loss of deprimerones in cancer DNA is responsible for higher template activity of deproteinized cancer DNA versus DNA from normal cells.

Supported by a grant from National Cancer Institute #RR 08061-10.

W-AM-Po69 KINETICS OF PHOTOREPAIR OF DNA IN *E. COLI* B_{s-1}. John Pendrys and Burt V. Bronk Departments of Physics and Microbiology, Clemson University, Clemson, S.C. 29631

A number of kinetic parameters of the photo-repair enzyme in *E. coli*. have been studied in the past with a variety of biological techniques. The assay of UV endonuclease sensitive sites gives the number of dimers remaining in the bacterial DNA after photo-reactivation by blacklight (wavelength 365 nm) and provides a different and possibly finer probe to explore site-to-site movement of this enzyme inside the bacterial cell.

We have irradiated a population of *E. coli*. B_{s-1} cells grown to log-phase ($5x10^7$ cells per ml) in HC salts (plus glucose, casamino acids, adenosine and thymidine) in HC salt(1,2) buffer at about 20° C. At a dose of 0.7 J/m^2 UV light (wavelength 260 nm) approximately 0.15dimers/10^7 daltons are put into the bacterial DNA. After a dark period of 10 minutes, photoreactivation with between 1200 and 2400 J/m^2 of blacklight causes an apparently constant number of dimers to be removed, indicating saturation of photoreactivation at the lower end of this blacklight dose range.

If we count the number of dimers repaired during the above treatment and assume an *E. coli*. genome of 2.5×10^9 daltons, we find between 30 and 70 effective photorepair enzyme molecules per genome, a result not inconsistent with values obtained by other means(3).

(1) Bronk, B.V. and Walbridge, D., Biophys. J. 31,381-392 (1980).
(2) Helmstetter, C.E. and Cooper, S., J. Mol. Biol. 31, 519-540 (1968).
(3) Harm,W., Harm,H. and Rupert,C.S.,Mut. Res. 6,371-385 (1968).

W-AM-Po70 KINETICS OF PHOTOREPAIR OF THE DNA IN CHICKEN EMBRYO FIBROBLASTS. Willem P. van de Merwe and Burt V. Bronk Departments of Physics and Microbiology, Clemson University, Clemson, S. C. 29631

We have determined the value of several new parameters influencing the efficiency of photorepair of pyrimidine dimers in the DNA of chick embryo fibroblasts. Estimates of the parameters were made by monitoring the disappearance of U.V. endonuclease sensitive sites (1,2).

Dark repair is a complication. After a U.V. dose of 10 J/m^2 of 260 nm wavelength light, which results in ∿2.4 dimers/10^7 daltons, the dimers are removed at a rate of about 0.1 dimers/10^7 daltons/hr. in the dark. After accounting for dark repair, the assay remains sufficiently sensitive to provide estimates for the times of site to site movement of repair molecules. These times appear to be substantially longer in chick cells than those previously observed in E. coli (3).

Black light of wave length ∿365 nm was used for photoreactivation. After 10 J/m^2 U.V. dose, at the time of maximum attachment of photorepair molecules to dimer sites, we find about 1.2 molecules/10^7 daltons attached. If we assume an exponential dependence for photoconversion of PR molecule-dimer complexes to repaired sites then the number of complexed sites remaining after a black light dose of D joules/m^2 is proportional to exp (-λD). On the basis of several experiments, our estimate for the value and reproducibility of λ is (1.5 ± 0.3) x 10^{-4} (J/m^2)$^{-1}$ for U.V. doses between 7.5 and 15 J/m^2.

1. Carrier, W. L. and Setlow, R. B., J. Bacteriol. 102: 178-186 (1970).
2. Patterson, M. C., Lohman P.H.M., and Sluyter, M. L., Mut. Res. 19, 245-256, (1973).
3. Harm, W., Harm, H. and Rupert, C. S., Mut. Res. 6, 371-185 (1968).

W-AM-Po71 THE STABILIZATION OF NEWLY DNA FILLED PHAGE HEADS. Harlee Strauss and Jonathan King. Biology Dept, MIT, Cambridge, MA 02139

The encapsulation of DNA into a preformed capsid and the subsequent stabilization of this condensed form of DNA are critical steps in phage assembly. We have been studying the conversion of semistable heads containing condensed, concentrically coiled DNA (Earnshaw and Casjens (1980) Cell 21, 319) into stable heads in the Salmonella bacteriophage P22.

Three phage encoded proteins, gp4, gp10, and gp26 act upon the semistable, newly DNA filled heads to convert them to extremely stable heads which, upon addition of the tail protein, will form infectious phage. Three classes of semistable heads are possible, those that accumulate when either gp4, gp10, or gp26 is removed from the cell (by mutation). We have determined the order of addition of these proteins by in vitro complementation of sucrose gradient purified semistable heads. In this assay, a phage infected cell extract containing all phage proteins except one of the head stabilization proteins is incubated with one class of semistable heads and the production of infectious phage is monitored. If the missing protein has already acted upon the semistable head, infectious phage will be formed. If the protein missing from the cell extract is still required for phage formation, no phage will be formed. We have determined that gp4 is the first protein to act upon the newly DNA filled heads and gp10 and gp26 are then added, apparently as a preformed complex. This sequence appears to be obligatory.

The immediate product of the DNA packaging reaction may be the 4$^-$ semistable head as this particle has not yet reacted with any stabilization proteins. Therefore, this structure may hold a clue to the driving forces of the DNA packaging reaction. We are now characterizing these particles.

W-AM-Po72 EFFECT OF NOVOBIOCIN ON MYCOPLASMA NUCLEOID STRUCTURE. Saibal K. Poddar and Jack Maniloff (Intr. by William A. Bernhard). Dept. of Microbiology, University of Rochester, Rochester, NY 14642

We have investigated how novobiocin (nov) stabilizes the Acholeplasma laidlawii folded chromosome and allows its isolation in low salt. Nov inhibits cell growth: inhibition of DNA replication is rapid; RNA and protein syntheses shut down more slowly. Spectrum analysis of nov-DNA mixtures indicated no nov-DNA interaction. The nucleoid was isolated by lysing cells in 0.07% Brij-58 in 0.1 M NaCl. The lysate obtained this way had a relative viscosity about 1.1-1.2. However, if cells were treated with 10 μg nov/ml before lysis, the lysate relative viscosity was only 1.005-1.020. Hence, the nov treated nucleoid must be a compact structure. This was confirmed by measurements of viscosity as a function of DNA concentration, which showed little concentration dependence of the viscosity for nucleoids from nov treated cells. This confirmed that these nucleoids behave like compact non-interacting particles. Sedimentation studies showed that nucleoids from nov treated cells sediment faster than nucleoids from untreated control cells. Double-label experiments, where both cellular DNA and protein were labeled, showed a 4-fold higher DNA:protein ratio in the nucleoid from nov treated cells than in the whole cell lysate. Hence, the rapid sedimentation rate of these nucleoids cannot be explained by incomplete lysis of nov treated cells and the nucleoids must have a compact structure. To be effective, the nov must be added to the cells before lysis and 5 min treatment is sufficient to produce the rapidly sedimenting nucleoid structure. Electron microscopic studies confirm the compact nucleoid structure.

W-AM-Po73 VACUUM ULTRAVIOLET CIRCULAR DICHROISM AND LINEAR DICHROISM OF SOME POLYNUCLEOTIDES. Gary C. Causley and W. Curtis Johnson, Jr., Department of Biochemistry and Biophysics, Oregon State University, Corvallis, OR 97331.

The optical properties of nucleic acids depend on the interactions among all of the transitions, including the higher energy transitions. However, the polarization and effect of the higher energy transitions is not well studied. Recently, we have been able to orient samples of homopolyribonucleic acids in a flow cell and obtain linear dichroic signals in the vacuum ultraviolet spectral region. Specifically, linear dichroism curves of polyadenylic and polycytidylic acid have been obtained to 175 nm. Data for both single stranded and double stranded forms of these compounds indicate that the allowed transitions in this region are all oriented in the plane of the bases. However, differences in the ratio of linear dichroism signal to isotropic absorbance (LD/A_{iso}) indicate that all of the transitions are not perfectly coplanar. These data are compared to the corresponding high energy circular dichroism curves that have been measured to 170 nm. (This work was supported by NSF grant PCM 76-81556.)

W-AM-Po74 IONIC-STRENGTH DEPENDENCE OF THE FLEXIBILITY OF DNA. Paul J. Hagerman, Dept. of Biochemistry/Biophysics/Genetics, University of Colorado Health Sciences Center, Denver, Colorado 80262.

A Monte Carlo analysis has been performed which provides a numerical relationship between the rotational diffusion coefficients and the persistence length (P) of short, wormlike chains (Hagerman and Zimm; results to appear elsewhere). The results of that analysis have been applied to the observed rates of decay of birefringence for a series of sequenced DNA fragments ranging in size from 104bp to 910bp. One advantage of the use of relatively short DNA molecules is that intramolecular excluded-volume effects are negligible. Under the conditions employed in this study, the DNA has been shown to be native. Furthermore, the rates of decay of birefringence are independent of the width and amplitude of the orienting pulse. It is observed that, subject to the restricted range of salt concentrations used in this study (less than 10mM), there is no strong ionic-strength dependence of P above 1mM for either Na^+ or Mg^{+2}, and that the limiting value for P is approximately 500 angstroms, consistent with values of P determined by other workers at much higher ionic strengths. Below 1mM, however, electrostatic contributions to P become significant. These observations are qualitatively consistent with the theoretical model for P, proposed independently by Odijk (Odijk, T. (1977) J. Polym. Sci. Polym. Phys. Ed., 15, 477-483; Odijk, T. and Houwaart, A.C. (1978) J. Polym. Sci. Polym. Phys. Ed., 16, 627-639) and by Skolnick and Fixman (Skolnick, J. and Fixman, M. (1977) Macromolecules, 10, 944-948). However, the observed increase in P with decreasing ionic strength below 1mM is less dramatic than that predicted by the Odijk-Skolnick-Fixman model.

(Supported by a Leukemia Society of America postdoctoral fellowship; NIH GM 28293 (P. Hagerman); and NIH GM 11916 (B. Zimm))

W-AM-Po75 BINDING OF POLYAMINES TO DNA. W. H. Braunlin, T. J. Strick, and M. T. Record, Jr. Dept. of Chemistry, University of Wisconsin, Madison, Wisconsin 53706.

In our work we have, by the technique of equilibrium dialysis, characterized the binding of the polyamines spermine and spermidine to DNA over a range of salt conditions, and as a function of temperature. We have also demonstrated that the effects of other small cations on polyamine binding to DNA can be consistently modelled as a competition for binding sites on the DNA. In this manner, we have obtained binding parameters over a range of solution conditions for the interaction of Mg^{2+} and putrescine with double helical DNA.

Current theory predicts that for the binding of a charged ligand to a rod-like polyelectrolyte, a plot of log K_{obs} vs. -log Na^+ should be linear, with a slope equal to the number of sodium ions released upon binding of the ligand to DNA, which should in turn be approximately equal to the charge on the ligand.[1] Further, it is expected that for a predominantly electrostatic interaction, the intercept of log K_{obs} vs. -log Na^+ at 1 M Na^+ should be small. These predictions are confirmed by our experiments. For spermine and spermidine we obtain respectively log $K_{obs,sp}$ = -3.9 log$[Na^+]$ - .52 and log $K_{obs,spd}$ = -2.7 log $[Na^+]$ at pH = 6.5. According to theory, the ΔH for a predominantly electrostatic interaction is expected to be small. In fact, we observe only small changes in K_{obs} for the binding of these polyamines over a temperature range of 4° - 37°C.

[1]Record, M. T., Jr., Anderson, C. F. and Lohman, T. M. (1978) Q. Rev. Biophys. 11, 103-178.

W-AM-Po76 DETECTION BY ESR OF FAST INTERNAL MOTIONS IN A B-DNA HELIX. A. M. Bobst, J. C. Ireland and P. W. Langemeier. Chemistry 172, University of Cincinnati, Cincinnati, OH 45221.

High molecular weight $(DUTT,dT)_n$ copolymers with DUTT/dT ratios of 0.01 and 0.025 were obtained enzymatically with calf thymus terminal deoxynucleotidyl transferase from pppDUTT and pppdT. DUTT is a dU residue site specifically spin labeled in position 5. An ESR titration of $(DUTT,dT)_n$ with $(dA)_n$ in 20 mM Tris (pH 8.1), 10 mM NaCl, 1mM EDTA buffer gave an end point at a 1:1 stoichiometry. The ESR spectra from the titration were analyzed with a two component model using the initial and final spectra as representative line shapes. The T_m and percent hypochromicity of 1% and 2.5% spin labeled $(DUTT,dT)_n$ complexed with $(dA)_n$ were essentially the same as for $(dT)_n \cdot (dA)_n$. Correlation times for $(DUTT,dT)_n$ and $(DUTT,dT)_n \cdot (dA)_n$ were computed with an axially symmetric rotational diffusion model. An isotropic Brownian rotational diffusion model with a τ_R of 2.2×10^{-10} s gave a line shape identical to the $(DUTT,dT)_n$ ESR spectrum at 25° C, whereas an anisotropic reorientation model was required to simulate the ESR spectrum of $(DUTT,dT)_n \cdot (dA)_n$ at 25° C with a $\tau_{R||}$ and a $\tau_{R|}$ of 1.1×10^{-9} s and 2.3×10^{-9} s, respectively. The mobility contribution from the leg linking the N-O· moiety to the nucleic acid matrix is presently not known, but, interestingly, correlation times calculated by ^{31}P NMR show similar mobilities for phosphate residues in DNA duplexes. Supported in part by NSF grant PCM 7801979.

W-AM-Po77 STRUCTURE OF DOUBLE-HELICAL NUCLEIC ACIDS AND ITS DISTORTION BY DRUGS: STACKING INTERACTIONS. Shih-Chung Kao, Christian G. Reinhardt, and Chun-che Tsai, Department of Chemistry, Kent State University, Kent Ohio 44242.

We have developed a generalized stereochemical scheme for comparing the stacking patterns between adjacent base-pairs with defined base sequences in double-helical nucleic acids, and for comparing the stacking patterns between adjacent base-pairs within the paired dinucleoside monophosphates of different drug-dinucleoside monophosphate complexes. This generalized stereochemical scheme has led us to define a set of unified structural parameters for comparing the structure of double-helical nucleic acids (DNA and RNA) and its distortion by binding to drugs. This generalized stereochemical scheme for comparing the base stacking patterns in double-helical nucleic acid fragments may be used to estimate the ring-current effects in the NMR of double-helical nucleic acids. Our current studies of using this generalized stereochemical scheme in comparing the structure of double-helical nucleic acids and its distortion by binding to intercalative drugs have provided important stereochemical features and structural concepts which have relevance in understanding a broad range of drug-DNA intercalations and drug-RNA intercalations.
(Supported by NIH Grant GM 24259)

W-AM-Po78 EFFECTS OF TRIAMINES ON THE DYNAMICS AND CONFORMATION OF VIRAL ϕ29 DNA. S. Allison and J.M. Schurr, Univ. of Washington (Intr. by T.M. Lohman)

Polyamines are ubiquitous in all living systems and bind strongly to DNA at low salt. Dynamic light scattering was employed to study the internal dynamics and radius of gyration R_G of DNA with bound spermidine in 0.01M NaCl, where condensation to form compact species does not occur. Only small changes in internal dynamics are effected by near saturation binding levels of spermidine although R_G is reduced significantly, probably due to intramolecular crosslinking. In the presence of spermidine, the pH profile of the plateau diffusion coefficient reveals a pronounced valley centered at pH 10.2 which is not observed in the absence of spermidine. This change is believed to result from a change in the mode of spermidine binding that is coupled to or associated with the premature titration of protons on the base ring nitrogens of thymine and guanine.

The combined techniques of electron microscopy and light scattering were used to study ϕ29 DNA condensed by triamines, principally spermidine, in 0.001M NaCl. The results for DNA condensed in 30uM spermidine at neutral pH are quantitatively consistent with a toroidal structure with a mean outer diameter of 1850 A°. At pH 10.2, condensed structures of a completely different size and shape are observed. These structures are more irregular in shape and more polydisperse than those observed at neutral pH. In addition to spermidine, certain homologs, in which the butyl group is replaced by longer pentyl through octyl groups, were also studied. Though all of the triamines condense DNA at 30uM, aggregation becomes a more prevalent occurence as the length of the end chain increases. This suggests that cross-linking may play an important role in the condensation process.

W-AM-Po79 TRIMETHYLPSORALEN AS A SITE SPECIFIC PROBE OF CHROMOSOME AND DNA STRUCTURE IN VIVO. Jonathan O. Carlson and David E. Pettijohn, University of Colorado Health Sciences Center, Denver, Colorado 80262.

When plasmid DNA, photoreacted with 4,5',8-trimethylpsoralen (me_3psoralen), was used as a substrate for HindIII restriction endonuclease, the number of sites that could be cleaved decreased exponentially with respect to the number of bound me_3psoralen adducts per DNA molecule. Similar inactivation of restriction sites for other endonucleases also occurred (EcoRI, BamHI, PstI, SalI, SmaI and BglI); however, the sensitivity of the HindIII site was substantially greater. For example, the HindIII site was inactivated at a rate 15 fold greater than the EcoRI. The simplest explanation is that me_3psoralen binds to the HindIII restriction site with greater affinity than to the EcoRI site, which is inactivated at a rate consistent with no preferential binding.

Since living cells are permeable to trimethylpsoralen, this affinity for HindIII sites may be used to probe the relative accessibility of HindIII sites in the DNA in vivo. Preliminary data relating the accessibility of the HindIII sites in SV40 DNA will be presented, which suggest that specific HindIII sites differ in their accessibility in vivo and in vitro.

W-AM-Po80 A PROTON NMR STUDY OF DRUG BINDING TO DNA, J. Feigon, W. Leupin, W.A. Denny*, and D.R. Kearns, Department of Chemistry, University of California-San Diego, La Jolla, CA, *New Zealand Cancer Society's Experimental Chemotherapy Research Laboratory, Auckland, New Zealand.

The hydrogen bonded imino protons of AT and GC basepairs in DNA give rise to two groups of resonances located between 10 and 15 ppm in proton NMR. Since few drug resonances appear this far downfield, this region provides a convenient window for monitoring changes in the DNA spectrum which are caused by drug binding. The resonance positions of the imino protons are susceptible to ring current shifts caused by bound drugs. We have developed methods for obtaining large quantities of short (<60 basepairs) random sequence natural DNA and have examined the effects of binding of over 70 different drugs and dyes to this DNA. The spectral changes observed on drug binding allow us to distinguish between drugs which bind by intercalation and drugs which bind on the outside of the DNA, and we are able to see some correlation with proposed AT and GC specificities. Further, some conclusions can be drawn about the kinetics of the drug binding, and we can see some specific protected or hydrogen bonded drug resonances. This work represents the first systematic lowfield proton NMR study of random DNA-drug interactions and demonstrates that the lowfield region provides valuable information on the nature of drug binding to DNA.

W-AM-Po81 THE INTERACTION OF DAUNOMYCIN WITH DNA. J.B.Chaires, N.Dattagupta, and D.M.Crothers*, Department of Chemistry, Yale University, New Haven, CT. 06511

Daunomycin is a potent antibiotic widely used in cancer chemotherapy. The drug is believed to act by intercalating into DNA, and subsequently inhibiting both replication and transcription. We report here results from equilibrium studies on the interaction of daunomycin with DNA. Daunomycin self-associates at moderate concentrations (0.01-1.0mM) in a buffer containing 6mM Na_2HPO_4, 2mM NaH_2PO_4, 1mM Na_2EDTA, and 0.185M NaCl, pH 7.1. Sedimentation equilibrium and proton NMR experiments are most consistent with an indefinite association model, characterized by an intrinsic association constant $K_a \simeq 1500 M^{-1}$, in contrast to reports that the self-association is best described by a simple dimerization model. Equilibrium dialysis and optical titration experiments on the binding of the drug to sonicated calf thymus DNA are most reasonably interpreted in terms of the neighbor exclusion model, yielding an association constant $K = 0.5\text{-}1.0 \times 10^6\ M^{-1}$ with the exclusion parameter equal to four base pairs. Competition dialysis experiments show that the drug has a slight preference for G-C base pairs as a binding site. Once bound, daunomycin dramatically stabilizes the DNA helix, increasing its T_m by some 20°C with 0.1 drug molecules bound per base pair. Transient electric dichroism experiments show that a length increase in the DNA results from drug binding. From the limiting values of the dichroism at infinite field, the drug appears to be oriented within the DNA with its long axis at 90° and its short axis tilted at 70° relative to the DNA helix axis. Supported by NIH Postdoctoral Fellowship GM 07092-02 (J.B.C.) and CA 15583 from the National Cancer Institute (D.M.C.)

W-AM-Po82 ^{1}H NMR STUDIES OF A DEOXYRIBOSYL DECAMER HELIX, d-(CCAAGCTTGG)$_2$ - NH RESONANCES AND CH RESONANCES OF THE BACKBONE REGION. L.S. Kan, D.M. Cheng, P.S. Miller and P.O.P. Ts'o, Division of Biophysics, The Johns Hopkins University, Baltimore, Md. 21205.

The synthesis and initial characterization of the short DNA helix, d-($C_1C_2A_3A_4G_5C_6T_7T_8G_9G_{10}$)$_2$ has been reported by our laboratory (Biochemistry 19, 4688, 1980). The CH resonances of the base protons at both helical and coil states were assigned unambiguously (Tm ≈ 60°C at strand conc. 6mM, 0.1M NaCl, pH 7.0, phosphate buffer). The NH-N hydrogen-bonded resonances in H_2O were measured at 0° to 60°C. Based on their relative stability, the NH-N resonances are assigned as follows: C_1G_{10} - 13.24 ppm (20°); G_2G_9 - 13.03 ppm (50°); A_3T_8 - 14.23 ppm (53°); A_4T_7 - 14.15 ppm (60°); G_5C_6 - 12.84 ppm (60°) (degree in bracket indicates the temperature of disappearance of the NH-N resonance due to exchange). The disappearance of the terminal C_1G_{10}-NH-N resonance at a temperature 40° below Tm, suggests the existence of rapid fraying motion at the end, which may be independent of the total length of the helix (Biochemistry 14, 4864, 1975). As for the characterization of C-H resonances, the entire ^{1}H NMR spectra of d-(CCAA) and d-(TTGG) including the pentose regions, were assigned and analyzed. At 25°C, the % of ^{2}E are 66,73,81,66 for Cp,pCp,pAp,pA in d-(CCAA); 69,75,77,64 for Tp,pTp,pGp,pG in d-(TTGG), respectively. The backbone conformations of both tetramers form gg(60-86%), gg'(76-91%) and the ϕ angle is either 200° or 281°. The complete analysis of d-(CCAAG) and d-(CTTGG), based on 500 and 600 MHz spectra, are also near completion. These studies allow us to analyze the conformation of the single-stranded form of the helix in great detail and also possibly the conformation of the backbone of the helical pentameric duplex, d-CCAAG·CTTGG, (Tm ≈ 35°C), and the decamer helix. (Supported by NIH CA 27111, GM 160066 and NSF PCN 77-25226).

W-AM-Po83 NATURAL ABUNDANCE CARBON-13 NMR SPECTROSCOPIC STUDIES OF NATIVE AND DENATURED DNA. Randolph L. Rill, George C. Levy, Peter R. Hilliard, Jr., Linda F. Levy, Chemistry Department, Florida State University, Tallahassee, Florida 32306, and Ruth Inners, NSF Southeastern NMR Facility, University of South Carolina, Columbia, South Carolina 29208.

Natural isotopic abundance carbon-13 NMR spectra of double and single-stranded DNA fragments of different length have been obtained at three magnetic fields: 37.7, 67.9 and 100.6 MHz. Short (<100 nucleotide pairs, np), intermediate (160 ± 30 np) and relatively long (300-1000 np) DNA samples were isolated from chromatin digested with micrococcal nuclease. Preliminary comparisons of NMR parameters as a function of DNA length, strandedness, and magnetic field, provide interesting new data on DNA conformational dynamics:

1) ^{13}C resonances for protonated sugar and base carbons of intermediate and short length DNA were resolved, with relatively narrow linewidths indicative of some rapid internal motions, possibly of restricted amplitude, for both sugar and base sites. The field dependences of the linewidths show that in native DNA, chemical shift dispersion resulting from nearest neighbor bases contributes significantly to sugar linewidths observed at high magnetic fields, whereas this contribution is absent in the single-stranded molecule.

2) Linewidths for the exocyclic C-5' sugar carbon reflect a relatively higher motional freedom than for other carbons in DNA.

3) ^{13}C T_1s and, more importantly, Nuclear Overhauser effects confirm that both sugar and base carbons in native DNA undergo complex dynamics characterized by short ($\gtrsim 10^{-9}$ sec) timescale motions, superimposed on slow overall tumbling. Native and single stranded DNA samples show comparable ^{13}C T_1s, while linewidths narrow three to five-fold and NOEs increase somewhat (from ~0.6 to ~1.1 for C-H carbons).

W-AM-Po84 A GENERAL PROCEDURE FOR THE ASSIGNMENT OF THE ^{31}P AND ^{13}C NMR RESONANCES OF OLIGONUCLEOTIDES. D.M. Cheng, L.S. Kan, P.S. Miller, E.E. Leutzinger, and P.O.P. Ts'o, Division of Biophysics, The Johns Hopkins University, Baltimore, Md. 21205.

While the ^{31}P NMR spectra of oligonucleotides are readily obtainable, the unambiguous assignment of the individual ^{31}P resonances has not been achieved. The main reason is that the ^{31}P NMR spectrum of an oligonucleotide, such as NpN'pN", cannot be deduced from its components, i.e. NpN' and N'pN". We present a general method for unambiguous assignment of the ^{31}P NMR of any oligonucleotide, the ^{1}H NMR spectrum of which at the furanose-backbone region can be completely characterized. In the NMR spectrum, each phosphorous nucleus is coupled to $H_{3'}$, $H_{4'}$, $H_{5'}$, and $H_{5"}$ of its neighboring pentose unit. Thus, if the ^{1}H NMR spectrum of the pentose-backbone region can be characterized with certainty, then the ^{31}P resonance can be assigned unambiguously through a double resonance technique. In practice, we specifically irradiate individual ^{31}P resonances of the oligonucleotides and observe the spectral changes of ^{1}H NMR spectrum, particularly the $H_{5'}$ and $H_{5"}$ region for assignment. We have assigned the six ^{31}P resonances in two tetranucleotides d-$C_pI$$C_pII$$A_pII$A and d-$T_pII$$T_pIII$$G_pI$G (I,II,III denote the order of the ^{31}P resonances in the spectra from low field to high field), as well as in the helical duplex of these two tetramers. The same double resonance technique was also used to solve the assignment problem of ^{13}C NMR spectrum of dinucleotides. For example, the two $^{13}C_2$, two $^{13}C_8$ and two $^{13}C_{1'}$ resonances in the ^{13}C NMR spectrum of d-ApA methyl phosphonate were successfully assigned for the first time by selective irradiation of the well-characterized ^{1}H resonances of H_2, H_8 and $H_{1'}$ of the dimer. This study illustrates the usefulness of the completely characterized ^{1}H resonances for the unambiguous assignment of ^{31}P and ^{13}C resonances of the oligonucleotides by double resonance technique. (Supported by NIH CA 27111, GM 160066 and NSF PCN 77-25226)

W-AM-Po85 PROTON NMR RELAXATION MEASUREMENTS OF THREE DNA RESTRICTION FRAGMENTS, T.A. Early, D. R. Kearns, W. Hillen*, and R. D. Wells*; Department of Chemistry, University of California - San Diego; La Jolla, Calif.; *Department of Biochemistry, University of Wisconsin; Madison, Wisc.

Extensive measurements of proton relaxation rates have been obtained at 300 MHz on three pVH 51 restriction fragments of 12, 43, and 69 base pairs in length. Relaxation rates for both the non-exchangeable and the exchangeable imino protons in Watson-Crick base pairs have been measured. From a study of the temperature dependence of the relaxation rates of the imino protons, the details of the events which preceed the helix-to-coil transition can be studied. At high temperature, the imino proton relaxation rates are a direct measure of the base pair opening rates and in the 12 base pair fragment, where individual imino resonances can be observed, the opening of individual base pairs can be directly monitored. These observations demonstrate that the opening of the AT base pairs occurs as a single base pair phenomenon without opening neighboring base pairs. At low temperatures where exchange of imino protons is slow, the imino proton relaxation data can be used to determine an effective rotational correlation time for the three fragments. These effective correlation times are compared with the predictions of two different hydrodynamic theories in order to obtain information about the flexibility of these DNA fragments in solution. Measurements on the relaxation behavior of the nonexchangeable protons in these molecules provide additional information about the local structural and dynamic properties of DNA.

W-AM-Po86 POLYMORPHISM OF THE PHOSPHATE-BACKBONE IN POLYNUCLEOTIDE COMPLEXES. J.L. Alderfer, M.W. Jackson*, and G. Hazel*, Department of Biophysics, Roswell Park Memorial Institute, Buffalo, New York 14263.

Phosphorous-31 nuclear magnetic resonance spectroscopy (P-31 NMR) is a useful technique for studying the backbone conformation of nucleic acids. High resolution P-31 NMR spectra have been obtained above and below the thermal denaturation temperature (Tm) for (1) poly-(A)$^+$•poly(A), (2) poly(A)•poly(U), (3) poly(U)•poly(A)•poly(U), and (4) poly(I)•poly(C). Above the Tm the spectral lines are generally sharp ($\nu_{\frac{1}{2}}$ <2 Hz) and consist of one or two resonances of expected intensity reflecting the homopolymer composition of the respective complexes. Below the Tm the spectral lines are somewhat broader ($\nu_{\frac{1}{2}}$ ∿20-50 Hz), presumably reflecting reduced correlation times of the base-paired complexes. Of particular interest is the observed number of phosphorous resonances for these complexes and their chemical shifts in the base-paired states (PPM at 30°C in aqueous solution referenced to trimethyl-phosphate): (1) poly(A)$^+$•poly(A): one resonance at -5.10; (2) poly(A)•poly(U): two at -4.10 and -4.45; (3) poly(U)•poly(A)•poly(U): three at -3.39, -3.84, and -4.36; and (4) poly(I)•poly(C): two at -4.03 and -4.54. In complexes where multiple resonances are observed, each is approximately of equal intensity. Except for the poly(U)•poly(A)•poly(U) complex, x-ray diffraction studies of the fibers of these complexes have been interpreted to have phosphate backbone conformations which are radially symmetric (possess a dyad symmetry axis). However, the present P-31 NMR studies indicate a model where only poly(A)$^+$•poly(A) has similar backbone conformations in each strand, while each of the other complexes have unique phosphate-backbone conformations for each strand. These observations suggest that base-sequence and the mode of base-pairing are important in determining polymorphism of the polynucleotide backbone.

W-AM-Po87 ALTERNATING ELECTRIC FIELD LIGHT SCATTERING FROM T4 BACTERIOPHAGE. Thomas J. Herbert. Department of Biology, University of Miami, Coral Gables, Fl 33124.

The dielectric properties of T4 bacteriophage were studied by alternating electric field light scattering. The intensity of light scattered from a solution of centro-symmetric particles which are partially oriented by a weak sinusoidal electric field consists of a constant component and a sinusoidal component with twice the frequency as that of the applied field. For non-centrosymmetric particles, such as T4 bacteriophage, the light scattering intensity consists of these terms plus a large component at the same frequency as that of the applied field. This single frequency term has a Lorentzian dependence upon frequency of the applied field and intensity proportional to the permanent dipole moment of the scatterer. Furthermore, at low scattering angles, the intensity of the single frequency component does not depend upon the exact shape of the scatterer but is a function of the degree of asymmetry of the particle. For T4 bacteriophage, knowledge of the distance between the center of mass of the particle and the center of mass of the head permits calculation of the permanent dipole moment. The resulting value for the permanent dipole moment of fiberless T4 particles is 22,989 ± 979 Debye. These and other results on bacteriophage particles will be discussed. (Supported by grants from the Research Corporation and the Petroleum Research Fund administered by the American Chemical Society.)

W-AM-Po88 A THEORY OF AGGREGATION IN THE THERMAL DENATURATION REGION OF MULTI-STRAND BIOPOLYMERS, John Shibata and J. Michael Schurr, Department of Chemistry, University of Washington, Seattle, Washington.

Dynamic light scattering experiments performed on DNA[1,2] and collagen[3] solutions have demonstrated that, contrary to widespread belief, these species actually aggregate in their thermal denaturation regions. Here we propose a theory that explicitly admits the possibility of aggregation of multi-strand biopolymers. It is found that the same secondary bonds responsible for stabilizing the native structure at low temperature will promote aggregation in the thermal denaturation region for sufficiently long chains. A requirement for both open and zippered regions dictates that the aggregation region does not extend far below the melting temperature. However its width, or extension on the high temperature side of the melting temperature, is a strongly increasing function of chain length and also cooperativity parameter.

The present theoretical results obtained for DNA and collagen with almost no adjustable parameters are in good qualitative agreement with a number of previously poorly understood experimental observations. The significance of such a spontaneous aggregation phenomenon for genetic recombination is noted.

1) J. M. Schurr, CRC Crit. Revs. Biochem. (1977)4, 370-430.
2) J. Wilcoxon, these abstracts.
3) J. C. Thomas and G. C. Fletcher, Biopolymers (1979) 18, 1333-1352.

W-AM-Po89 A DYNAMIC LIGHT SCATTERING STUDY OF THE VARIATION OF DNA FLEXIBILITY WITH TEMPERATURE. Jess Wilcoxon, Department of Chemistry, University of Washington, Seattle, WA.

Internal and translational diffusion of clean viral ϕ29 DNA was studied to determine whether local denaturation or softening of the helical backbone was occurring for temperatures less than the melting temperature T_m. It was found that the rigidity remained approximately constant from 0° to 70°C, which indicates that local denaturation does not occur to a significant extent. In the optical thermal transition region $70° \leq T \leq 80°C$, softening occurred but no single-strand formation was observed. All data for $T \leq 70°C$ could be accurately described by a unique Rouse-Zimm model with constant rms subchain extension independent of T.

At T=80°C the translational diffusion coefficient (corrected for viscosity and temperature changes) decreased abruptly and remained low up to 92°C, which indicates aggregation of the DNA in the upper denaturation region. No indication of single-strand DNA was observed until T≈92°, where a very rapid component with the anticipated single-strand diffusion coefficient was observed in the correlation functions, which became strongly bi- or multi-exponential at that temperature. Gel electrophoresis studies revealed aggregates that did not migrate.

W-AM-Po90 TORSION DYNAMICS, FLUORESCENCE DEPOLARIZATION, AND NMR RELAXATION OF DNA. J. Michael Schurr, John H. Shibata, Stuart A. Allison, and John C. Thomas, Department of Chemistry, University of Washington, Seattle, Washington.

The decay of the fluorescence polarization anisotropy (FPA) of ethidium bromide bound to DNA has been studied over a range of time spans from 0-18 ns to 0-120 ns with the aid of a picosecond dye laser. These FPA data were fitted to 3 different functional forms: (1) the Initial Exponential Decay Zone formula of a recently developed rigid-rod and torsion spring model for the torsion dynamics of DNA; (2) the Intermediate Zone formula of that same model; and (3) a single-exponential-plus-baseline. Only the Intermediate Zone formula fits the data from all different time spans well with the same set of physical parameters. Intermediate Zone relaxation rules out the existence of distributed torsion soft-spots, or joints, in the range from 1 in 20 to 1 in 1000 base-pairs and allows determination of the torsion elastic constant. Effects of bound spermidine at pH 7.6 and 10.2 on the torsion dynamics will be described.

The FPA monitors the correlation function $\langle P_2[\underline{\mu}(0)\cdot\underline{\mu}(t)]\rangle$, where $\underline{\mu}(t)$ is the instantaneous unit vector along the transition moment of the fluorophore. NMR dipolar relaxation of 31P monitors fourier transforms of the same correlation function, but with $\underline{\mu}(t)$ now the instantaneous unit vector connecting the P and H nuclei. A physically realistic expression for this correlation function incorporating (1) end-over-end diffusion of the local helix-axis, (2) overdamped reorientations of the P-H vector in a local harmonic well within the nucleotide unit, and (3) the already measured contribution of the collective torsional deformations has been derived, and applied to calculate T_1, T_2 and NOE. Much smaller amplitudes of local reorienting motion are required to fit the literature data than believed previously.

W-AM-Po91 THE BINDING OF INITIATION FACTOR 3 TO POLYRIBONUCLEOTIDES. B. F. Schmidt*, K. T. Twombly*, L. J. Mengle*, and T. Schleich, Division of Natural Sciences, University of California, Santa Cruz, CA 95064

We have used sedimentation partition chromatography to determine the affinity of E. coli IF3 for different polynucleotides under various conditions. Observed association constants, at pH 7.0 and 22° C, for poly(A) range from 3×10^2 M^{-1} at 230 mM NaCl to 2×10^5 M^{-1} at 85 mM salt. The binding of IF3 to poly(U) is not significantly different from that of poly(A) which suggests that IF3 has little preference for base type, at least in non-specific binding. The effect of monovalent cation concentration on the association constants indicates that the dominant factor in complex formation is the release of cations from the polynucleotide. We calculate that 8 monovalent cations are released from poly(A) or poly(U) upon the binding of one protein molecule. The binding of IF3 to poly(U) at pH 7.0, is reduced in the presence of 10 mM $MgCl_2$, at NaCl concentrations less than 230 mM, but to a lesser degree than predicted from binding theory. Poly(C), which is double-stranded at pH 5.5, binds IF3 40 times stronger than when it is single-stranded at pH 7.0 (10 mM $MgCl_2$ and 85 mM NaCl). However, poly(U), which is single-stranded at pH 5.5 and pH 7.0, shows no significant difference in its affinity for IF3 at these two pH values. Thus, it appears that IF3 has a stronger affinity for double-stranded than single-stranded structures, and shows no significant preference for purine or pyrimidine containing polynucleotides. (Supported by NIH Grant GM 23951 to T.S.)

W-AM-Po92 INVESTIGATION OF CONFORMATIONAL CHANGES OF RNA THROUGH ULTRAVIOLET THERMAL PERTURBATION DIFFERENCE SPECTROSCOPY (TPDS). D. Fréchet*, R. Ehrlich, J. Gabarro-Arpa and P. Remy (Introduced by P.O.P. Ts'o), IBMC,67084 Strasbourg-Cédex, France.

High resolution optical studies provided evidence for fine cooperative transitions in thermal denaturation of RNA. Analysis of the spectral dispersion of the optical signal was undertaken in order to gain additional insight about the structural parameters involved. This analysis is based on a systematic study of the TPDS of mono-, di-, oligo-, and polynucleotides. Significant changes in UV spectra of the mononucleotides were observed upon temperature elevation; these changes are attributed to temperature dependent hydration changes of the bases, and are observable also in di- and oligonucleotides. These spectral changes due to dehydration are superimposed upon the spectral changes due to unstacking of bases, a process which was found to be dependent on base composition and base sequence. The effect of stacking geometry on TPDS was noted in the studies on chain length dependence. In the study of trimers, TPDS revealed the interaction of the terminal bases resulting in the bulging out of the mid-base. The specific spectral effect due to base-base hydrogen bonding was observed upon interaction of purines and pyrimidines in non-aqueous solvents. Similar spectral changes were noted in the premelting process of polynucleotide complexes. However, the spectral changes observed in the melting process of synthetic polynucleotide complexes, tRNAs and 5S RNA could not be described satisfactorily by a linear combination of following parameters: unstacking of the bases using single-stranded polynucleotides as model, hydration changes using mononucleotides as model and base-base hydrogen-bonds rupture using premelting optical changes as calibration. Additional parameters may be obtained from the analyses of defined short helices. *Present address: Division of Biophysics, Johns Hopkins Univ., School of Hygiene, Baltimore, Maryland 21205.

W-AM-Po93 MISMATCHES AND BULGE LOOPS IN DEOXYRIBO-OLIGONUCLEOTIDES: A THERMODYNAMIC STUDY, Luis A. Marky, Sharon Kozlowski, and Kenneth J. Breslauer, Department of Chemistry, Rutgers University, New Brunswick, New Jersey 08903.

A series of deoxyribo-oligonucleotides of specific sequences were synthesized and investigated by temperature-dependent uv absorption spectroscopy and differential scanning calorimeter. The stabilizing and destabilizing effects of mismatches, dangling ends and bulge loops were thermodynamically characterized. Replacement of a Watson-Crick GC base pair by a GT mismatch in a dodecamer duplex (dCGCGAATTCGCG) reduced the duplex stability by over 20°C. The calorimetric data reveal this destabilization to be enthalpic in origin. Addition of one extra nucleotide resulted in the formation of a "bulge loop" which also destabilized the helix by nearly 20°C. In contrast, however, this destabilization was entropic in origin.

The thermodynamic results are discussed in terms of specific molecular interactions. This work was supported by NIH Grant GM-23509.

W-AM-Po94 DATA BASE FOR NUCLEIC ACID SEQUENCES R.M. Schwartz, H.R. Chen, M.O. Dayhoff, W.C. Barker, L.T. Hunt, and B.C. Orcutt, National Biomedical Research Foundation, Georgetown University Medical School, Washington, D.C. 20007

We have assembled a computer data base of currently correct, up-to-date, nucleic acid sequence data containing more than 300,000 residues from over 320 sequences. A convenient retrieval system (see abstract by Orcutt, et al.) makes this data base accessible and intellectually comprehensible. Each sequence entry is identified by its nucleic acid name, species, strain, and higher taxonomic group. References and tables of important biological features are provided with each entry. Information on linear or circular nucleic acid configuration, single- or double-stranded structure, total length, and base composition is also provided. The data base currently includes complete genomes of bacteriophages, plant viruses, viroids and mammalian tumor viruses; primary RNA transcripts including introns and coding regions; mature mRNAs; complete sequences of plasmids, transposons, and insertion sequences; and control regions, such as promoters and origins of replication. In addition to displaying the data base using a video computer terminal, we will also provide alignments and other illustrative materials to clarify the functional and evolutionary relationship among the sequences. Supported by NIH grant GM-08710 and NASA contract NASW-3317.

W-AM-Po95 DATA RETRIEVAL FROM THE NUCLEIC ACID SEQUENCE DATA BASE. B.C. Orcutt, R.M. Schwartz, H.R. Chen, J.A. Fredrickson, and M.O. Dayhoff. National Biomedical Research Foundation, Georgetown University Medical Center, Washington, D.C. 20007.

Interactive dial-up access to a large-scale data base of nucleic acid sequences is currently available. Any computer terminal with a telephone connection device can be used for remote access. No background in computer programming or data retrieval systems is required. Sequences can be found by searching for the nucleic acid name, the species name, a keyword in the text of the ancillary information, or an author name. Nucleic acid name, species name, authors, references, comments, annotation table, composition, and the sequence can be displayed. Also, an overall view of the features in the annotation table can be displayed. A sequence can be searched for a matching string of nucleotides. Sequences can be constructed by splicing segments of a sequence from the data base. The spliced sequence, its complement, or the protein translated from either can be obtained. Lists of sequences from higher taxonomic groups and sequences ordered by length and nucleotide composition are maintained. Supported by NASA contract NASW 3317 and NIH grant GM-08710.

W-AM-Po96 COMPUTER ANALYSIS OF NUCLEOTIDE AND PROTEIN SEQUENCES. M. I. Kanehisa and W. Goad, Theoretical Division, Los Alamos Scientific Laboratory of the University of California, Los Alamos, New Mexico 87545.

We have developed an interactive computer program for analysis of nucleotide and protein sequences. The program is designed for use at the Nucleic Acid Sequence Library which is being established in the Los Alamos Scientific Laboratory. The program includes all the features of the Korn-Queen program (Methods in Enzymology. Vol. 65, p. 595, 1980). In addition, it offers the Sellers-Goad method for finding homology regions, the calculation of evolutionary distances, and the prediction of secondary structures. All of these may be used for protein sequences as well.

The similarity of two sequences is defined by a metric for nucleic (or amino) acid match, replacements, and deletions, and represented in terms of the standard deviation unit of the similarity of randomized sequences (random sequences with the same compositions). The metric for amino acids is taken from the mutation data in related proteins accumulated by Dayhoff and colleagues (Atlas of Protein Sequence and Strucutre, Vol. 5, p. 101, 1972). The metric for nucleic acids is then determined by calculating the similarity in both nucleic acid sequences and translated protein sequences in coding regions of small viruses. The metric for nucleic acids is used to search for repeated, symmetry, and dyad symmetry regions within a sequence, and for locally homologous regions of two sequences.

Work supported by the U.S. Department of Energy.

W-AM-Po97 SEARCHING FOR HOMOLOGOUS/ANALOGOUS DNA SUBSEQUENCES. Walter Goad, Theoretical Division, Los Alamos Scientific Laboratory, University of California, Los Alamos, NM 87545.

With large quantities of nucleic acid sequence data available in computer-readable form, it is useful to be able to locate within long and very long sequences those subsequences that resemble each other in some way. "Some way" may mean sequences that are the same but for a few base replacements or insertion/deletion of bases or groups of bases from the one sequence or the other, or the same but for codon replacements/deletions/insertions, or take up similar secondary structures ... and so on.

Sellers[1] recently offered a definition of "locally close" subsequences and announced an algorithm for isolating them that starts from the Needleman-Wunsch path-through-a-matrix formulation of the problem. We have implemented the Sellers algorithm but finding it insufficiently discriminating against resemblances of little or no interest, have explored various modifications. A modification which involves primarily a conditioning of the underlying metric increases the discrimination to what seems an acceptable level, and provides a powerful and computationally efficient tool.

Both particular and statistical results will be presented.

(Work supported by the U.S. Department of Energy.)

[1]P.H. Sellers, Proc. Nat. Acad. Sci. 76, 3041(1979).

W-AM-Po98 SEQUENCE DEPENDENCE OF DIMER CONFORMATIONAL FEATURES. B. Van Assen. Department of Chemistry, Rutgers University, New Brunswick, N.J. 08903.

Catalogs of the sterically allowed, stacked conformers of the ribodinucleoside monophosphates UpA and ApU have been constructed. Semiempirical potential functions have been used to estimate the base-stacking energies of the cataloged conformers. The structural features of the conformers are described by computed extents of base overlap and distances and angles between base planes. The ranges of conformations and stacking parameter values characteristic of the ApU and UpA dimers are slightly different. The relative numbers of ApU and UpA stacked conformers and their relative extents of overlap substantiate qualitatively, if not quantitatively, the stacking propensities deduced from NMR coupling constants. The ranges of stacking energies characteristic of the sequence isomer catalogs are similar. Furthermore, calculations of base-backbone interaction energies indicate that base-stacking energies alone are not sufficient to describe fully the relative stabilities and conformational differences of stacked UpA and ApU structures. Patterns of base overlap drawn from the catalogs show that the orientation of uracil H(5) relative to adenine is a function of base sequence. This sequence dependence may be partially responsible for observed differences in the chemical shifts of H(5) in UpA and ApU. Recent NMR studies have attributed such shift differences solely to differences in the handedness of base stacks and dimer stacking propensities. Because the helical organization of polynucleotides is sensitive to variations in chain conformation, a comparison of the fine structure of heteropolynucleotides comprising alternating UpA and ApU catalog members with that of standard A-RNA merits attention. The modeling of nucleic acid dynamics with collections of such double-stranded heteropolynucleotides may facilitate a description of the conformational changes involved in the "breathing" phenomenon. (Supported by USPHS Grant GM-20861 awarded to W. K. Olson.)

W-AM-Po99 CLONING AND ORGANIZATION OF MITOCHONDRIAL DNA FROM PARAMECIUM PRIMAURELIA AND PARAMECIUM TETRAAURELIA. Donald J. Cummings, Jane L. Laping, and Peter E. Nolan. Department of Microbiology and Immunology, University of Colorado School of Medicine, Denver, Colorado 80262.

Studies from our laboratory have shown that mitochondrial (mt) DNA from four different species of Paramecium aurelia is a linear molecule, 14 μm in length. Molecular hybridization experiments revealed that species 1, 5, and 7 mt DNA were quite similar. Except for the genes coding for ribosomal RNA, species 4 mt DNA had less than 25% homology with the other species. The major region of non-homology was that containing sequences necessary for initiation of DNA replication.

To better understand the structure and function of mt DNA from quite similar organisms, we have undertaken cloning and physical mapping of restriction enzyme fragments from Paramecium primaurelia (species 1) and Paramecium tetraaurelia (species 4). Fragments from four endonucleases, Pst I, Bam HI, EcoRI and Hind III were cloned successfully and restriction maps were constructed for each. The only fragments which have not yet been cloned were those located at the ends of these linear molecules. In general, the maps for species 1 and species 4 were comparable but differences did emerge. The details of these maps and possible consequences will be presented.

W-AM-Po100 INTERACTION OF MESO TETRA(4-N-METHYLPYRIDYL)PORPHINE WITH d(ATGCAT). James C. Howard and Robert J. Fiel, Department of Biophysics, Roswell Park Memorial Institute, Buffalo, New York 14263.

High resolution proton magnetic resonance and circular dichroism(CD) spectra were obtained for aqueous solutions (μ = 0.2 and 0.5) of the intercalator meso Tetra(4-N-methylpyridyl)porphine (T4MPyP), the hexadeoxynucleotide d(ATGCAT), and their mixtures for several ratios of base pairs to intercalator to determine the structure of the T4MPyP•d(ATGCAT) complex. The temperature was varied from 5°C to 80°C to cause the hexadeoxynucleotide to undergo a helix to coil transition. Upfield shifts (with respect to internal 0.5 mM t-BuOH) of all nucleic acid resonances and the porphyrin Hβ resonance were observed. The magnitude of the shifts depended on the temperature and the ratio of base pairs to porphyrin. No changes in the chemical shift of any pyridyl group protons were observed. A negative CD band was induced at about 440 nm with a small positive band at about 425 nm which is similar to that observed for some T4MPyP•calf thymus DNA complexes. Analysis of the data indicates that binding of T4MPyP to d(ATGCAT) stabilizes the duplex form and occurs at the ends with an asymmetry similar to that for T4MPyP intercalated into calf thymus DNA.

This work was supported in part by grant NIH-ES-07051-02 from the N.I.H.

W-AM-Po101 REVERSING ELECTRIC FIELD TRANSIENT BIREFRINGENCE STUDY OF THE FLEXIBILITY OF DNA RESTRICTION FRAGMENTS. John G. Elias* and Don Eden Yale University, New Haven, CT 06511.

The transient electric birefringence of monodisperse DNA restriction fragments ranging from 64 to 5000 base pairs has been studied as a function of length and counterion concentration. The high sensitivity of our apparatus, 4×10^{-12}, has permitted measurements to be made at concentrations of 5μg/cm^3 in low electric fields. For all fragments a rapid transient occurs upon field reversal. For the small, <267 base pair, and very large, >4000 base pair, fragment this is the only transient. However for intermediate size fragments the shape of the signal changes dramatically. As shown in the Figure there is a maximum in the signal before steady state orientation is achieved and then upon field reversal the rapid transient is followed by a larger maximum. The behavior is that which is expected for a polarization component perpendicular to the principal axis of the polyanion. The amplitude of the effect is a function of both the size of the fragment and the counterion concentration. We shall discuss the effect in terms of the flexibility of the DNA. Supported in part by NIH Grant SO7-RR-07015.